



Centro de Investigación Científica de Yucatán, A.C.

Posgrado en Ciencias Biológicas

YUCCA-mediated biosynthesis of the auxin IAA is required during the somatic embryogenic induction process in *Coffea canephora*

Tesis que presenta

Miguel Ángel Uc Chuc

En opción al título de

DOCTOR EN CIENCIAS

(Ciencias Biológicas: Opción Bioquímica y Biología Molecular)

Mérida, Yucatán, México

AÑO 2020

CENTRO DE INVESTIGACIÓN CIENTÍFICA DE YUCATÁN, A. C.
POSGRADO EN CIENCIAS BIOLÓGICAS



RECONOCIMIENTO

Por medio de la presente, hago constar que el trabajo de tesis de Miguel Angel Uc Chuc titulado **YUCCA-mediated biosynthesis of the auxin IAA is required during the somatic embryogenic induction process in *Coffea canephora*** fue realizado en la Unidad de Bioquímica y Biología molecular, en el laboratorio 24 del Centro de Investigación Científica de Yucatán, A.C. bajo la dirección del(a) Dr.(a) Víctor Manuel Loyola Vargas, dentro de la opción de Bioquímica y Biología Molecular, perteneciente al Programa de Posgrado en Ciencias Biológicas de este Centro.
Atentamente.

Dra. Cecilia Hernández Zepeda

Directora de docencia

Mérida, Yucatán, México, a 04 de noviembre de 2020

DECLARACIÓN DE PROPIEDAD

Declaro que la información contenida en la sección de Materiales y Métodos Experimentales, los Resultados y Discusión de este documento proviene de las actividades de experimentación realizadas durante el período que se me asignó para desarrollar mi trabajo de tesis, en las Unidades y Laboratorios del Centro de Investigación Científica de Yucatán, A.C., y que a razón de lo anterior y en contraprestación de los servicios educativos o de apoyo que me fueron brindados, dicha información, en términos de la Ley Federal del Derecho de Autor y la Ley de la Propiedad Industrial, le pertenece patrimonialmente a dicho Centro de Investigación. Por otra parte, en virtud de lo ya manifestado, reconozco que de igual manera los productos intelectuales o desarrollos tecnológicos que deriven o pudieran derivar de lo correspondiente a dicha información, le pertenecen patrimonialmente al Centro de Investigación Científica de Yucatán, A.C., y en el mismo tenor, reconozco que si derivaren de este trabajo productos intelectuales o desarrollos tecnológicos, en lo especial, estos se registrarán en todo caso por lo dispuesto por la Ley Federal del Derecho de Autor y la Ley de la Propiedad Industrial, en el tenor de lo expuesto en la presente Declaración.

Nombre y firma

A handwritten signature in black ink, appearing to read 'Miguel Angel Uc Chuc', written in a cursive style.

Miguel Angel Uc Chuc

Este trabajo se llevó a cabo en la Unidad de Bioquímica y Biología Molecular de Plantas del Centro de Investigación Científica de Yucatán, y forma parte del proyecto titulado “modificación del genoma de plantas superiores utilizando CRISPR/Cas9 para estudiar el proceso de diferenciación celular”, con el número del proyecto 1515, bajo la dirección del Dr. Víctor Manuel Loyola Vargas.

AGRADECIMIENTOS

Gracias al CONACYT por la beca Num. 448534 otorgada y por el financiamiento del proyecto “modificación del genoma de plantas superiores utilizando CRISPR/Cas9 para estudiar el proceso de diferenciación celular”, con el número del proyecto 1515, bajo la dirección del Dr. Víctor Manuel Loyola Vargas.

A mí director de tesis, Dr. Víctor Manuel Loyola Vargas; primero por haberme aceptado en su equipo de trabajo y segundo por su apoyo, confianza y por creer en mí.

A mí comité tutorial conformados por la Dra. Clelia De la Peña Seaman, Dr. Geovanny Nic Can, Dr. Stefan De Folter y el Dr. Víctor Manuel Loyola Vargas, por sus críticas y consejos durante estos cuatro años.

Al comité de examen de grado, Dra. Clelia De la Peña Seaman, Dr. Stefan De Folter, Dr. Geovanny Nic Can, Dr. Enrique Castaño de la Serna, Dr. Felipe Augusto Vazquez Flota, Dr. Víctor Aguilar Hernández y al Dr. Víctor Manuel Loyola Vargas.

Agradezco profundamente a la M.C. Rosa María Galaz Ávalos por su valioso apoyo en el HPLC y por todo su ayuda en estos cuatro años.

A la M. C. Ángela F. Ku González por apoyo y paciencia con el uso del microscopio confocal.

A la M. C. Cleyre Pérez-Hernández, por su valiosa colaboración en auxinas.

Al Dr. Víctor Aguilar Hernández y a la M. C. Ligia Brito Argáez por su apoyo y colaboración en el LC-MS/MS.

A mis padres, la Sra. Aida María y el Sr. Benjamín, así como también a mis apreciables y distinguidas hermanas, mil gracias por su apoyo.

A mis amigos del laboratorio núm. 24 y compañeros del la Unidad de Bioquímica.

DEDICATORIAS

Este trabajo va dedicado a mis queridos padres, la Sra. Aida Maria y el Sr. Benjamín.

INDEX

CHAPTER I.....	9
BACKGROUND.....	9
1. COFFEE	9
1.1. SOMATIC EMBRYOGENESIS (SE).....	9
1.2. GENE EXPRESSION DURING THE SE.....	11
1.3. GENES INVOLVED IN THE SE	12
1.4. AUXIN BIOSYNTHESIS	15
1.5. YUCASIN: A POWERFUL INHIBITOR OF THE ACTIVITY OF YUCCA ENZYMES	22
1.5 AUXIN TRANSPORT	23
HYPOTHESIS.....	27
GENERAL AIM	27
SPECIFIC AIMS.....	27
JUSTIFICATION	27
EXPERIMENTAL STRATEGY.....	27
CHAPTER II.....	29
YUCCA-MEDIATED BIOSYNTHESIS OF THE AUXIN IAA IS REQUIRED DURING THE SOMATIC EMBRYOGENIC INDUCTION PROCESS IN <i>COFFEA CANEPHORA</i>	29
2.1 INTRODUCTION.....	30
2.2 MATERIALS AND METHODS	33

2.2.1 PLANT MATERIAL AND GROWTH CONDITIONS.....	33
2.2.2 INDUCTION OF SOMATIC EMBRYOGENESIS IN <i>C. CANEPHORA</i>	33
2.2.3 EXTRACTION OF AUXINS AND THEIR CONJUGATES	33
2.2.4 HIGH-PERFORMANCE LIQUID CHROMATOGRAPHY	34
2.2.5 LIQUID CHROMATOGRAPHY-MASS SPECTROMETRY OF AUXINS	34
2.2.6 PREPARATION OF SEEDLINGS IN THE PRESENCE OF 3- ¹⁴ C-TRP	35
2.2.7 YUCASIN INHIBITION ASSAY	36
2.2.8 PLANT TISSUE SAMPLING	36
2.2.9 REAL-TIME QUANTITATIVE ANALYSIS OF GENE EXPRESSION.....	36
2.3.0 HISTOLOGICAL ANALYSES	37
2.3.1 IMMUNOLocalIZATION ASSAYS.....	37
2.3.2 CONTROLS OF IAA IMMUNOLocalIZATION.....	38
2.3.3 STATISTICAL ANALYSIS	38
2.4 RESULTS.....	39
2.4.1 THE INDUCTION PROCESS, HISTOLOGY AND EXPRESSION PROFILING OF THE CcYUCs TRANSCRIBED DURING SE IN <i>C. CANEPHORA</i>	39
2.4.2 IDENTIFICATION AND CONTENT OF FREE IAA AND CONJUGATED IAA.	42
2.4.3 ENDOGENOUS FREE IAA ACCUMULATIONS AND LOCALIZATION DURING THE SE INDUCTION PROCESS	49
2.4.4 EFFECT OF THE INHIBITION OF AUXIN IAA BIOSYNTHESIS BY YUCASIN DURING THE SE INDUCTION PROCESS IN <i>C. CANEPHORA</i>	52

2.4.5 RESTORATION OF SOMATIC EMBRYOGENESIS BY EXOGENOUS ADDITION OF IAA	55
2.4.6 DISCUSSION.....	58
SUPPLEMENTARY MATERIAL.....	63
CHAPTER III.....	69
IDENTIFICATION, ANALYSIS AND MODELLING OF THE YUCCA PROTEIN FAMILY IN GENOME-WIDE OF <i>COFFEA CANEPHORA</i>	69
3.1. INTRODUCTION.....	70
3.2 MATERIALS AND METHODS	72
3.2.1 SEARCHING OF CcYUC PROTEINS IN <i>C. CANEPHORA</i>	72
3.2.2 MULTIPLE- SEQUENCE ALIGNMENTS AND PHYLOGENETIC TREE CONSTRUCTION	72
3.2.3 PREDICTION OF ISOELECTRIC POINT, MOLECULAR MASS, TRANSMEMBRANE HELIX, SUBCELLULAR LOCALIZATION, SIGNAL PEPTIDE AND PHOSPHORYLATION SITES IN CcYUCs PROTEINS IN <i>C. CANEPHORA</i>	73
3.2.4 BUILDING OF THREE-DIMENSIONAL STRUCTURES (3D), MODELLING AND MOLECULAR DOCKING OF SELECTED CcYUCs PROTEINS IN <i>C. CANEPHORA</i>	73
3.2.5 PLANT MATERIAL.....	74
3.2.6 YUCASIN TREATMENT.....	74
3.2.7 IAA IMMUNOLocalIZATION IN LEAVES EXPLANT OF <i>C. CANEPHORA</i>	75
3.3 RESULTS	76
3.3.1 IDENTIFICATION OF THE CcYUC PROTEIN FAMILY IN <i>C. CANEPHORA</i>	76
3.3.2 PHYLOGENETIC ANALYSIS AND IDENTIFICATION OF MOTIFS IN CcYUC PROTEINS.....	77
3.3.4 BIOINFORMATICS ANALYSIS OF CcYUC PROTEINS IN <i>C. CANEPHORA</i>	82

3.3.5 3D STRUCTURE PREDICTION AND MODELING OF THE CcYUC PROTEINS FAMILY	88
3.3.6 MOLECULAR DOCKING	95
3.3.7 IMMUNOLOCALIZATION AND INHIBITION OF IAA BIOSYNTHESIS	97
3.4 DISCUSSION.....	100
CHAPTER IV	105
GENERAL DISCUSSION.....	105
CHAPTER V	107
5.1 CONCLUSIONS.....	107
PERSPECTIVES	108
REFERENCES.....	¡ERROR! MARCADOR NO DEFINIDO.

LIST OF FIGURES

Figure 1.1 mRNA in situ hybridization <i>BBM</i> embryos and seeds.....	14
Figure 1.2 Overexpression of <i>BBM</i> <i>Theobroma cacao</i> gene (<i>TcBBM</i>) induces an increase in the SE.....	15
Figure 1.3 A, <i>YUC4</i> and B, <i>YUC9</i> are expressed in the suspensor at 16 cell stage...	19
Figure 1.4 Auxin transport during embryogenesis in <i>A. thaliana</i>	25
Figure 2.1 SE induction process in <i>C. canephora</i>	40
Figure 2.2 Histological analysis during the SE induction process in <i>C. canephora</i> ..	41
Figure 2.3 Content of IAA and its conjugates during pre-treatment and induction of SE in <i>C. canephora</i>	44
Figure 2.4 Gene structure and protein sequence of <i>CcYUC1</i> in <i>C. canephora</i>	47
Figure 2.5 Expression levels of individual <i>CcYUC</i> genes during the induction of SE in <i>C. canephora</i>	48
Figure 2.6 Free IAA immunolocalization during the SE induction process in <i>C. canephora</i>	50
Figure 2.7 Free IAA immunolocalization during day zero of the SE induction process in <i>C. canephora</i>	51
Figure 2.8 Effect of yucasin during the induction of SE in <i>C. canephora</i>	53
Figure 2.9 Quantification of the IAA endogenous content in leaf explants of <i>C. canephora</i> treated with 5 μ M yucasin.....	54
Figure 2.10 Effect of yucasin on the production of somatic embryos during the induction process in <i>C. canephora</i>	55

Figure 2.11 The exogenous addition of IAA restores somatic embryogenesis in explants previously treated with 100 μ M yucasin.....	57
Figure 3.1 <i>C. canephora</i> genome analysis	76
Figure 3.2 Alignments of multiple sequences of CcYUC proteins family in <i>C. canephora</i>	78
Figure 3.3 Phylogenetic tree of CcYUC proteins family in <i>C. canephora</i>	79
Figure 3.4 Phylogenetic tree of CcYUC/AtYUC proteins family of the <i>C. canephora</i> and <i>A thaliana</i>	81
Figure 3.5 Predicted transmembrane helix (TMH) in the amino acid sequence of A) CcYUC10 Cc01_g20210 and B) CcYUC Cc01_g 20250 auxin biosynthetic proteins in <i>C. canephora</i>	84
Figure 3.6 Prediction of CcYUC protein phosphorylation sites in <i>C. canephora</i>	87
Figure 3.7 Homology predictions of the 3D structures of nine CcYUC proteins in <i>C. canephora</i>	89
Figure 3.8 Modeling of the 3D structures of nine proteins of the CcYUC family in <i>C. canephora</i>	91
Figure 3.9 Alignment of the CcYC proteins family in <i>C. canephora</i>	92
Figure 3.10 Alignment and identification of FAD and NADPH motifs of CcYUC proteins in <i>C. canephora</i>	94
Figure 3.11 CcYUC2–FAD–NADPH–IPA complexes.....	96
Figure 3.12 Trp-Dependent IAA biosynthesis mechanism and YUC protein functional activity inhibition by yucasin in <i>C. canephora</i>	99
Figure 3.13 Endogenous immunolocalization of free IAA in leaf explants of <i>C. canephora</i>	100

LIST OF TABLES

Table 1. Total radioactivity present in each sample of <i>C. canephora</i> plantlets analyzed.....	44
Table 2. CcYUC genes family selected for analysis by qRT-PCR and primers.....	46
Table 3. CcYUC family in <i>C. canephora</i> used in this study.....	83
Table 4. The table below shows the prediction of signal peptide, most likely cleavage site and subcellular location of CcYUCs enzymes in <i>C. canephora</i>	85
Table 5. Information on the phosphorylation sites of the selected CcYUCs enzymes in <i>C. canephora</i>	86

ABBREVIATIONS

Somatic Embryogenesis	SE
Growth Regulators	GR
YUCCA	Flavin monooxygenase
DAI	Days post- induction
IAA	Indole-3-acetic acid
IPyA	Indole-3-pyruvic acid
Kin	Kinetina
NAA	Naphthalen acetic acid

RESUMEN

A pesar de la existencia de una investigación considerable sobre la embriogénesis somática (ES), el mecanismo molecular que regula la biosíntesis de las auxinas durante el proceso de inducción de la ES sigue siendo desconocido. El ácido indol-3-acético (AIA) es una auxina que se sintetiza en las plantas a través de cinco vías. La vía biosintética más frecuentemente utilizada en esta síntesis es la conversión de triptófano a ácido indol-3-pirúvico (IPyA) por las enzimas triptófano aminotransferasas de *Arabidopsis* (TAA) seguido de la conversión del IPyA a AIA por enzimas codificadas por los genes *YUCCA* (*YUC*) de la familia de flavina monooxigenasas; sin embargo, no está claro si la biosíntesis del AIA mediada por *YUC* está involucrada en la inducción de la ES. En este estudio, se indica que el aumento de AIA observado durante el pretratamiento para la inducción de la ES en *Coffea canephora* (MS suplementado con ácido 1-naftaleneacético (NAA) 0.5 μ M y cinetina (Kin) 2.32 μ M durante 14 días) se debe a su biosíntesis *de novo*. Mediante qRT-PCR, se determinó que la expresión de genes *CcYUCs* es consistente con la señal del AIA libre encontrada en los explantes durante la inducción de la ES. Además, el uso de yucasina, un inhibidor de las enzimas *YUC*, reduce la señal de AIA libre en los explantes foliares y disminuye drásticamente el desarrollo de la ES. La adición de AIA restaura el proceso de ES en explantes tratadas con yucasina. Para obtener información detallada de la familia de proteínas *YUC*, se presenta una caracterización profunda basada en un análisis filogenético y bioinformático que incluye la predicción proteica de una hélice transmembrana hidrofóbica (TMH), un péptido señal, su localización subcelular, sitios de fosforilación, y modelado y acoplamiento molecular de las proteínas *CcYUC*. Nuestros hallazgos sugieren que la familia de proteínas *CcYUC* están altamente conservadas en la ruta de biosíntesis de las auxinas y que la biosíntesis y la localización del AIA desempeñan un papel esencial durante el proceso de inducción de la ES en *Coffea canephora*.

ABSTRACT

Despite considerable research on somatic embryogenesis (SE), the molecular mechanism that regulates the biosynthesis of auxins during the SE induction process remains unknown. Indole-3-acetic acid (IAA) is an auxin that is synthesized, in plants, through five pathways. The biosynthetic pathway more frequently used in this synthesis is the conversion of tryptophan to indol-3-pyruvic acid (IPyA) by tryptophan aminotransferases of *Arabidopsis* (TAA). The followed step is converting IPyA to IAA by enzymes encoded by *YUCCA* (*YUC*) genes of the flavin monooxygenase family; however, it is unclear whether YUC-mediated IAA biosynthesis is involved in SE induction. In this study, we report that the increase of IAA observed during SE pre-treatment (plants in MS medium supplemented with 1-naphthaleneacetic acid (NAA) 0.5 μ M and kinetin (Kin) 2.32 μ M for 14 days) is due to its *de novo* biosynthesis. By qRT-PCR, we demonstrated that *CcYUCs* gene expression is consistent with the free IAA signal found in the explants during SE induction. Also, the use of yucasin to inhibit YUC enzymes' activity reduces the signal of free IAA in the leaf explants and dramatically decreases SE's induction. The exogenous addition of IAA restores the SE process in explants treated with yucasin. We presented an in-depth characterization based on the phylogenetic and bioinformatic analysis for more detailed information on the YUC family of proteins. This analysis includes predicting hydrophobic transmembrane helix (TMH), signal peptide, subcellular localization, phosphorylation sites, modelling, and docking molecular of *CcYUC* proteins. Our findings suggest that the *CcYUC* proteins family is highly conserved in the auxin biosynthesis pathway. That biosynthesis and the localization of IAA play an essential role during the induction process of the SE in *Coffea canephora*.

INTRODUCTION

Unlike animals, plants have a high capacity for regeneration of new individuals identical to the mother from a cell or groups of cells without the need for fertilization. This regeneration mechanism is known as somatic embryogenesis (SE) (Vogel, 2005; Nic-Can et al., 2013). SE is the development of structures similar to a zygotic embryo from somatic cells (Tvorogova et al., 2019; Loyola-Vargas and Ochoa-Alejo, 2016). It can also be the process by which somatic cells, under induction conditions, generate competent cells that undergo a series of morphological, biochemical, and molecular changes to give rise to somatic embryos without the fusion of gametes (Quiroz-Figueroa et al., 2006). SE provides an invaluable tool for the genetic improvement of plant species that cannot be propagated sexually (Ma et al., 2015).

The study of the biochemical and molecular mechanisms of SE allows us to identify the factors involved during the induction process of the somatic embryo (Ma et al., 2015) and determine how best to apply them to the genetic improvement of a range of plant species (Ma et al., 2015; Santana-Buzzy et al., 2004). Furthermore, SE is an example of totipotency because the somatic cells respond directly to a stimulus leading to the somatic embryo's development and formation. Therefore, SE is an excellent system for studying cellular differentiation and dedifferentiation (Magnani et al., 2017).

SE is a complex process that involves many factors including plant species, tissue type (explant), culture medium, exogenous growth regulators and changes in endogenous growth regulators, and nitrogen and carbon source (Nic-Can et al., 2013; Quiroz-Figueroa et al., 2001; Fuentes-Cerda et al., 2001). Besides, somatic cells can activate the genetic machinery necessary for the transcription of genes involved in SE induction (Quiroz-Figueroa et al., 2002), implicating the alteration of cell wall composition and changes in growth regulators, genetic expression, and epigenetic regulations in this process (De-la-Peña et al., 2015).

It has been proposed that plant growth regulators, mainly indole-3-acetic acid (IAA), play a crucial role in mediating the signal transduction that leads to the reprogramming of gene expression. This change is followed by a series of cell divisions that induce disorganized

growth (callus) or lead to direct SE (Dudits et al., 1991). IAA is a molecule that controls almost all aspects of plant growth and development (Tsugafune et al., 2017). Its biosynthesis is crucial for plant homeostasis, including embryo development, fruit ripening, organogenesis, and plant architecture (Nonhebe, 2015; Paque and Weijers, 2016). However, the auxin's action is determined by its synthesis and distribution in tissue, mainly by its polar transport from cell to cell (Petrášek and Friml, 2009; Peer et al., 2011).

The route most conserved and providing the most direct way to produce IAA in plants is from tryptophan via two enzymatic reactions consisting of TRYPTOPHAN AMINOTRANSFERASE OF ARABIDOPSIS (TAA) and YUC flavin monooxygenase of the indole-3-pyruvic acid (IPyA) pathway (Tsugafune et al., 2017; Zhao et al., 2001; Mashiguchi et al., 2011).

Genetic studies have demonstrated that YUC functions as the rate-limiting step of the IPyA pathway, indicating that YUC plays a crucial role in developmental processes regulated by cellular IAA levels (Tsugafune et al., 2017). Biochemical and molecular studies have shown that these gene families (TAA and YUC) participate in the IAA biosynthesis pathway in several plant species, including *Arabidopsis thaliana*, *Zea mays*, and *Oryza sativa* (Zhao, 2014; Brumo et al., 2014). It has been reported that IAA biosynthesis through YUC is necessary for the establishment of the basal part of the embryo and the onset of embryonic organs (Cheng et al., 2017). Previous findings indicated that auxin biosynthesis location plays an essential role in many growth and development processes, including embryogenesis (Zhao, 2010).

Cheng et al., (2006) overexpressed *YUC1*, *YUC2*, *YUC4*, and *YUC6* genes, and their results indicate an increase in the production of auxin in *Arabidopsis* seedlings. Also, they determined the expression of *YUC1* and *YUC4* at the apical meristem and primordia of young leaves (Cheng et al., 2006; 2007). Single or double mutants showed no adverse effect, unlike quadruple mutants that caused severe effects on the seedlings (Cheng et al., 2007). Accordingly, due to the *YUC* genes family's redundant functions, it is not easy to access reverse genetic approaches to understand IAA biosynthesis's physiological role (Tsugafune et al., 2017). Hence, the use of specific inhibitors to overcome the redundant activity of target genes has emerged as a useful tool for genetic studies (Tsugafune et al., 2017).

Despite the various studies in this area, the genes regulating IAA auxin biosynthesis during embryogenesis are unknown (Cheng et al., 2007). Endogenous intracellular levels remain unclear during the SE induction process. There the possibility that *de novo* IAA biosynthesis plays an essential role in the SE because previous reports have shown that auxin biosynthesis is dynamic during embryogenesis (Ribnicky et al., 2002).

Our primary goal in this work was to determine whether the YUC-mediated IAA biosynthesis is involved during the SE induction process in *Coffea canephora*. To solve it, we used qRT-PCR to measure the transcript levels of *CcYUCs* and used a specific yucasin inhibitor to block the biosynthesis of the auxin IAA. Yucasin is a potent specific YUC enzyme inhibitor (Nishimura et al., 2014).

In this study, we found that *CcYUC1*, *CcYUC1-putative*, *CcYUC4*, and *CcYUC-Like* genes have dynamic expression patterns when the induction of the SE process. We showed a correlation between the *CcYUCs* expression pattern and the location of the free IAA auxin signal at the beginning of the induction of the SE process. Furthermore, forming a local endogenous IAA gradient in specific tissues was crucial during the SE induction process in *C. canephora*. On the other hand, treatment with yucasin inhibited SE, but exogenous IAA addition restored the embryogenic process. Our data show that the YUC-mediated IAA biosynthesis is crucial for SE in *C. canephora*.

CHAPTER I

BACKGROUND

1. Coffee

Coffea belongs to the Rubiaceae family and has been identified two genera: *Coffea* and *Psilanthus*. The *Coffea* genus comprises more than 100 species. Commercially, the most important specie is *Coffea arabica*. *Coffea canephora* Robusta variety ($2n = 22$) is the second specie with. The major economic importance is not only by the volume of production but also by the cultivable area (Nolasco 1985). Also, *C. canephora* has a high degree of resistance to water stress and high temperatures and diseases; it also has high caffeine content. *Coffea arabica* ($2n = 44$) is less resistant to diseases, lower caffeine content, and is the most commonly used beverage (Bertrand et al., 2000).

For several years, different research groups have been working to improve coffee production through biotechnological applications and the support of such valuable tools like molecular biology (Anthony et al., 1997). The development of plant tissue culture techniques has been of great value to both agriculture and biotechnology. Tissue culture is essential to solving plant biology questions, for example, elucidating metabolic pathways, genetic improvement, somaclonal variation, and production of compounds of pharmaceutical interest (Loyola-Vargas and Ochoa-Alejo 2012). The SE as a tool of tissue culture is perhaps the best way to regenerate plants; however, some physiological, biochemical, and molecular mechanisms that take place when the cell becomes competent are still unknown (Rojas-Herrera et al., 2002; Quiroz-Figueroa et al., 2006).

1.1. Somatic Embryogenesis

During the life cycle of plants, embryogenesis is crucial in many species (De Vega-Bartol et al., 2013). Different molecular aspects of reproductive biology have been discussed widely (Petrasek, 2011).

The SE is the formation of an embryo from a cell or group of cells without gametes fusion. It can be done by a series of cell dedifferentiation (Pierik, 1990; Quiroz-Figueroa et al., 2006.) or somatic cells. The somatic cells, which under specific induction conditions, can

generate embryogenic cells that will undergo morphological, biochemical, and molecular changes until they form a somatic embryo (Zimmerman, 1993). The SE is the best example of totipotency because the somatic cells respond adequately to a stimulus leading to the somatic embryo's development and formation. Therefore, SE is a system for the study of cellular, differentiation and dedifferentiation (Magnani et al., 2017). Besides, SE is one of the most used tools for propagation and regeneration of higher plants (Priyono et al., 2010). Due to this feature, it has become a valuable technique for the study of plant species with agronomic and biotechnological interest (Quiroz et al., 2006).

A somatic embryo undergoes various development stages known as globular, heart, torpedo, and cotyledon to become a complete plant (Quiroz et al., 2002). Between zygotic and somatic embryogenesis exists a significant similarity during developmental stages except that SE enters a dormant (Zimmerman, 1993). The SE differs from the ZE (zygote embryogenesis) because the first can manipulate or control a wider range of factors *in vitro* than the ZE (Santana et al. 2007). Different explants can be used for the induction; however, in the genus *Coffea*, the best source is the young foliar tissue (Etienne, 2005).

It has been reported that SE in *Coffea* can be achieved in two ways, directly and indirectly. The directly way only requires a specific ratio of auxin and cytokinins; the indirect way requires the induction of an embryogenic callus under a specific medium supplemented with growth regulators (GR) and then another culture medium without GR (Quiroz et al., 2002., Rojas et al., 2002).

The induction of SE is a complex process that involves many factors, including plant species, tissue (explant), culture medium, exogenous growth regulators, nitrogen and carbon source, and *in vitro* conditions (Nic-Can et al., 2013; Quiroz-Figueroa et al., 2001). Also, the SE process can be affected by the IAA auxin, the same one that regulates the development and growth of the plant (Petrasek, 2011). Ayil-Gutiérrez et al. (2013) reported that IAA plays an essential role during the induction of SE in *C. canephora*; its homeostasis is crucial to understand the role of auxins during the process of SE induction.

1.2. Gene expression during the SE

Up today, the signal that activates somatic cells to become totipotent and gives rise to a whole plant is unknown. Although there are works that studied the cellular and molecular changes that control the formation of the somatic embryo, it is not clear the genetic and biochemical mechanisms that govern the SE's development. Biochemistry and molecular biology studies will help understand the mechanisms leading this cell capacity during the SE.

The SE can start from a cell or group of cells described by Loyola-Vargas et al. (1999) and Quiroz-Figueroa et al., (2002). They observed that somatic cells are originated from mesophyll cells or cells with the rapid epidemic mitotic division. Somatic cells can be distinguished from other cells at the leaf tissue because they are isodiametric, with dense cytoplasm and prominent nuclei, which undergo a series of organized divisions until a complete embryo, similar to the ZE (Quiroz et al., 2002). Besides, somatic cells can activate the genetic machinery necessary for the transcription of genes involved in the induction of SE (Quiroz-Figueroa, 2002). Several factors are implicated for the induction of SE, including alteration of the cell wall composition, changes in growth regulators, genetic expression, and epigenetic regulations (De la Peña et al., 2015).

Several works have documented the expression of genes involved during the SE. Recent studies showed an expression pattern of auxin response genes (*ARF*) during the SE induction process in *C. canephora* (Quintana-Escobar et al., 2019). Experiments performed by Magnani et al. (2017) determine the presence of the AP2/ERF transcription factor *WOUND INDUCED DEDIFFERENTIATION 1 (WIND1)*, which showed the same pattern of expression as *BABY BOOM (BBM)* and *Somatic Embryogenesis Receptor Kinase (SERK1)*, suggesting that they might play a crucial role in obtaining embryogenic competence.

Once these genes are activated, a program of gene expression is carried out, establishing a pattern in plant tissue (Quiroz-Figueroa et al., 2006). It has been proposed that growth regulators (GR) play a crucial role in mediating signal transduction leading to the reprogramming of gene expression, followed by a series of cell divisions that induce disorganized growth (callus) or growth. It is leading to polarized SE (Dudits, 1991).

Activation response by auxin may be the main event to gene expression and cell division in reprogramming the physiological state, which leads to embryogenic with the competition that gives rise to somatic embryo (Quiroz-Figueroa et al., 2006).

In recent years, a particular field of interest has been the study of the mechanisms regulating cell identity and the maintenance of undifferentiated cells in the meristems of the plant (Schoof, 2000). Understanding the mechanisms that govern this embryogenic process will lead us to lay the groundwork for future use in the propagation, improvement, and genetic manipulation. The SE can be an effective way of regeneration to obtain genetically modified cells, as well as a valuable tool for the multiplication of plant species with agronomic interest (Rojas-Herrera, 2002).

1.3. Genes involved in the SE

During the embryogenic process, somatic cells are induced to form embryogenic cells capable of generating a whole plant; this capacity is known as cell totipotency and is characteristic of plant cells. Such a change in development involves a series of events related to molecular recognition of internal signals and external stimuli (Chugh, 2002). GRs play a crucial role in plants' development and growth, mainly auxin IAA *in vitro* culture (Quiroz-Figueroa et al., 2006). 2,4-dichlorophenoxyacetic acid is a synthetic analogue of auxin, and its exogenous addition induces genetic expression during SE in many plant cultures (Dunits et al., 1991). It has been suggested that auxin signalling and stress are key for cellular reprogramming leading to embryogenesis (Quiroz-Figueroa et al., 2006).

The ability of the embryogenic system may be the result of several factors such as the presence or absence of specific receptor of the GR, alterations in balance or equilibrium of endogenous GR, chromatin remodelling, epigenetic regulation (acetylation and methylation), and transcription factors (Jimenez, 2001; Quiroz-Figueroa et al., 2006; Feng and Jacobsen, 2011). Although the embryogenic process has been widely studied, few genes have been associated with SE's induction. Some of them are the homeobox (HB) gene family *LEAFY COTYLEDON LEC* (Stone et al., 2001), *BBM* (Boutilier et al., 2002), the *WOX* family (*WOX2*, *WOX8*, *WUSHEL*) (Zuo et al., 2002; Tvorogova et al., 2019) and *SERK*. *SERK* is an essential receptor for auxin-mediated signalling (Baudino et al., 2001).

It has been reported that the SE in *A. thaliana* can be achieved by ectopic expression of transcription factors such as *LEC* (Stone *et al.*, 2001), *BBM* (Boutillier *et al.*, 2002). Previous studies showed that the embryogenesis-associated genes *BBM*, *LEC1*, *WOX2*, and *SERK* were identified and analyzed in somatic embryos of the *European larch* *L. decidua* Mill (Rupps *et al.*, 2016). *LdLEC1* and *LdWOX2* are mainly expressed during early embryogenesis, whereas *LdBBM* and *LdSERK* reveal increased expression during later development. Temporal and spatial expression studies revealed a specific *LdLEC1* signal in young embryo heads' outer cell layers, whereas mature embryos showed a homogeneous expression (Rupps *et al.*, 2016). Other genes found in *A. thaliana* like *FUS3*, *ABI4*, are transcription factors that encode proteins during embryogenesis induction (Gaj *et al.*, 2005).

The *LEC1* gene encodes a protein related to domain-B-ACTIVATED PROTEIN HEME 3 (HAP3) subunit CCAAT-box binding factors (CBF) (Lotan *et al.*, 1998). *LEC1* is predominantly expressed at the beginning and the end of the seed development phase (Ledwon and Gaj, 2010). It has been reported that *LEC1* regulates the genes of auxin biosynthesis (Junker *et al.*, 2012). *YUCs* genes family encoding flavin mono-oxygenases proteins involved in auxin biosynthesis in *A. thaliana* (Cheng *et al.*, 2006). In previous work, it was shown that *LEC1* binds to the *YUC10* promoter to activate gene transcription, which causes an increase in the endogenous auxin concentration during embryogenesis in *A. thaliana*. It has been suggested that *LEC1* plays a role in the control of *YUC10* expression and, therefore, affects the synthesis of auxins in the embryo (Junker *et al.*, 2012). Overexpression of *LEC2* leads to the formation of the embryo and callus formation, and cotyledons. Previously with *A. thaliana* mutants, it has been reported that *LEC* genes have its function at the end of embryogenesis to initiate and/or maintain embryo maturation and germination repress (West *et al.*, 1994).

Guo *et al.* (2013) promoted somatic embryogenesis as a study model using tobacco plants in which they overexpressed *LEC2* and *LEC1* genes. In *LEC2* transgenic plants, there is an increased production of somatic embryos, and the regeneration of the plant was done in a culture medium without exogenous GR. However, *LEC1* transgenic plants were not able to regenerate in the same culture medium.

Another essential transcription factor is *BBM*; it belongs to the AP2 family and is expressed in meristems and root. Ectopic expression of *BBM* in *A. thaliana* induces somatic embryos' spontaneous formation from seedlings (Boutilier et al., 2002). Also, *BBM* is a specific transcription factor that regulates a wide range of developmental processes in plants (Boutilier et al., 2002). The AP2/ERF proteins have been divided into two distinct subfamilies based on the number of DNA binding domains that can have (one or two). *BBM* belong to the AP2 subfamily (Boitilier et al., 2002).

On the other hand, it has been found that the expression of the *BBM* gene is present during the development of a zygotic embryo. Analysis by RT-PCR and *in situ* mRNA (Figure 1.1) hybridization pattern spatio-temporal expression of the *BBM* gene in cultured Brassica microspores and developing seeds of *A. thaliana* was determined. Transcripts of *BBM* find genes present in embryogenic cultures four days old but were not detected in non-embryogenic cultures of the same age. These transcripts (*BBM*) were detected subsequently globular to cotyledonary stage embryos developing microspore-derived (Boutilier et al., 2002).

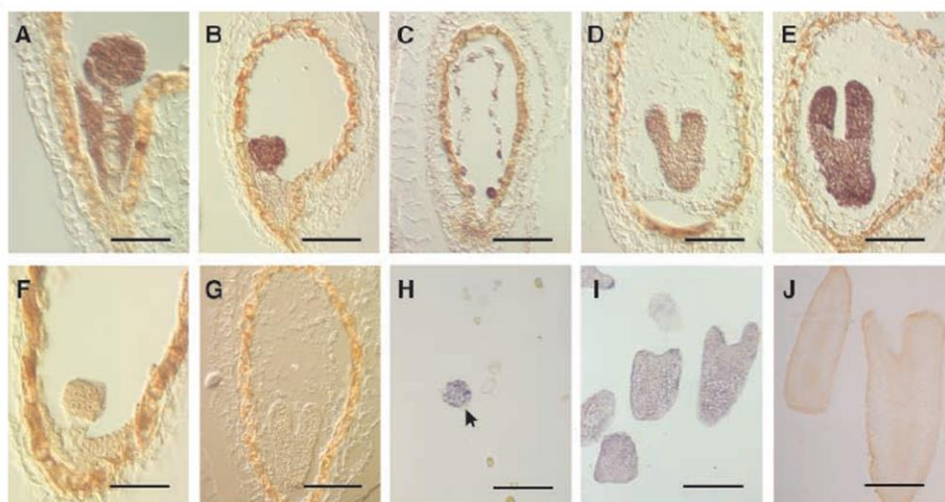


Figure 1 mRNA in situ hybridization *BBM* embryos and seeds. *Brassica* embryo sections microspores and seeds derived from *A. thaliana*. *AtBBM* **A-E** were hybridized; *BnBBM* of **H-I**; *AtBBM* **F** and **G**; *BnBBM* **J**. digoxigenin UTP labelled probes. The hybridization transcript is indicated purple-brown. **A-G** longitudinal sections of *A. thaliana* seeds. **H**, globular stage embryo (arrow) and microspores undeveloped cultured during 8 days old of the *Brassica*. **I-J**, *Brassica* embryo culture fourteen days old (Boutilier et al., 2002).

A *BBM* ortholog was identified and characterized in *Theobroma cacao*. The expression profile showed that it is present at SE and ZE. The overexpression of *BBM* T. sheets causes an increase in cocoa production SE (**Figure 1.2**) but a decrease in conversion to plants (Florez et al., 2015).

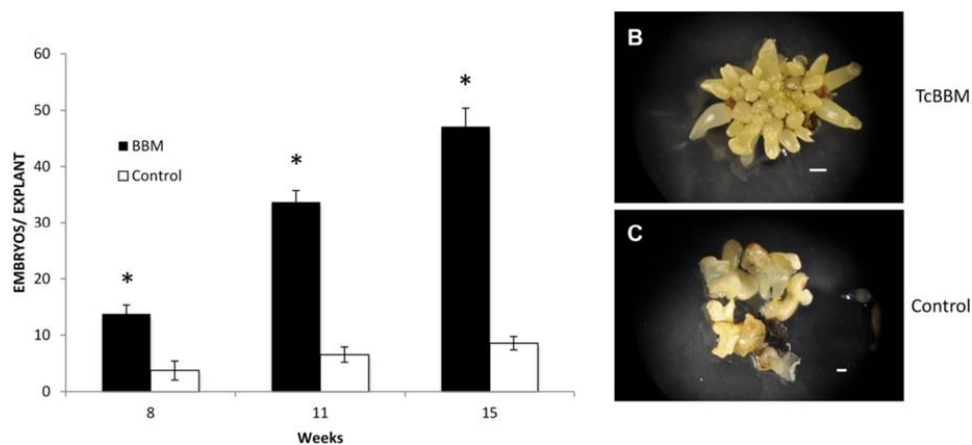


Figure 2 Overexpression of *BBM Theobroma cacao* gene (*TcBBM*) induces an increase in the SE. A, number of embryos produced by explant compared to wild type (control). Error bars represent one standard deviation. **B**, embryo production of transgenic plants (*BBM*) and wild type **C** (Florez et al., 2015).

*WOX*s family genes form a family of transcription factors in plants that participate in a wide range of processes. *WOX* genes were first identified as determining cell fate during embryo development and playing important roles in maintaining stem cell niches in the plant (Costanzo et al., 2014). Nowadays, it is known that *WOX1* play an essential role in the formation of lateral organs, while *WOX2* is active during the formation of embryogenic cells (Van der Graaff et al., 2009). Besides, *WOX3* promotes cell proliferation, and lateral organ formation (Van der Graaff et al., 2009) whereas *WUSCHEL* (*WUS*) is expressed in the apical meristem organization's center to regulates meristem stem cells (Van der Graaff, 2009). Among *WOX* genes the ectopic expression of *WUS* can induce embryogenic callus formation and generate somatic embryos in *A. thaliana*, *tobacco* and *coffee* plants (Arroyo-Herrera et al., 2008).

1.4. Auxin biosynthesis

Auxins control almost all aspects of plant development and their biosynthesis is a crucial process (Paque and Weijers, 2016). IAA, with a structure resembling that of Trp including indole and carboxyl functions, is the predominant auxin form, behaving as a weak organic

acid in aqueous solutions (Friml et al., 2003; Paque and Weijers, 2016). Although auxin concentrations affect cell division, differentiation, phyllotaxis, organogenesis, and embryogenesis, synthesis and polar cell to cell transport play a central role in those effects (Petrasek and Friml, 2009; Cheng et al., 2006; 2007; Grones and Friml, 2015; Paque and Weijers, 2016).

It is of vital importance to know exactly where auxin is synthesized in plants. It has long been held that auxin is synthesized in young developing leaves. However, it is now known that auxin can be synthesized in many different plant tissues (Chandler, 2009). Plants had five biosynthetic pathways to produce IAA, four tryptophan (Trp) dependent, and one Trp independent. Trp synthesis is one of the most complicated amino acids, involving five steps from chorismate (Woodward and Bartel, 2005).

During the last 70 years, several researcher groups have shown in *A. thaliana* that the IAA biosynthetic pathway begins with the amino acid Trp (Stepanova et al., 2011). Five ways can do IAA synthesis; four from Trp-dependent and one Trp-independent pathway:

1. By decarboxylation to produce tryptamine (TAM).
2. To cause oxygenation, Indole-3-acetamide (IAM).
3. By transamination to produce indole-3-pyruvic acid (IPyA).
4. For oxygenation to produce indole-3-acetaldoxime (IAOx) (Woodward and Bartel, 2005).
5. Trp-independent pathway.

The most studied and accepted pathway for auxin biosynthesis is from the Trp-dependent route through two enzymatic steps involved tryptophan aminotransferases of Arabidopsis (TAA) and YUC flavin-containing monooxygenases (FMO) (Zhao, 2014). FMO enzymes are widespread in nature and perform a wide variety of redox reactions, including hydroxylation, reduction, monooxygenation, DNA repair, and cellular signalling (Macheroux et al., 2011). In plants, the YUC protein family belongs to a class of FMO exclusively involved in auxin biosynthesis (Zhao et al., 2001).

Previous studies have demonstrated that plants use Trp as a substrate, which is converted to IPyA as an intermediary for IAA production (Mashiguchi et al., 2011; Zhao, 2014). Enzymes of the TAA family use Trp to catalyze the conversion in IPyA as an intermediary

molecule for IAA biosynthesis (Tao et al., 2008). The following reaction is converting IPyA into IAA catalyzed by members of the YUCs family, which are key enzymes for IAA biosynthesis (Zhao, 2001; Mashiguchi et al., 2011). The IPyA pathway is the first route of IAA biosynthesis and is the most conserved and complete in plants (Zhao, 2014).

Recombinant TAA1 proteins catalyze the conversion of IPyA from Trp *in vitro* (Stepanova et al., 2008). Mutants of the *taa* family showed a significant decrease in IAA and IPyA concentrations. Unlike in the induction of *TAA1*, the concentrations of IAA and IPyA increased endogenously in *Arabidopsis* (Mashiguchi et al., 2011). The family of *TAA* genes plays an important role during the development and growth of plants. Mutations in the *taa* genes cause severe deficiency in auxin in different biological processes, including floral development, lateral root formation, and embryogenesis (Stepanova et al., 2008).

On the other hand, numerous studies have determined the *YUCs* genes' role during plant development (Zhao, 2012); e.g., overexpression of *YUCs* genes causes hypocotyl elongation in *Arabidopsis* (Zhao et al., 2001). In *maize*, it has been reported that mutations in the *yuc* genes cause a reduction of IAA levels affecting the vegetative development (Bernardi et al., 2012). In *Arabidopsis*, there are 11 *YUCs* genes encoding enzymes for IAA biosynthesis. In this model, different studies have been carried out to determine the *YUCs* genes' function during plant development (Cheng et al., 2007). The overexpression of *YUCs* increase the production of IAA in seedlings of *Arabidopsis*; unlike *yuc* mutants in which the expression and content of both IPyA and endogenous IAA decrease drastically (Mashiguchi et al., 2011; Kasahara, 2015).

Cheng et al., (2007) overexpressed the genes *YUC1*, *YUC2*, *YUC4*, and *YUC6*, and their results indicate an increase in the production of auxin in *Arabidopsis* seedlings. Also, they determined the expression of *YUC1* and *YUC4* at the apical meristem and primordia of young leaves (Cheng et al., 2006). It is important to mention that single or double mutants showed no adverse effect, unlike quadruple mutants that caused severe effects on the development of the seedlings (Cheng et al., 2007).

The presence of a second auxin in plants, phenylacetic acid PAA, has been reported, even at levels similar to IAA in plant tissues (Sugawara et al., 2015); however, the physiological activity of PAA is not as marked as IAA (Wightman and Lighty, 1982). It has been

suggested that PAA biosynthesis is carried out through the phenylpyruvate intermediate from the amino acid phenylalanine (Phe) (Sugawara et al., 2015). *In vitro* experiments have shown PAA production through phenylpyruvate by the recombinant enzymes AtYUC6 and AtYUC2 (Dai et al., 2013; Sugawara et al., 2015). However, Cook and colleagues demonstrated that although YUC enzymes can convert PAA *in vitro*, these enzymes are unlikely to act the same way *in vivo* (Cook et al., 2016; Cook, 2019). In *Zea mays* defective endosperm (*de18*) mutants, the enzyme ZmYUC1 results in complete loss of function (Bernardi et al., 2012). Using this mutant, IAA levels were significantly reduced but not endogenous PAA levels in the wild type (Bernardi et al., 2012). These results suggest that ZmYUC1 does not participate in PAA biosynthesis (Cook et al., 2016). In a greater magnitude of triple mutants in *A. thaliana* (*yuc1*, 2, and 6), the PAA content is not affected (Sugawara et al., 2015). But, interestingly, *in vitro*, AtYUC2 and AtYUC6 produce PAA (Dai et al., 2013). Overall, today, it is known that the TAA/YUC pathway is highly conserved throughout the plant kingdom (Stepanova et al., 2011).

Several studies suggest that the Trp-dependent pathway for IAA biosynthesis through *YUC* genes could be determinant for the development of embryogenesis (Nonhebel, 2015). It has been shown that IAA biosynthesis is essential for vascular pattern formation, seedling growth, zygote embryogenesis, and organogenesis (Cheng, 2006; 2016; Stepanova et al., 2008). Also, it has been reported that during embryogenesis, auxin biosynthesis plays a critical role because previous studies have shown that auxin biosynthesis is dynamic during embryogenesis (Ribnicky et al., 2002; Ayil-Gutiérrez et al., 2013). IAA regulates the *de novo* root organogenesis in Arabidopsis (Liu et al., 2014; Xu et al., 2017; Yu et al., 2019). Liu and colleagues reported that endogenous auxin is critical for cell transition. The blockade of auxin transport causes a decrease in auxin concentration, therefore, loss of regeneration of *de novo* organogenesis in Arabidopsis (Liu et al., 2014).

It is important to mention that regeneration responds to detachment or wounding generated to the explant (leaf). In Arabidopsis, *de novo* root organogenesis begins after a wound to the explant in a growth medium without growth regulators in the dark. After 12 hours, the auxin levels significantly increased (Liu et al., 2014; Chen et al., 2016). The *YUC1* and *YUC4* genes are activated quickly after wounding (within 4 hours), suggesting

that these two genes participate in the production of endogenous auxin in leaf explants (Chen et al., 2016).

Production of IPyA-dependent auxin in zygotic *Arabidopsis* embryos has been investigated through the gene expression pattern of *YUC1* to *YUC11* (Mashiguchi et al., 2011; Cheng et al., 2007). Only the *YUC4* and *YUC9* genes were specifically expressed in the suspensor at the early embryogenesis (**Figure 1.3**) (Chen et al., 2007; Robert et al., 2013). Also, double mutations were made (*yuc3+yuc9* and *yuc4+yuc9*). The segregation of the progeny of the double mutations in the *yuc* did not show any defect in its basal expression. However, they produced seedlings with apical defect, number and aberrant form of cotyledons.

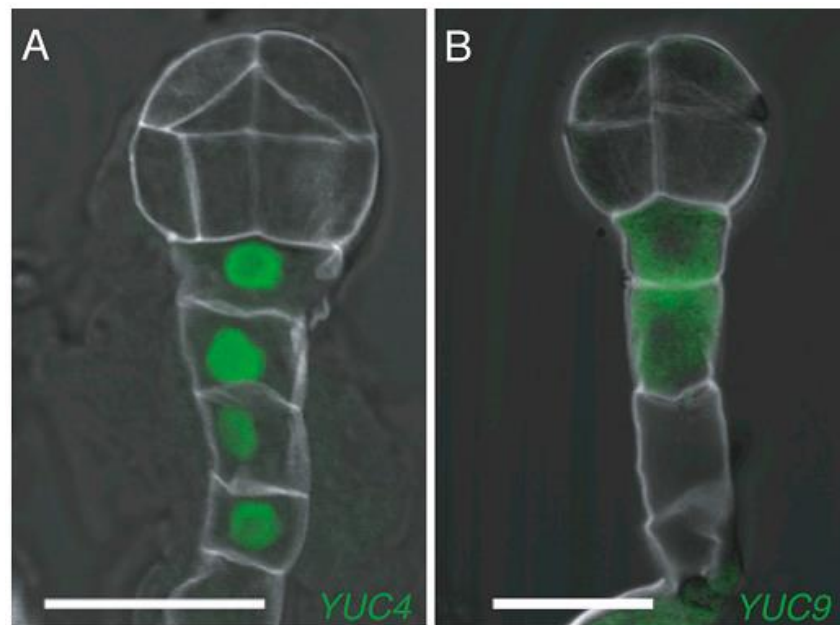


Figure 3 Spatio-temporal distribution of YUC gene expression during the onset development of embryogenesis in *Arabidopsis*. A, *YUC4* and B, *YUC9* are expressed in the suspensor at 16 cell stage (Robert et al., 2013).

Combinations have been made with *taa* and *yucca* mutants causing developmental defects. Quadruple mutants in *yuc1*, *yuc4*, *yuc10*, *yuc11* and triple mutants in *taa1*, *tar1*, and *tar2* causing fail in the development of the basal part of the embryo in *Arabidopsis* (Cheng et al., 2007a; Stepanova et al., 2008).

Studies made in maize with *yuc* and *taa* mutants showed similar results as the obtained in *Arabidopsis*, which indicates that both families of genes are crucial for development and that also participate in the same pathway of IAA biosynthesis in plants (Phillips et al., 2011).

The redundant function of the proteins YUC has been reported. For example, both *YUC1* and *YUC4* are expressed in discrete groups of cells throughout embryogenesis. Their expression patterns overlap with *YUC10* and *YUC11* during embryogenesis (Cheng et al., 2007). On the other hand, single or double mutants do not affect development, unlike the quadruple mutants of *yuc1 yuc4 yuc10 yuc11* fail to develop a hypocotyl and a root meristem (Cheng et al., 2007). Reverse genetics approaches are useful for studying the functionality of YUCs. However, the use of specific inhibitors outweighs the redundant function (Nishimura et al., 2014; Chen et al., 2016).

Our group has shown that the induction of SE in *C. canephora* requires at least one exogenous auxin before or during the process (Ayil-Gutierrez et al., 2013). Exogenous auxin (1-naphthaleneacetic acid NAA) appears to be essential for the induction of SE. In leaf explants of *C. canephora*, the exogenous auxin NAA induces the biosynthesis of endogenous IAA accompanied by the expression of genes of the *YUC* family during the process of induction of the SE (Ayil-Gutierrez et al., 2013).

The exogenous addition of auxin causes an increase in the endogenous concentration in cell suspensions of *Daucus carota* (Michalczyk et al., 1992). In *Medicago falcata*, the SE induction process is related to increased endogenous auxin concentration (Ivanova et al., 1994). Therefore, it seems that an increase in endogenous auxin content is crucial to turn on the SE induction mechanism (Ayil-Gutierrez et al., 2013). In *C. canephora* and other plant species, the exogenous addition of auxin or a ratio of auxin and cytokinins is required for the induction of SE (Quiroz-Figueroa et al., 2006).

Our protocol used young leaves of *C. canephora* seedlings *in vitro*, incubated in a solid medium Murashige and Skoog (MS) supplemented with NAA and kinetin (Kin) for 14 days in the dark (pre-treatment). Then, the SE is induced in a liquid medium Yasuda with 6-benzyladenine (BA) 5 μ M in darkness (Quiroz-Figueroa et al., 2006).

The expression of the *YUC1* gene increases in the pre-treatment period and its expression was maintained until day 21 after the induction of SE in *C. canephora* (Ayil-Gutierrez et al., 2013), suggesting that the increase in auxin content is *de novo* biosynthesis and this is essential for the beginning of the SE.

The above mentioned indicates that the machinery of auxin biosynthesis through the *YUCs* genes is crucial at the beginning of the proembryo and necessary for developing the embryo structures (Robert et al., 2013). Besides, IAA biosynthesis, polar transport, and conjugation mechanisms are factors that regulate the homeostasis of IAA for the control of the regulation of the SE (Ayil-Gutierrez et al., 2013). SE is a complex biological process that involves many factors, and the biosynthesis of IAA is only one part. It has been observed that *mir160* and *mir165/mir166* regulate auxin biosynthesis through *YUC* via *LEC2* during the SE in *Arabidopsis* (Wójcik et al., 2017). Also, it is suggested that low concentrations of ethylene can activate the auxin biosynthesis during the SE induction process (Bai et al., 2013).

Despite the great effort that scientific research has provided a clearer picture in the last decade of the enzymes involved in auxin biosynthesis, several questions regarding this process's biochemical mechanisms and subcellular localization have not been elucidated. There are few reported studies in maize and *Arabidopsis* of auxin biosynthetic activity can be found in microsomal fractions (Kriechbaumer et al., 2015; 2016), and some of auxin biosynthetic proteins showed endoplasmic reticulum (ER)-localization, due to transmembrane helix (TMH) (Kriechbaumer et al., 2016). Eleven members of the *AtYUCs* family have been found to exist in *A. thaliana*, of which *AtYUC4.2* is a splice variant located on the ER in flower (Kriechbaumer et al., 2012). Similarly, *AtYUC5*, *AtYUC8*, and *AtYUC9* were localized in the ER of the root, the rest of the *AtYUC* proteins in the cytosol (Poulet and Kriechbaumer, 2017).

There are still many unresolved questions on the subject of auxin biosynthesis and how it impacts its homeostasis regulation during the development of the SE. Although several models propose the mechanisms of auxin biosynthesis, we still need to understand how it is regulated at the transcriptional level, protein, and epigenetic level.

1.5. Yucasin: a powerful inhibitor of the activity of YUCCA enzymes

Trp is initially converted by TAA to produce IPyA, which is then oxidized to IAA by YUC proteins (Zhao et al., 2001). Previous studies suggest IPyA as a substrate for YUC proteins (Stepanova et al., 2008; Tao et al., 2008). A biochemical study of YUC6 showed that YUC catalyzes the oxidative decarboxylation of IPyA (Dai et al., 2013). Mutations of *yucs* gene family may not affect IAA content or phenotype, due to the functional redundancies of *YUCs* family members (Zhao, 2014). This makes it difficult to analyze and understand the function of auxin and IAA biosynthesis pathway using genetic approaches. The use of chemical components is a powerful strategy that employs small molecules as probes to dissect biological processes (Dejonghe and Russinova, 2014).

These small chemicals can be applied to any tissue and at any time in the plant life cycle, using the appropriate concentrations, to interfere with protein function (Kakei et al., 2015; 2017). Therefore, pharmacological approaches using small inhibitory molecules result in advantageous in studying essential functions and tissue specificity of target molecules. These small inhibitory molecules can be applied to analyze various vegetables and crops (Kakei et al., 2015). In this manner, pharmacology is a remarkably useful approach to analyze the growth and development of plants, including SE.

Various inhibitory have been used to study auxin metabolism. For example, the 1-naphthylphthalamic acid (NPA) acts as a specific IAA efflux inhibitor (Nagashima et al., 2008), and another small molecule, L -kynurenine (Kyn), has been identified as a potent auxin biosynthesis inhibitor that targets TAA1 (He et al., 2011). Another inhibitor is 5-(4-chlorophenyl)-4H-1,2,4 -triazole-3-thiol, also known yucasin, an IAA biosynthesis inhibitor, targets the YUC enzyme. The compound was identified as the most potent inhibitor of IAA biosynthesis during a chemical library's screens using an *in vivo* system with maize coleoptiles (Nishimura et al., 2014). It has been shown that yucasin strongly inhibited the enzymatic activity of recombinant AtYUC1-His *in vitro* and also yucasin inhibits a wide range of YUC proteins in Arabidopsis (Nishimura et al., 2014).

On the other hand, treatments with 200 μ M of yucasin affected the free IAA content and blocked *de novo* root organogenesis in Arabidopsis leaf (Chen et al., 2016). It has been suggested that yucasin is a substrate analogue of FMO and functions as a competitive

inhibitor of YUC1, with a higher binding affinity than the substrate IPyA. The thiol group of yucasin may be important for its interaction with YUC (Nishimura et al., 2014). Thus, yucasin offers a useful tool to determine the mechanisms of IAA biosynthesis via the YUC protein and to identify uncharacterized proteins involved in IAA biosynthesis during the SE induction process.

1.6 Auxin transport

The concentration of auxin is variable in all the plant tissues, being young leaves the best source of synthesized auxin. Unequal distribution is crucial for the correct development (Paque and Weijers, 2016).

IAA's homeostasis and distribution depend on several factors, such as biosynthesis, conjugation, and transport. The free IAA is responsible for performing the physiological functions in the plant but must be transported from cell to cell to perform the physiological functions, and for this to happen, the formation of a concentration gradient of IAA is necessary (Benková et al., 2003). The auxin concentration gradient is carried out by transmembrane transporters that regulate their flux for the control of many development processes, including embryogenesis, vascular formation, lateral organ development, and tropism (Naramoto, 2017; Krecek et al., 2009).

The IAA auxin, being a weak acid in its protonated form under physiological pH conditions, can freely cross the cells' plasma membrane. However, once inside the cell, the IAA is deprotonated, acquiring charge; therefore, it can no longer cross the plasma membrane; it needs auxin-specific carriers (Swarup et al., 2005; Grones and Friml, 2015). The transport of IAA through the cells is unidirectional and involves energy consumption in the form of ATP. This transport occurs in the basipetal form in stems and roots. Although in roots, the transport can be in both directions, acropetal at the central cylinder and basipetal at the epidermis (Rashotte et al., 2003).

Although the IAA indole group's hydrophobic nature allows the association with the plasma membrane, the negative charge of the carboxyl group dissociated with the molecule prevents it from crossing the plasma membrane. Therefore, the IAA can no longer move passively and requires outbound specific carriers such as PIN (pin-formed) and ABCB

(ATP-binding cassette protein subfamily B) carrier. Therefore, the auxin output of the cell is ultimately an active process dependent on energy (Kleine et al., 2009).

After being synthesized, the IAA must be transported polarly towards the root parenchyma cells through associated vascular tissue and the xylem and phloem; however, flow from cell to cell of IAA is polar. Polar auxin transport is a complex process regulated by the action of proteins such as AUX1, PIN, and ABCB (Rashotte et al., 2003). In *A. thaliana*, the PIN family is composed of eight integral membrane proteins is divided into two subclasses, according to the length of the hydrophobic domain (Zazimalová et al., 2007). The polar location of the PINs is important for the development of the embryo, organogenesis, tropism, among other development processes (Zazimalová et al., 2010).

On the other hand, the superfamily ABCB is one of the largest and the best known and studied. Several studies indicate that transporters ABCB1 and ABCB19 are involved in transporting auxins in plants and play a crucial role during plant growth and development (Tusnady et al., 2006). In *A. thaliana*, it has been reported that the PIN and ABCB proteins are involved in the transport of IAA. The ABCB proteins need energy in the form of ATP to transport the IAA from cell to cell (Rashotte et al., 2003). The importance of cooperation between these transporters (PIN and ABCB) seems to be buffering when the levels of auxin synthesis change or when the conjugations are induced (Weijers et al., 2005).

The function of the auxin transporters in the plasma membrane is to carry out a quick transport of the auxin with a specific direction established by the auxin gradient for the development of the plant and also the development of embryogenesis (Zazimalová et al., 2010; Nishimura et al., 2012).

During embryogenesis, all-important structural features of the plant body are established. Studies on the ZE in *A. thaliana* showed that during the development process are involved PIN1, PIN4, and PIN7 auxin efflux carriers (Petrasek et al., 2011). In the same study reported that PIN1 is responsible for the distribution of auxin during proembryo formation. It has been shown that ABCB1 as ABCB19 contributes to the auxin efflux during the proembryo development stage. While ABCB1 is found in all cells and suspensor cells proembryo, ABCB19 is restricted to the proembryo forming cells (Petrasek et al., 2011).

During the globular stage, PIN1 is located in the apical part with PIN4. During this stage, the flow of auxin, which until then had been acropetal, now goes to basipetal, the apical part to the hypophysis is reversed. To complete this flow, the polarity of PIN7 is shifted from apical to basal localization in the uppermost suspensor cells by the endocytic recycling process (Petrasek et al., 2011). At this moment, apical to the basal polarity of auxin flow is established. Thus, a maximum concentration of auxin in the cells to be future cotyledons well as hypophysis occurs. Auxin transport to the hypophysis, as well as to the formation of the cotyledons, is carried out by PIN1 (**Figure 1.4**) (Michniewicz et al., 2007).

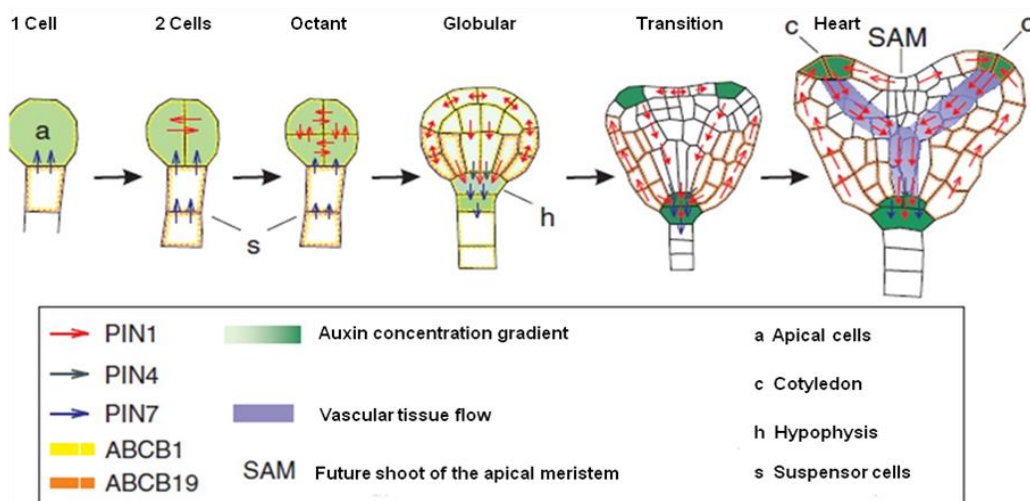


Figure 4 Auxin transport during embryogenesis in *A. thaliana*. Auxin efflux during the different stages of embryonic development using as a model the zygotic embryogenesis in *A. thaliana* mediated by transporters PIN and ABCB type (Petrasek and Friml, 2009).

Great numbers of experiments provide evidence of the importance of membrane dynamism in PINs' polar location (Naramoto, 2017; Oochi et al., 2019). Although PINs may be anchored in the plasma membrane's polar domain, it has been proposed that PINs continuously undergo recycling between the plasma membrane and endosomal compartments, fulfilling functions of regulation of the polar location of the PINs (Tanaka et al., 2013). This dynamism has seen changes in response to environmental signals or during the development of the plant (Naramoto, 2017; Adamows and Frim, 2015).

Besides, the subcellular traffic of PINs' is highly regulated. Previously, it was thought that the activity of the phosphatase PPA2 mediated the change of direction of auxin flow during embryogenic development. PPA2, together with a PID protein kinase, regulate the polar

transport orientation of auxins (Furutani et al., 2004; Michniewicz et al., 2007). However, recent research has shown that phosphorylation of PINs does indeed regulate the flow of auxin (Weller et al., 2017).

PINs are phosphorylated by a protein kinase family (D6PK) and PINOID proteins (PID) (Zourelidou et al., 2009; 2014). D6PK is located at the basal part of the plasmatic membrane and regulates the auxin efflux activity of the basally localized PINs (Zourelidou et al., 2009; 2014). Unlike PIN, that is located in the plasma membrane and regulates both the flow and the PINs (Weller et al., 2017). The localization of D6PK is regulated by the level of auxin and the composition of the phospholipids of the plasma membrane (Barbosa et al., 2014; 2018). Similarly to D6PK, the PIN is also regulated by phospholipids' composition (Jia et al., 2016). Another key element is the mitogen-activated protein kinase (MAPK/MPK); it also regulates auxin flow activity by phosphorylation of the PINs (Jia et al., 2016). These findings suggest a complex system of regulation of the PIN proteins that coordinate the auxin polar transport and its location in the plasma membrane .

In summary, plant cells display distinct developmental plasticity and the process of SE well illustrates this unique phenomenon. During onset SE, somatic cells undergo numerous molecular changes, followed by induction of a new embryonic pathway of development (Zimmerman, 1993). Most frequently, SE is induced *in vitro* under an appropriate growth regulators environment applied to cultured somatic cells or tissue (Jimenez 2001), and the induction phase seems to be the most intriguing in terms of the genetic control of the embryogenic transition. Early molecular events provide a critical step for SE initiation, and thus for the identification of key genes determining the SE-induction phase. The expression of transcription factors is auxin-dependent upregulation and found to be associated with the induction phase of SE. Auxin biosynthesis is one of the first key events and is carried out by *YUC* genes that encode enzymes involved in IAA auxin biosynthesis (Zhao, 2014). As mentioned earlier in this Chapter I, auxin controls various processes of growth and development. But, to exert its function, auxin must be transported through PIN (Petrasek et al., 2011) and ABCB (Tusnady et al., 2006) type proteins for signal translation [activation of *BBM*, *WOX* and *LEC* genes) allowing that somatic cells are converted into embryonic cells (Boutilier et al., 2002; Van der Graaff et al., 2009; Guo et al. 2013; Costanzo

et al., 2014). Knowledge of these genes has high practical utility in plant biotechnology, and for the improvement of somatic embryo production in recalcitrant plants.

Therefore, the question to be addressed in this project is:

Does the IAA biosynthesis is mediated by the YUC enzymes during the SE induction process in *C. canephora*?

HYPOTHESIS

YUC enzymes are involved on the auxin-dependent somatic embryogenesis in *C. canephora*.

GENERAL OBJECTIVE

To evaluate if YUC enzymes mediate IAA biosynthesis during the SE induction process in *C. canephora*.

SPECIFIC OBJECTIVES

1. To Identify, analysis, modeling and docking molecular of YUC protein family in Genome-wide of *Coffea canephora*.
2. Histology analysis of SE induction process.
3. To determine the profile expression of *YUC* genes by qRT-PCR during the SE induction process.
4. To evaluate the effect of the yucasin inhibitor during of SE induction process.
5. To determine the localization and distribution of IAA in the coffee explants during SE induction process.

JUSTIFICATION

SE is a biological process in which a series of morphological, biochemical, and molecular events leads to the formation of the somatic embryo, with auxin playing a central role in it. However, molecular mechanisms regulating auxin biosynthesis during SE induction remains only partially understood. Hence, approaching the mechanisms of auxin

biosynthesis during these events will allow us a deeper insight into the basic biology process of SE opening future possibilities for biotechnological applications in crop improvement.

EXPERIMENTAL STRATEGY

In this section, the overall experimental strategy is described. First, candidates to *YUC* gene family members were identified by bioinformatic analysis of the *C. canephora* genome (Denoeud et al., 2014). In parallel, induction of somatic embryogenesis was performed *in vitro* by exposing *C. canephora* seedlings to pre-treatment with Kin and NAA, simultaneously with Yucasin, an inhibitor of the YUC protein function, for 14 days. After seedling pretreatment, leaf sections were used as explant for induction of SE in Yasuda medium containing BA. Tissue samples were collected every 7 days throughout 28 days after induction. The collected tissues were used for the analysis of expression the six *CcYUC* genes retrieved by bioinformatics, as well as for IAA localization and quantification (Figure 1.5).

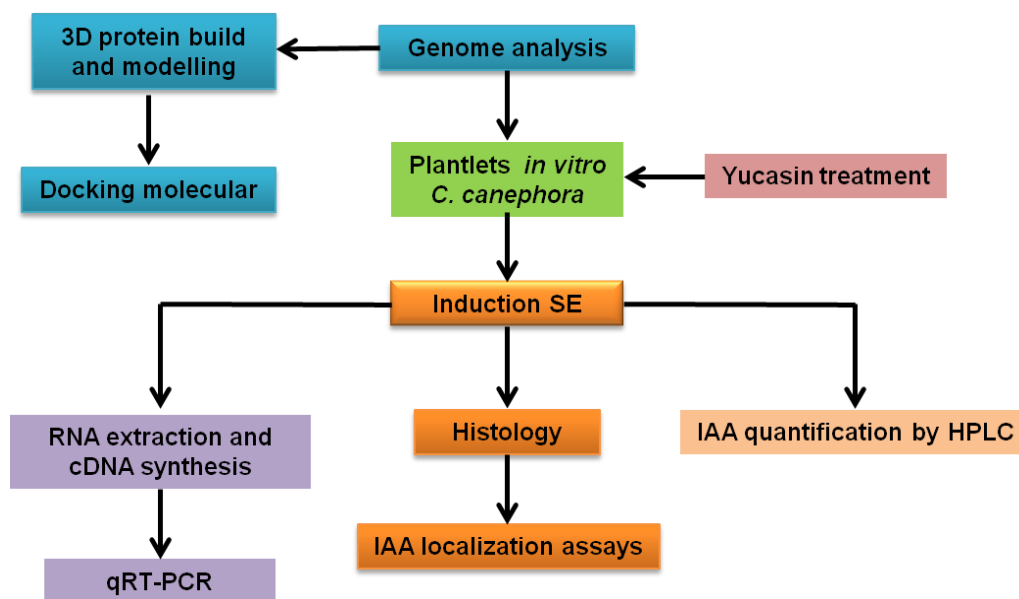


Figure 1.5 General diagram of the workflow carried out in this job.

As a first point, the bioinformatic analysis (blue). The second point, *in vitro* plantlets (green) and the inhibitor treatment (Brown), were used; then qRT-PCR analysis (purple); followed by the induction of SE, histology, localization (orange) and quantification of IAA (pink).

CHAPTER II



International Journal of
Molecular Sciences



Article

YUCCA-mediated biosynthesis of the auxin IAA is required during the somatic embryogenic induction process in *Coffea canephora*

¹Miguel A. Uc-Chuc, ¹Cleyre Pérez-Hernández, ¹Rosa María Galaz-Ávalos, ¹Ligia Brito-Argáez, ²Victor Aguilar-Hernández, ¹Víctor M. Loyola-Vargas*

¹Unidad de Bioquímica y Biología Molecular de Plantas. Centro de Investigación Científica de Yucatán, A.C. Calle 43 No. 130 x 32 y 34 Colonia Chuburná de Hidalgo CP. 97205 Mérida, Yucatán, México

²Catedrático CONACYT, Unidad de Bioquímica y Biología Molecular de Plantas, Centro de Investigación Científica de Yucatán, Mérida, México.

* Correspondence: vmloyola@cicy.mx (V.M.L.V.)

Article published: 3 July 2020. Int. J. Mol. Sci. 21, 4751; doi:10.3390/ijms21134751

Abstract: Despite the existence of considerable research on somatic embryogenesis (SE), the molecular mechanism that regulates the biosynthesis of auxins during the SE induction process remains unknown. Indole-3-acetic acid (IAA) is an auxin that is synthesized, in plants, through five pathways. The biosynthetic pathway more frequently used in this synthesis is the conversion of tryptophan to indol-3-pyruvic acid (IPyA) by tryptophan aminotransferase of *Arabidopsis* (TAA) followed by the conversion of IPyA to IAA by enzymes encoded by *YUCCA* (*YUC*) genes of the flavin monooxygenase family; however, it is unclear whether *YUC*-mediated IAA biosynthesis is involved in SE induction. In this study, we report that the increase of IAA observed during SE pre-treatment (plants in MS medium supplemented with 1-naphthaleneacetic acid (NAA) 0.54 μ M and kinetin (Kin) 2.32 μ M for 14 days) is due to its *de novo* biosynthesis. By qRT-PCR, we demonstrated that *YUC* gene expression is consistent with the free IAA signal found in the explants during the induction of SE. In addition, the use of yucasin, to inhibit the activity of *YUC* enzymes, reduces the signal of free IAA in the leaf explants and dramatically decreases the induction of SE. The exogenous addition of IAA restores the SE process in explants treated with yucasin. Our findings suggest that the biosynthesis

and the localization of IAA play an essential role during the induction process of the SE in *Coffea canephora*.

Keywords: auxin; *Coffea canephora*; localization; somatic embryogenesis; YUCCA; yucasin.

2.1 Introduction

Plants, unlike animals, have a high capacity for regeneration of new individuals identical to the mother from a cell or groups of cells without the need for fertilization. This regeneration mechanism is known as somatic embryogenesis (SE) (Vogel, 2005; Nic-Can et al., 2013). SE is the development of structures similar to a zygotic embryo from somatic cells (Tvorogova et al., 2019; Loyola-Vargas and Ochoa-Alejo, 2016). It can also be the process by which somatic cells, under induction conditions, generate competent cells that undergo a series of morphological, biochemical, and molecular changes to give rise to somatic embryos without the fusion of gametes (Quiroz-Figueroa et al., 2006). SE provides an invaluable tool for the genetic improvement of plant species that cannot be propagated sexually (Ma et al., 2015).

The study of the biochemical and molecular mechanisms of SE allows us to identify the factors involved during the induction process of the somatic embryo (Ma et al., 2015) and determine how best to apply them to the genetic improvement of a range of plant species (Ma et al., 2015; Santana-Buzzy et al., 2004). Furthermore, SE is an example of totipotency because the somatic cells respond directly to a stimulus leading to the development and formation of the somatic embryo. Therefore, SE is an excellent system for the study of cellular differentiation and dedifferentiation (Magnani et al., 2017).

SE is a complex process that involves many factors including, plant species, tissue type (explant), culture medium, exogenous growth regulators and changes in endogenous growth regulators, and nitrogen and carbon source (Nic-Can et al., 2013; Quiroz-Figueroa et al., 2001; Fuentes-Cerda et al., 2001). In addition, somatic cells can activate the genetic machinery necessary for the transcription of genes involved in SE induction (Quiroz-Figueroa et al., 2002), implicating the alteration of cell wall composition and changes in

growth regulators, genetic expression and epigenetic regulations in this process (De-la-Peña et al., 2015).

It has been proposed that plant growth regulators, mainly indole-3-acetic acid (IAA), play a crucial role in mediating the signal transduction that leads to the reprogramming of gene expression. This change is followed by a series of cell divisions that induce disorganized growth (callus) or lead to direct SE (Dudits et al., 1991). IAA is a molecule that controls almost all aspects of plant growth and development (Tsugafune et al., 2017). Its biosynthesis is crucial for plant homeostasis, including embryo development, fruit ripening, organogenesis, and plant architecture (Nonhebe, 2015; Paque and Weijers, 2016). However, the action of auxin is determined by its synthesis and distribution in tissue, mainly by its polar transport from cell to cell (Petrášek and Friml, 2009; Peer et al., 2011).

The route most conserved and providing the most direct way to produce IAA in plants is from tryptophan via two enzymatic reactions consisting of TRYPTOPHAN AMINOTRANSFERASE OF ARABIDOPSIS (TAA) and YUC flavin monooxygenase of the indole-3-pyruvic acid (IPyA) pathway (Tsugafune et al., 2017; Zhao et al., 2001; Mashiguchi et al., 2011).

Genetic studies have demonstrated that YUC functions as the rate-limiting step of the IPyA pathway, indicating that YUC plays a crucial role in developmental processes regulated by cellular IAA levels (Tsugafune et al., 2017). Biochemical and molecular studies have shown that these gene families (TAA and YUC) participate in the pathway of IAA biosynthesis in several plant species including *Arabidopsis thaliana*, *Zea mays* and *Oryza sativa* (Zhao, 2014; Brumo et al., 2014). It has been reported that IAA biosynthesis through YUC is necessary for the establishment of the basal part of the embryo and onset of embryonic organs (Cheng et al., 2017). Previous findings indicated that the location of auxin biosynthesis plays an essential role in many growth and development processes, including embryogenesis (Zhao, 2010).

Cheng et al., (2006) overexpressed *YUC1*, *YUC2*, *YUC4*, and *YUC6* genes, and their results indicate an increase in the production of auxin in *Arabidopsis* seedlings. Also, they determined the expression of *YUC1* and *YUC4* at the apical meristem and primordia of young leaves (Cheng et al., 2006; 2007). Single or double mutants showed no adverse

effect, unlike quadruple mutants that caused severe effects on the development of the seedlings (Cheng et al., 2007). Accordingly, due to redundant functions of the *YUC* genes family, it is difficult to access reverse genetic approaches to understand the physiological role of IAA biosynthesis (Tsugafune et al., 2017). Hence, the use of specific inhibitors to overcome the redundant activity of target genes has emerged as a useful tool for genetic studies (Tsugafune et al., 2017).

Despite the various studies in this area, the genes regulating IAA auxin biosynthesis during embryogenesis are not known (Cheng et al., 2007), and endogenous intracellular levels remain unclear during SE induction process. There the possibility that de novo IAA biosynthesis plays an essential role in the SE because previous reports have shown that auxin biosynthesis is dynamic during embryogenesis (Ribnicky et al., 2002).

Our primary goal in this work was to determine whether the YUC-mediated IAA biosynthesis is involved during the SE induction process in *Coffea canephora*. To solve it, we used qRT-PCR to measure the transcript levels of *CcYUC* and used a specific yucasin inhibitor to block the biosynthesis of the auxin IAA. Yucasin is a powerful specific YUC enzyme inhibitor (Nishimura et al., 2014).

In this study, we found that *CcYUC1*, *CcYUC1-putative*, *CcYUC4*, and *CcYUC-Like* have dynamic expression patterns at the moment of the induction of the SE process. We showed that there exists a correlation between the *CcYUC* expression pattern and the location of the free IAA auxin signal at the beginning of the induction of the SE process. Furthermore, the formation of a local endogenous IAA gradient in specific tissues was crucial during the SE induction process in *C. canephora*. On the other hand, treatment with yucasin inhibited SE, but exogenous IAA addition restored the embryogenic process. Our data show that the YUC-mediated IAA biosynthesis is crucial for SE in *C. canephora*.

2.2 Materials and methods

2.2.1 Plant material and growth conditions

C. canephora plantlets were propagated and maintained under in vitro photoperiod conditions 16/8 h ($150 \mu\text{mol m}^{-2} \text{s}^{-1}$) at $25 \pm 2 \text{ }^\circ\text{C}$ in MS inorganic culture medium [(Murashige and Skoog, 1962), Phyto Technology Laboratories, M524]. The MS medium contains $29.6 \mu\text{M}$ thiamine-HCl (Sigma, T3902), $550 \mu\text{M}$ myo-inositol (Sigma, I5125), $0.15 \mu\text{M}$ L-cysteine hydrochloride hydrate (Sigma, C8277), $16.24 \mu\text{M}$ nicotinic acid (Sigma, N4126), 87.64 mM sucrose and 0.25% (w/v) CultureGel TM Type I-Bio Tech Grade (Phyto Technology Laboratories, G434), pH 5.8. Plantlets were subcultured every 6 weeks by in vitro transplantation of shoot intermodal segments to fresh maintenance media.

2.2.2 Induction of somatic embryogenesis in *C. canephora*

For the induction of SE, we started with four-month-old plantlets of *C. canephora* cultured *in vitro* conditions. A batch of plantlets was selected and placed in a semisolid medium for pre-treatment. The culture medium was MS medium, supplemented with $0.54 \mu\text{M}$ NAA (Sigma N1145) and $2.32 \mu\text{M}$ Kin (Sigma K0753-5G), for fourteen days under photoperiod conditions (16 h light/8 h dark) at $25 \pm 2 \text{ }^\circ\text{C}$. For the induction of SE, leaves two and three were used. The explants were cut into circles of approximately 0.25 cm in diameter and transferred to Yasuda liquid medium (Yasuda *et al.*, 1985) supplemented with $5 \mu\text{M}$ BA (Phyto Technology Laboratories, B800). The cultures were incubated in the dark at $25 \pm 2 \text{ }^\circ\text{C}$ and shaking (100 rpm) for 56 days (Quiroz-Figueroa *et al.*, 2006). Samples were taken 0, 7, 14, 21 and 28 days after induction (dai) of SE.

2.2.3 Extraction of auxins and their conjugates

For the extraction of auxins and their conjugates, 100 mg of tissue was used from days -14, -9, -4 of pre-treatment; on day 0 of the induction of SE and 0.02, 0.04, 1, 7, 14 and 21 days after the induction of SE. The samples were stored at $-81 \text{ }^\circ\text{C}$ until use. The frozen tissue was ground with liquid nitrogen and mixed with one ml of acidic water (the pH was adjusted to 2.8 with HCl). The mixture was transferred to a test tube with an additional ml of acidic water. The mixture was stirred for one min with one ml of a solution of butylated hydroxytoluene (Acros Organics 112992500), and then one ml of ethyl acetate (CTR

Scientific 00184) was added. The mixture was stirred for one min and the supernatant recovered. Then 2 ml of ethyl acetate was added, stirred for one min, and the supernatant was recovered. This operation was repeated once more. From this mixture, 3 ml of the organic phase was taken and evaporated with nitrogen gas. The dried sample was resuspended in one mL of the mobile phase, filtered through a Millipore filter (0.22 μM) and analyzed using high-resolution liquid chromatography (HPLC) (60% acetonitrile; JT Baker 9017-03: 40% water containing 0.5% (v/v) acetic acid; CTR Scientific 00500). The standards used were IAA (I1250, Sigma) and IAA-Ala (345911, Sigma). Preparation of IAA-Glu, IAA-Leu, IAA-Asp was previously reported (Ayil-Gutiérrez *et al.*, 2013; Rodríguez-Sanz *et al.*, 2014).

2.2.4 High performance liquid chromatography

For the analysis of the samples, an Agilent Technologies 1200 high-resolution liquid chromatograph (HPLC) consisting of a quaternary array of pumps (Agilent Technologies G1311A) connected to an automatic injector (Agilent Technologies G1329A) was used. 20 μL of the tissue extract was injected and subjected to chromatography with an isocratic elution system with a flow rate of 0.6 mL min⁻¹ in a C18 reverse-phase column (Phenomenex) of 250 mm x 4.6 mm. The samples were analyzed with a fluorescence detector (Agilent Technologies G1321A) at an emission length of 280 nm and an excitation length of 340 nm. The presence of compounds in the analyzed samples was determined by the retention times of IAA and of IAA-Ala, IAA-Leu, IAA-Glu, and IAA-Asp conjugates (Figures S1, S2 and S3), for which co-injections of the standards and the samples were analyzed, to determine if they coelute. The calibration curves were performed with free IAA and the conjugate standards using the area under each curve for each compound.

2.2.5 Liquid chromatography mass spectrometry of auxins

LC-MS/MS analysis was performed using a Thermo LTQ Orbitrap, equipped with a heated-electrospray ionization (HESI-II) source with sheath gas set to 60, auxiliary gas set to 20, source temperature set to 310 °C, and spray voltage 4 kV in a positive mode. To determine the chemical fragmentation of auxins, a solution of an individual auxin at a concentration of 100 $\mu\text{g mL}^{-1}$ in methanol:water (80:20; v/v) was directly infused on LTQ Orbitrap at 5 $\mu\text{L min}^{-1}$. The collision energy dissociation (CID) parameter for auxins was

optimized to yield either parent ion-dependent product ions (M+H)⁺ and nearly 20% of the parent ion. Chromatographic separations were performed using a reverse-phase ZORBAX Eclipse XDB C18 (150 x 4.6 mm i.d., 5 μm particle size, 80 Å pore size) column (Agilent Technologies, G1321A). A gradient of 0.1% formic acid in water (solvent A) and 0.1% formic acid in acetonitrile (solvent B) was used during LC separations. A flow rate of 0.3 mL min⁻¹ was used, and the injection volume was 2 μL. The gradient program was 5% B at 0 min, to 20% B at 20 min, to 30% at 32 min, to 80% at 34 min, to 100% at 36 min, kept at 100% for 2 min and then to 5% at 40 min and kept at 5% for 6 min. Retention time and spectra were processed with raw Xcalibur data files.

2.2.6 Preparation of seedlings in the presence of 3-¹⁴C-Trp

Seedlings were incubated in the presence of 3-¹⁴C-Trp (NEN-Dupond; 1.85 MBq 55 mC mmol⁻¹) during the 14 days of pre-treatment in MS liquid medium supplemented with NAA 0.54 μM and Kin 2.32 μM. Auxins were isolated on days -14, -9, -7, -4 and 0 of pre-treatment. To monitor the incorporation of labelled Trp into the IAA, the auxinic extract was run on a silica TLC plate with an alumina fluorescent indicator Kieselgel 60 F254 (Merck, 105554). Five μL of the leaf extract incubated with 3-¹⁴C-Trp and 5 μL of the Trp standards (0.25 μL; Sigma, T0254, 1G), indol-3-pyruvic acid (IPyA, 1 μL; Sigma, L7017-1G) and IAA (0.25 μL; Sigma 45533-250 mg) were applied to the plates. The samples were run for 3 cm using a mixture of chloroform:ethyl acetate (50:50) as the mobile phase and Salkowski reagent was used as a developer. Bands were identified by the R_f of the compounds. The silica of each band was scraped, deposited in vials with scintillation liquid, and the radioactivity of each was quantified in a scintillation counter (Beckman 6500).

To track the destiny of all of the radioactivity used, we used the following protocol. Once the auxins were extracted from pre-treatment seedlings that were incubated in the presence of 3-¹⁴C-Trp, 5 μL of the total of 100 μL of the leaf extract was placed on a chromatographic plate, as well as Trp, IPyA, and IAA standards. The spots were developed with the Salkowski reagent (stain compounds containing an indole group). Each spot on the plate was associated with the corresponding standards. Each spot was scraped off the plate and placed in a scintillation vial to count the radioactivity present. In order to be certain that there were no radioactive compounds outside those marked by the

developer, the areas between the spots were cut, and the radioactivity was determined. No radioactive label was detected in any case.

2.2.7 Yucasin inhibition assay

Yucasin, an inhibitor of the YUC protein function in the auxin biogenesis pathway, [5-(4-chlorophenyl)-4H-1, 2, 4-triazole-3-thiol (Santa Cruz Biotechnology, 233161)] was added to the pre-treatment semisolid medium at concentrations of 5, 10, 20, 50 and 100 μM for fourteen days under dark conditions. Leaf explants of *C. canephora* plantlets treated with yucasin were transferred to the SE induction medium (Quiroz-Figueroa, 2006). Yucasin was dissolved in dimethyl sulfoxide (DMSO, Sigma, D8418) and IAA was dissolved in EtOH (J. T. Baker). As a control DMSO was added to the semisolid pre-treatment medium. The experiments were performed in biological triplicate. The effect of the different concentrations of the yucasin was analyzed by quantifying the number of embryos formed after 56 days.

2.2.8 Plant tissue sampling

The plant tissue samples were collected at different times from day zero (D0), seven (D7), fourteen (D14), twenty-one (D21) and twenty-eight (D28). Samples collected 0, 7, 14, 21 and 28 dai of SE were used for performing immunolocalization assays. Day -14 (at the beginning of the pre-treatment), 0, 7, 14, 21 and 28 dai were used for the analysis of quantitative genetic expression.

2.2.9 Real-time quantitative analysis of gene expression

The total RNA extraction was performed following the manufacture instructions for TRI reagent (Sigma, 93298). 100 mg of plant tissue was used for RNA extraction. The integrity and purity of the RNA were evaluated by 1% agarose electrophoresis and spectrophotometry (NanoDrop 2000, Thermo Scientific). Five mg of total RNA was used for cDNA complementary DNA synthesis using a SuperScript II reverse transcriptase kit (Invitrogen) following the manufacturer's protocol. Quantification of gene expressions by qRT-PCR was carried out with Applied Biosystems equipment using the Step One program. The Coffee Genome Hub page was consulted (<http://coffee-genome.org/>) and the genome database of *C. canephora* was downloaded for the design of specific primers

described in table 4.1 to analyze the *CcYUCs* genes. With the support of the *C. canephora* transcriptome (Quintana-Escobar et al., 2019), an analysis was carried out to determine which genes could be the main participants during the induction process of SE. After identifying the *CcYUCs* candidate genes, the coding sequences (CDS) of the specific genes were downloaded and the design of the primers was carried out in the Primer3plus program (<http://www.bioinformatics.nl/cgi-bin/primer3plus/primer3plus.cgi/>). The primers for each gene were tested by an in-situ PCR in Sol Genomics (<http://solgenomics.net/>).

2.3.0 Histological analyses

The plant tissues were fixed in FAA solution [10% formaldehyde (Fischer BioReagents, BP531), 5% acetic acid (Sigma, 695092), and 50% ethanol (Meyer, 0390)] for 72 h in dark conditions at 4 °C. A gradient of sucrose (10, 20, 30%) was made to embed the samples in a PB buffer [10 mM sodium phosphate dibasic (Sigma, S3264) and 2 mM potassium phosphate monobasic (Sigma, P5655)], pH 7.2 (adjusted with NaOH 1 N), adding three to six drops of Leica tissue freezing medium (Leica Biosystem, Code 14020108926) to the gradients of 20 and 30%, respectively. Each gradient was changed after 1 h at 4 °C. Subsequently, the samples were embedded in a Leica tissue freezing medium (Leica Biosystem, Code 14020108926) at -26 °C. The blocks were sectioned at 10 and 30 µm with a cryostat (Leica Biosystem CM1950) with low profile blades (Thermo Scientific, 1407060). Sections of 30 µm were collected on glass slides. The samples were stained with calcofluor white (18909-1000 ML-F Fluka Analytical Sigma-Aldrich) for 1 h. The images were obtained using a confocal laser scanning microscope (Olympus, FV1000 SW) and the FV10 ASW 3.1 viewer software. The calcofluor white signal was detected using the excitation wavelength of 380 nm; the emission wavelength was 475 nm.

2.3.1 Immunolocalization assays

Immunofluorescence was performed with modifications of the protocols previously described (Nic-Can et al., 2013; Márquez-López et al., 2018). In this method, we eliminated the use of paraffin and replaced it with the Leica tissue freezing medium (Leica Biosystem, Code 14020108926) to embed the tissues. In addition, we did not use the sodium citrate buffer, Tween, and we skipped the heating step of the slides. In short, the slides with sample tissue (previously rinsed with 0.1% poly-L-lysine in H₂O) were washed

three times with sterile distilled water to remove excess Leica tissue freezing medium, then washed three times with the PB buffer, pH 7.2 (adjusted with NaOH 1 N). Sections were blocked with 3% bovine serum albumin (BSA, Sigma, A2153) in PB for 1 h at 4 °C. After three rinses with PB, sections were incubated overnight with anti-IAA mouse monoclonal antibody (Sigma, A0855) diluted 1:100 in 1% BSA in PB buffer. After three rinses with PB buffer, sections were incubated for 3 h in darkness with Alexa Fluor 488-labeled anti-mouse IgG antibody (Invitrogen, A-11001) diluted 1:100 in PB. After three washes with PB buffer, the tissue sections were treated with 10 µL of Vectashield mounting medium and DAPI to stain the DNA (Vector Laboratories, H-1200) and stored in the dark for 1 h at 4 °C. The images were obtained using a confocal laser scanning microscope (Olympus, FV1000 SW) and the FV10 ASW 3.1 viewer software. The IAA signal was detected using an excitation wavelength of 488 nm; the emission wavelength was 520 nm. The DAPI staining signal was detected using the excitation wavelength of 405 nm; the emission wavelength was 461 nm. The immunolocalization assay experiments were performed independently three times.

2.3.2 Controls of IAA immunolocalization

Negative controls were performed by replacing the antibody first by PB buffer. The anti-IAA mouse antibody was incubated with a solution of 5 mg mL⁻¹ synthetic IAA at a 1:2 (v/v) ratio at 4 °C overnight; the pre-blocked antibody solution was used as the primary antibody for immunofluorescence, following the same protocol and conditions described above.

2.3.3 Statistical analysis

The data processed to make the graphs and the statistical analysis were made with the ANOVA variance analysis program using the Origin Pro 2017 64 bit software, ver. 94E (Data Analysis and Graphing Software). Significance values were determined by the Tukey test. The differences were considered significant at $P \leq 0.05$.

2.4 RESULTS

2.4.1 The induction process, histology and expression profiling of the *CcYUCs* transcribed during SE in *C. canephora*

The pre-treatment stage (plants in MS medium supplemented with NAA 0.54 μM and Kin 2.32 μM for 14 days) and growth regulators are essential for SE in *C. canephora*. To induce SE, we used foliar explants of plantlets maintained in Murashige and Skoog (MS) medium for 14 days under photoperiod conditions (see materials and methods). Then the explants were transferred to an auxin-free medium supplemented with benzyladenine (BA, 5 μM). The samples were collected 56 days after induction (dai) (**Figure 2.1A**) and the number of somatic embryos counted (**Figure 2.1B**). During the induction process, we observed a rapid proliferation of proembryogenic cell mass at the edge of the explant wound 14, 21, and 28 dai. By 56 dai all the developmental stages of the somatic embryos were found (G, globular; H, heart; T, torpedo, and C, cotyledonar; (**Figure 2.1A**). The total embryo production per flask was 402.3. Two hundred ninety-eight were embryos in the G stage followed by 48.6 embryos in the H stage, 31.3 in the T stage, and 24.3 in the C stage (**Figure 2.1B**).

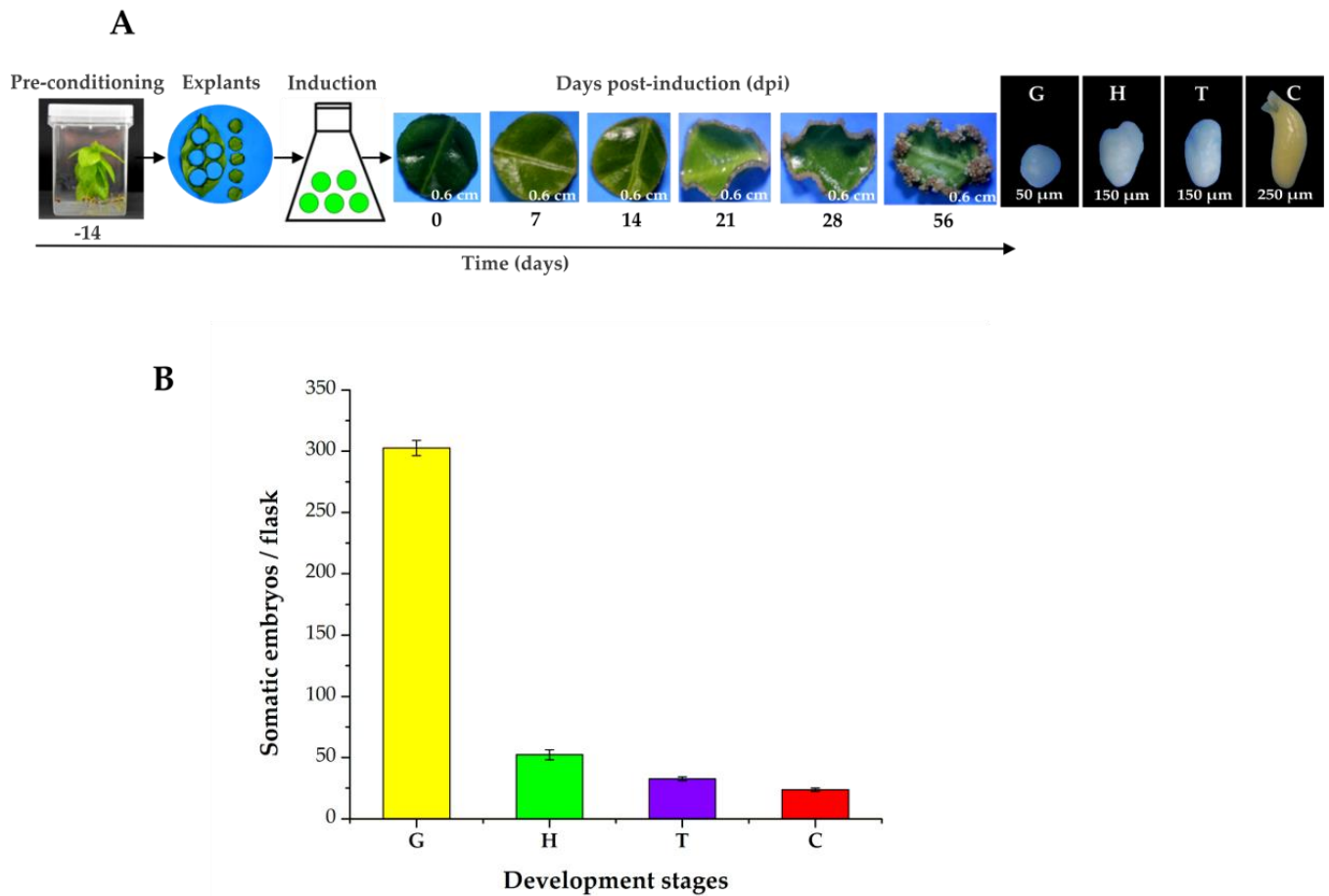


Figure 5 SE induction process in *C. canephora*. **A**, on day -14 (beginning of the pre-treatment), *C. canephora* plantlets are incubated in a pre-treatment medium (MS medium supplemented with NAA 0.54 μM and Kin 2.32 μM) for 14 days. After 14 days, explants are transferred into the induction medium (Yasuda medium supplemented with 5 μM benzyladenine) under photoperiod conditions (16/8 h) for 56 dai. **B**, total embryo production per flask was 402.3. The values corresponding to the different developmental stages were globular (**G**, 298), heart (**H**, 48.6), torpedo (**T**, 31.3), and cotyledonar (**C**, 24.3). The bars over the columns represent the mean value \pm SE of three independent experiments.

Transversal cuts of the explants were analyzed during the SE induction process, in order to observe the changes that are carried out in the explant and the formation of the first embryogenic structures. The results showed that at the beginning, the explant tissues are composed of spongy and palisade mesophyll cells (**Figure 2.2A**). The structure of the explant showed almost no change during the first 14 days of the induction of SE (Figures **2.2B**, **2.2C**). After 21 days in the induction medium, the first embryogenic cells appeared. These first structures are located near the vascular tissue (**Figure 2.2D**). These new cells are small, circular, and have a very dense cytoplasm (**Figure 2.2E**). Twenty-eight dai, there was an increase in the proembryogenic mass, with most of them emerging from spongy mesophyll cells (**Figure 2.2F**). The formation of the proembryos is the result of the coordinated growth of a series of organized cell divisions that will give rise to the somatic embryos.

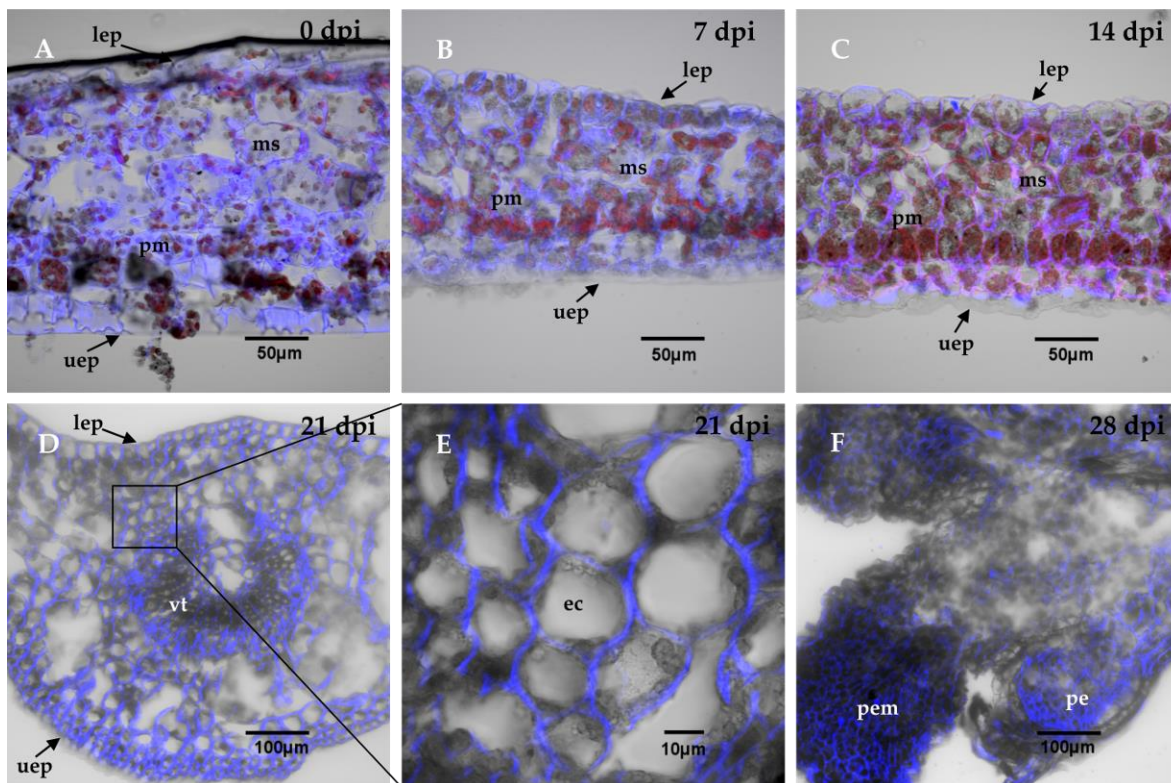


Figure 6 Histological analysis during the SE induction process in *C. canephora*. The leaf explants is composed of parenchymal cells of the spongy mesophyll, **sm**, and palisade mesophyll, **pm**. There are no changes in the explant cell structure as shown in panel **A** which corresponds to the induction day (0 Day); **B**, 7 dai and **C**, 14 dai. **D**, from 21 dai, the appearance of

embryogenic cells, **ec**, is observed near the vascular tissue, **vt**. **E**, a close-up view of the explants after 21 dai shows the dense embryogenic cells. **F**, after 28 dai, the **pe** proembryons are formed. The cell wall is stained with calcofluor white and chlorophyll is indicated in red. Other abbreviations: proembryogenic mass, **pem**; upper epidermis, **uep**; lower epidermis, **lep**. 0, 7, 14, 21, 28 dai of SE 30 μm cross-sections.

2.4.2 Identification and content of free IAA and conjugated IAA.

IAA is found in the cells in free and conjugated form. In all the systems in which the IAA conjugates have been measured, they are more than 90% of the total auxin. We used liquid chromatography-mass spectrometry (LC-MS/MS) and compared the retention times and fractionation patterns of standards and the auxins extracted from the explants. In this way, we identified free IAA and its conjugates with aspartic acid (Asp), glutamic acid (Glu), alanine (Ala), and leucine (Leu). The elution and fractionation patterns correspond perfectly between the standard and the samples (**Supplementary material S1-S5**). With this certainty, we proceeded to quantify the free IAA and its conjugates. The amount of IAA-Asp determined was only at the trace level, so the quantification was performed in the other three conjugates and free IAA (**Figure 2.3**).

The endogenous initial free IAA content was $0.22 \text{ nmol g}^{-1} \text{ FW}$ and increased more than nine times during the pre-treatment of the seedlings in the presence of NAA and Kin (**Figure 2.3**), and reached a maximum content of $2.06 \text{ nmol g}^{-1} \text{ FW}$ fourteen days after the start of the pre-treatment. The explants were taken from these plantlets to start the induction of SE. The free IAA content decreased rapidly during the first hour of explant incubation in the induction medium of the SE and was maintained at levels of 0.1 to $0.5 \text{ nmol g}^{-1} \text{ FW}$ for the next six days. Its level increased again with the appearance of the first embryonic structures.

The IAA conjugates are a significant part of IAA homeostasis (Rampey et al., 2004; Zhand and Peer, 20017), so they were assessed throughout the entire process (**Figure 2.3**). The conjugate with glutamic acid was more than 85% of the total IAA content. Fourteen days of pre-treatment produced an endogenous level of $98 \text{ nmol g}^{-1} \text{ FW}$ of IAA-Glu. After the induction of SE, the IAA-Glu content decreased seven times in just 24 hours and practically disappeared seven days after the induction of SE.

The conjugates with alanine and leucine made up 12.6% of the total IAA. These conjugates are very important for homeostasis of IAA since they can be hydrolyzed and contribute to free IAA. The IAA-Ala increased from 2.49 nmol g⁻¹ FW at the beginning of the pre-treatment to 11 nmol g⁻¹ FW at the time of induction and decreased very quickly during the next 21 days. The IAA-Leu conjugate decreased during the first seven days of pre-treatment, and by the time of the induction of SE, returned to its initial levels. This conjugate decreased very rapidly during the first hours of the induction of SE and then began to increase to levels ranging from 2.5 to 5.5 nmol g⁻¹ FW in the following days (**Figure 2.3**).

To determine whether the increase in IAA content observed during pre-treatment of *C. canephora* seedlings was due to *de novo* biosynthesis, 3-¹⁴C-Trp was used as has been done in *A. thaliana* (Hull et al., 2000; Sugawara et al., 2009) and *Solanum lycopersicum* (Liu et al., 2012).

Firstly, we performed a standard thin plate chromatography, and ran real non-radioactive samples and identified the compounds by LC-MS. This experiment gave us the confidence to associate radioactive spots with their identity. The result of incubation in the presence of 3-¹⁴C-tryptophan (Trp) can be seen in **Table 1**. As the days of the pre-treatment progressed, there was an increase in the radioactivity associated with the IAA. This result suggests that the IAA biosynthesis was *de novo* from Trp. A 7-fold increase in the IAA content was observed between day -9 and day zero (**Table 1**). The marked Trp only began to accumulate on days -4 and 0, possibly due that the cells had reached a maximum biosynthesis of IAA.

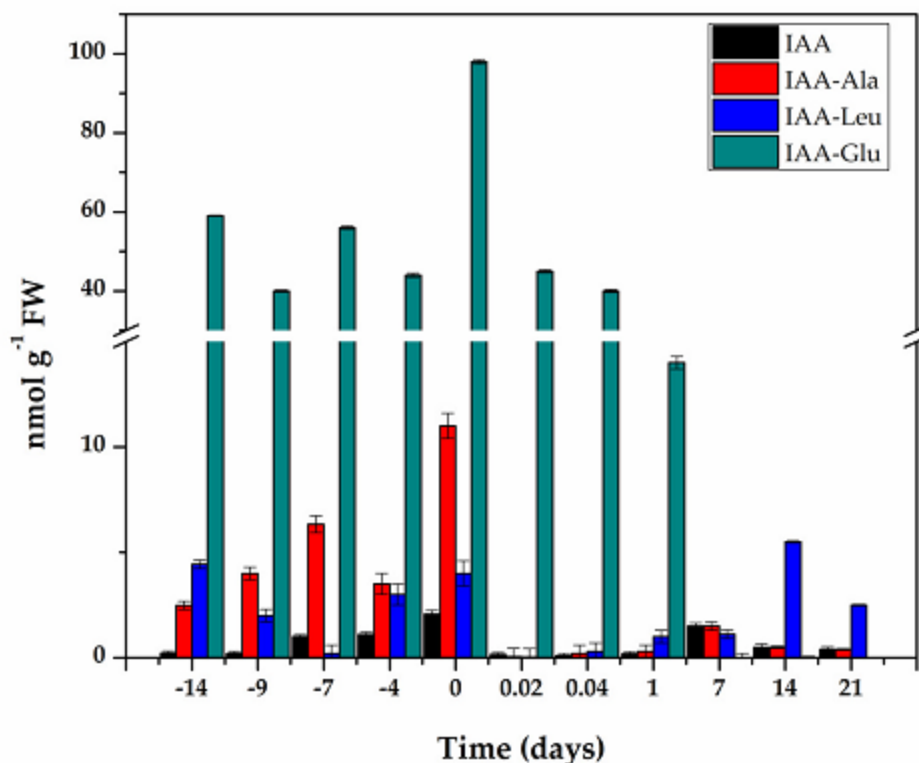


Figure 7 Content of IAA and its conjugates during pre-treatment and induction of SE in *C. canephora*. One hundred mg of leaf tissue was collected (days -14, -9, -4, and zero). Samples were also collected at 0.02, 0.04, 1, 7, 14, and 21 days after SE induction. Samples were analyzed as described in materials and methods. All analyses were carried out with three biological replicates from at least two different experiments. The bars represent the standard error ($n = 3$).

Table 1. Total radioactivity present in each sample of *C. canephora* plantlets analyzed.

Sample		Days			
		-9	-7	-4	0
Leaf extracts	IAA	154	174	274	1 093
	Trp	0	0	34	40
Leaves in medium		287	764	755	1 131

Medium	2,306,388	1,845,858	1,537,818	2,283,948
Stem	-	-	-	5 860
Root	-	-	-	-
Total counts per minute	2,306,829	1,846,796	1,538,848	2,292,033
Initial total cpm = 2,679,807				

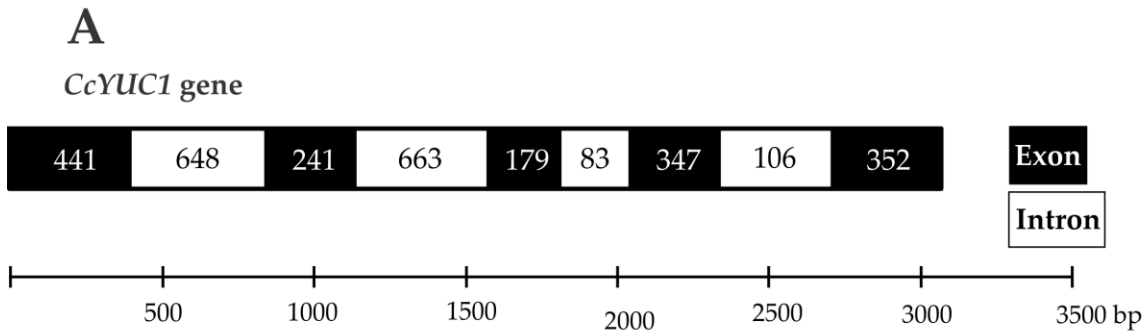
In an experiment using a radioactive label, it is important to determine the fate of the entire radioactive label. Therefore, we measured the radioactivity present in each of the fractions of the experiment. A part of the radioactivity will be in the tissues and other part in the culture medium. In the case of tissues, radioactivity was not only determined in the explants used to induce SE, but also in the rest of the plant. The extraction of auxins present in the stem of the plants was also performed and their radioactivity was measured. From days -9, -7 and -4 the stem was not extracted because it was submerged in the liquid medium and it would not be possible to determine how much radioactivity was due to the auxin present in the stem and how much radioactivity was external pollution; but this determination was done on day zero. The seedlings were incubated in 10 mL of pre-treatment medium to which the radioactivity was added; 10 μ L was taken to count in the scintillator. 2,679,807 cpm was added to each experimental unit (**Table 1**). As can be seen in **Table 1**, the destination of most of the radioactivity used in each experimental unit could be determined.

SE is a complex process that involves multiple factors, including the biosynthesis of IAA through the pathway TAA/YUC (TRYPTOPHAN AMINOTRANSFERASE OF ARABIDOPSIS/YUCCA) (Zhao, 2018). To test whether the *CcYUCs* genes are participating during the SE induction process in *C. canephora*, we performed a quantitative expression analysis of *CcYUC* transcript levels. First, we determined how many *YUC* genes were in the genome of *C. canephora* [<http://coffee-genome.org/>] (Denoëud et al., 2014). The search yielded eight *CcYUC* genes. Two copies of the *CcYUC1* gene and two copies of the *CcYUC10* gene were found throughout the genome. At the same time, we performed an analysis of the transcriptome of *C. canephora* (Quintana-Escobar et al., 2019). The results showed the presence of five transcripts of *CcYUC* gene products during the induction of SE. Two of these five transcripts belonged to the *CcYUC1*. The locus of

the *CcYUC1* gene is located on chromosome six in the genome of *C. canephora* and structurally consists of five exons, four introns with a length of 3,060 base pairs (**Figure 2.4A**). The reading frame of the *CcYUC1* gene predicted a 519-amino acid protein, 59 kDa molecular mass with FAD motifs (**Figure 2.4B**) characteristic of flavin monooxygenase enzymes. To have a complete picture of the participation of the *CcYUC* family during the induction of ES, we analyzed the expression of seven *CcYUC* genes, including the two copies of the *CcYUC1* gene, *CcYUC3*, *CcYUC4*, *CcYUC6*, and *CcYUC10* genes and one *CcYUC*-Like gene (**Table 2**).

Table 2. *CcYUC* genes family selected for analysis by qRT-PCR and primers.

Gen	Accession	Sequence 5'-3'	Size bp
<i>CcYUC1</i>	Cc06_g12600	Fw: CACGGATTCTTTGGGAGGGG Rv: CCACCCCAAATGGGTAGCA	179
<i>CcYUC1-putative</i>	Cc06_07530	Fw: TGGTAAGGTGTTGCATTCCA Rv: AGCTAGGAAGCACCCAGTGA	197
<i>CcYUC3</i>	Cc00_g00330	Fw: CTTTCGAGGATGGAGCTTTG Rv: AAAGTGCAGGAGCAAGTCGT	165
<i>CcYUC4</i>	Cc11_g01360	Fw: ATGCCTGTGGGTTGATG Rv: AAGAATGACAGAAGGGACAC	101
<i>CcYUC6</i>	Cc08_g08920	Fw: GAGGGCTTCCCAACTTATCC Rv: CTTCAATCCCACCGTCCTTA	159
<i>CcYUC10</i>	Cc01_g20210	Fw: TCCAAACCTAGTCCTTGAGAG Rv: GACAGAACTGTTTAGCCAGG	98
<i>CcYUC-Like</i>	Cc00_g00340	Fw: GATCGAACTCTGACCCCTGA Rv: TGGCAACTTTAGCAACATCG	184



B

CcYUC1 nucleotide sequence

MAIFSKIGIVGAGISGIAAAKQLRKYDPIIFEATDSLGGVWKHCSYRSTKLQTPRCDYEFSDFPWTQR
 DNSSFPTHLEVLEYLHSYATHFGVVELIKFSSKVVEIRFVGNHANDPDDQVNSNGYGNLLNGQPV
 WEVAVQTSESDTVEWYAFELLVICTGKYGDVPIIPQFPHNKGPEVFKGQVLHSLDYCKLDEENSVQL
 LKDKKVVVVGYYKSAIDLAVECAKANQGPDGQPCTIVVRTLHWITPHYSIWGLPFYLFYSTRASQF
 LHERPNQGILRNIFCKLLSPVRNAMSKIIESYLVWRLPLEKYGLKPDHHPFVEDYGSCQMAILPEELFE
 EAEKGMIDFKKASKWCFWEGGVFEFDDNTKLEADVLLATGFDGKRKLRNILEPFRSLLETGEMM
 PLYRGTIHLPLPNMAFVGYIESVSNLHTAEIRCKWLSRLADNYFKLPSVGQMLEQTQKEMGIMRKT
 RFYKRSCISTFSINHTDEICEEMGWKSWRKNNWLAEAFSPYCSQDYQEQQHID

519 aa 59 kDa

Figure 8 Gene structure and protein sequence of *CcYUC1* in *C. canephora*.

A. The length of the *YUC1* gene is 3060 bp base pairs and the structure consists of five exons, and four introns. B. The *YUC1* gene coding sequence produces a 519 aa amino acid protein with a molecular mass of 59 kDa. In bold letters the FAD binding-motif.

The analysis of the *CcYUC* expression was performed by qRT-PCR for samples of the -14, 0, 7, 14, 21, and 28 dai of SE. Among the *CcYUC* analyzed, it was found that the *CcYUC1* gene was especially highly expressed, and its transcription level showed a distinguishably substantial increase on the zero days of SE induction (up to 6.8-fold) (**Figure 2.5A**). During days 7, 14, 21 dai of SE, the transcriptional activity of *CcYUC1* decreased but then had a slight increase 28 dai (up to 1.2-fold). In contrast, *CcYUC1*-putative was only expressed on day zero (**Figure 2.5B**), and *CcYUC4* had two expression peaks, on day zero (up to 4.2-fold) and 28 dai (up to 2.7-fold), respectively (**Figure 2.5C**).

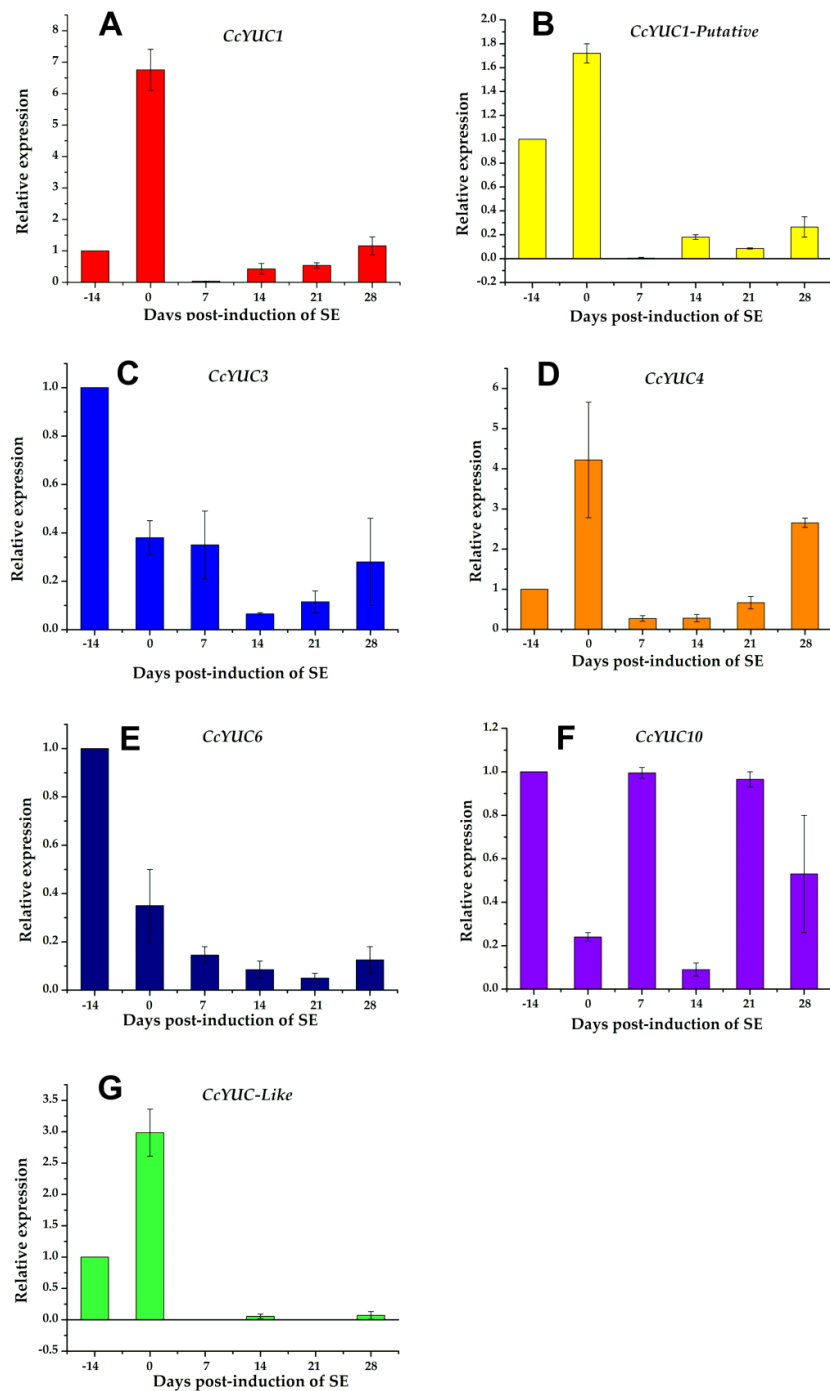


Figure 9 Expression levels of individual *CcYUC* genes during the induction of SE in *C. canephora*. **A**, *CcYUC1*; **B**, *CcYUC1-putative*; **C**, *CcYUC3*; **D**, *CcYUC4*; **E**, *CcYUC6*; **F**, *CcYUC10* and **G** *CcYUC-like*. Actin was used as an

internal qRT-PCR reference. The bars over the columns represent the mean value \pm SE of three independent experiments.

CcYUC3 (**Figure 2.5D**) and *CcYUC6* (**Figure 2.5E**) genes showed low levels of transcripts compared to -14 during the entire SE induction process. *CcYUC10* had very similar expression times 7 and 21 dai of SE (**Figure 2.5F**). The *CcYUC*-like gene was expressed only during the pre-treatment stage, with a 3-fold increase at the end of the pre-treatment and just before the explants were introduced into the induction medium (**Figure 2.5G**). Once in the explant was in the presence of the induction medium, the expression of the *CcYUC*-like gene disappeared. Of the seven analyzed *CcYUC* genes, four genes, including *CcYUC1*, *CcYUC1*-putative, *CcYUC4*, and *CcYUC*-Like, were up-regulated on day zero, while *CcYUC3* and *CcYUC6* were down-regulated during the SE induction process. The behavior of *CcYUC10* did not follow a definite pattern along the stages of induction of SE.

2.4.3 Endogenous free IAA accumulations and localization during the SE induction process

To investigate whether there is a specific localization of IAA in leaf explants of *C. canephora* during the process of SE induction, we used an anti-IAA mouse monoclonal primary antibody specific for free IAA and an Alexa Fluor 488-labeled anti-mouse IgG secondary antibody.

Previously, it was reported that auxin response gradients were established in specific regions of the embryonic callus and were responsible for SE (Rodríguez-Sanz et al., 2015; Márquez-López et al., 2018).

Cross-sections of leaf tissue, 30 μ M thick, were made of explants of *C. canephora* leaf during the process of induction of SE. After pre-treatment, we observed the cells that were part of the tissue structure. This tissue is made of spongy and palisade mesophyll cells (**Figure 2.6A, 2.6G**). In addition, although no morphological change was observed between the control explants and those treated with 100 μ M yucasin, there was a difference in the thickness of the explant. In tissues treated with 100 μ M yucasin, it was observed that the thickness of the tissue was thinner compared to the control (**Figure 2.6A, 2.6G**). It is possible that the yucasin inhibitor could cause this effect.

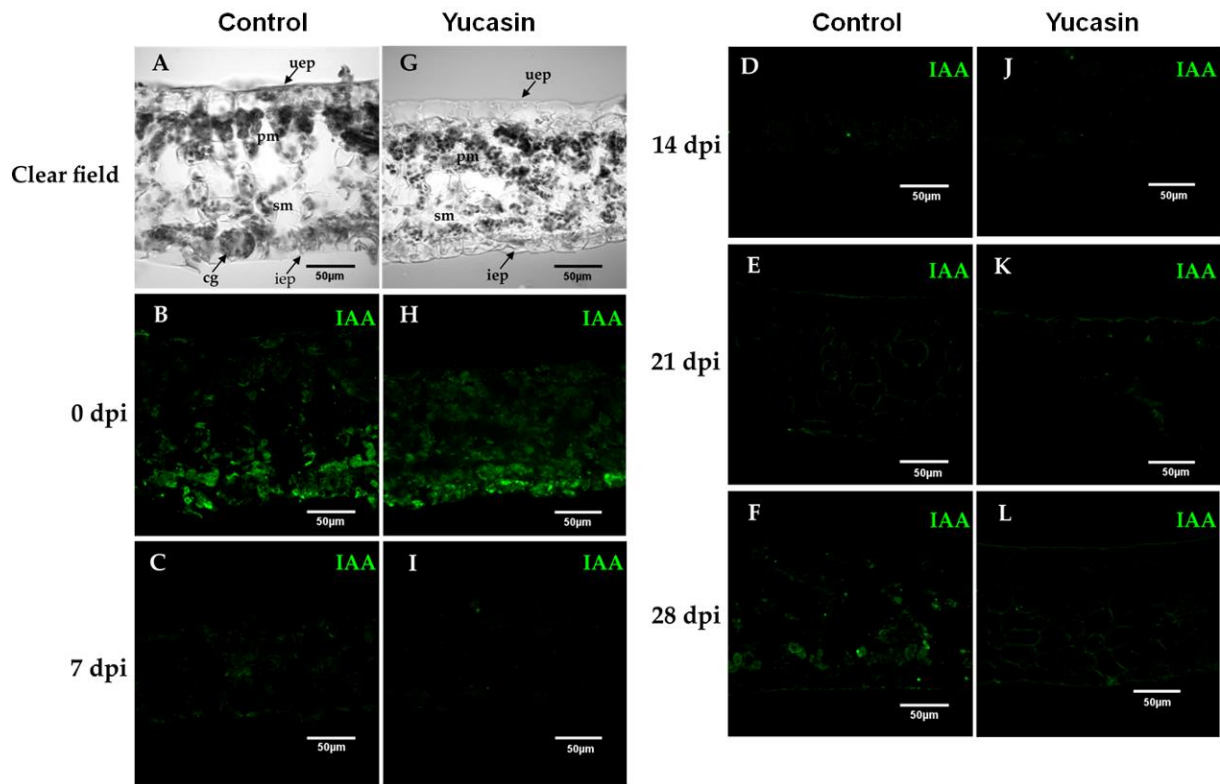


Figure 10 Free IAA immunolocalization during the SE induction process in *C. canephora*. Confocal images of longitudinal sections of leaf explants during 0, 7, 14, 21, and 28 dai of SE without (A, B, C, D, E, F) and with yucasin (G, H, I, J, K, L). A, G, Transmitted light differential interference images of a longitudinal section of leaves during the induction of SE. B, H (0 days); C, I (7 dai); D, J (14 dai); E, K (21 dai); F, L (28 dai). IAA was visualized with the Alexa 488 chromophore bonded to the antibody 224 that recognizes the antibody-IAA (green). **Upper** epidermis, **uep**; lower epidermis, **lep**; spongy mesophyll, **sm**; palisade mesophyll, **pm**.

In our study, on day zero, we found a strong free IAA signal during the SE induction process (Figure 2.6B). The signal decreased from seven dai (Figure 2.6C) through 14 dai (Figure 2.6D). At 21 dai (Figure 2.6E), the IAA signal began to increase. Seven days later, the increase of the IAA signal was much more significant (Figure 2.6E), and was localized at the edges of the explants and in the cell wall of the spongy mesophyll cells (Figure 2.6E).

On the other hand, the immunolocalization assays of free IAA of the yucasin-treated samples revealed important changes in the IAA signal accumulation pattern. At day zero of the SE induction process, we found a free IAA auxin signal in explants treated with 100 μ M yucasin (**Figure 2.6H**). The free IAA signal found was less intense than in the control samples (**Figure 2.6B**). The IAA signal disappeared from day 7 to day 21 after the induction of SE (**Figure 2.6I,J,K**). An essential difference from the control samples was the decrease in the IAA signal, in the presence of the yucasin, at 28 dai (**Figure 2.6L**) compared with the control at the same stage (**Figure 2.6F**).

The next step was to determine, intracellularly, the location of the IAA signal (**Figure 2.7**). The endogenous accumulation of free IAA was located in the interior chloroplasts and nucleoplasm of spongy mesophyll cells (**Figure 2.7B**).

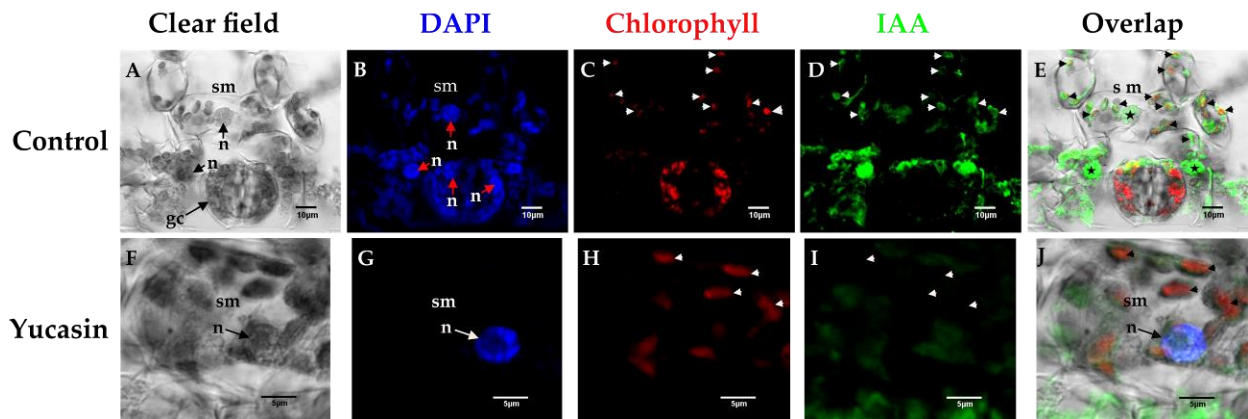


Figure 11 Free IAA immunolocalization during day zero of the SE induction process in *C. canephora*. Confocal microscopy images of cross-sections of leaf explants during 0 dai of SE. **A**, clear field; **B**, nuclei staining with blue DAPI; **C**, red chlorophyll signal; **D**, free IAA signal in green, and **E** overlapping of the free IAA and chlorophyll signal. Note that there is IAA in the chloroplasts (short white arrows) and nucleoplasm (bold stars) of the spongy mesophyll, **sm**, cells; **F**, light field; **G**, nuclei staining with DAPI in blue; **H**, chlorophyll signal in red; **I**, free IAA signal in green colour; **J**, overlapping of IAA signal, chlorophyll, and DAPI on day zero SE induction. IAA is not in the chloroplasts or the nucleoplasm of the spongy mesophyll cells but the cytosol. Mesophyll cells, **sm**; palisade mesophyll, **pm**; nucleus, **n**.

In control tissues, numerous chloroplasts were located within the spongy mesophyll cells (**Figure 2.7A**). These cells had prominent nuclei (**Figure 2.7B**). The free IAA signal was found both in the chloroplasts and in the nuclei of the spongy mesophyll cells (**Figure 2.7E**). We show that free IAA of mouse anti-IAA monoclonal primary antibodies was specific (**Figure 2.7D**) and the signal was not mixed with chlorophyll (**Figure 2.7C**). In treatments with 100 μM of yucasin, the free IAA signal was found in the cytosol (**Figure 2.7I**) and not in the chloroplasts or nuclei (**Figure 2.7-J**), as in the control.

2.4.4 Effect of the inhibition of auxin IAA biosynthesis by yucasin during the SE induction process in *C. canephora*

Several studies have shown that the pathway of IAA biosynthesis in most plants is through two simple steps from tryptophan, mediated by TAA and YUCs (Zhao et al., 2001; Stepanova et al., 2011; Zhao, 2012). The tryptophan-dependent pathway for IAA biosynthesis through *YUC* genes could be a determining factor for the development of embryogenesis (Nonhebel, 2015). At the same time, different groups have shown that an increase in the amount of IAA is required to initiate the induction of SE (Ayil-Gutiérrez et al., 2013; Rodríguez-Sanz et al., 2014). Our results (**Figure 2.3**) show an increase in the IAA signal during the pre-treatment phase. To test whether CcYUC-mediated IAA biosynthesis is required for the SE induction process, we used the auxin biosynthesis inhibitor, yucasin, which specifically inhibits the function of YUC proteins (Nishimura et al., 2014).

The results show that the efficiency in the formation of proembryogenic mass was severely affected by the treatment in a dose-dependent way (**Figure 2.8A**). Twenty-one dai, the explants treated with the inhibitor showed a decrease in proembryogenic mass formation, particularly at 20, 50, and 100 μM of yucasin (**Figure 2.8A**). After 56 dai of SE, all of the explants coming from plants incubated in the presence of yucasin during pre-treatment showed signs of damage, including tissue necrotization and phenolization (**Figure 2.8A**). The treatments with 50 and 100 μM of yucasin completely inhibited the development of the proembryogenic mass from 28 dai on (**Figure 2.8B**).

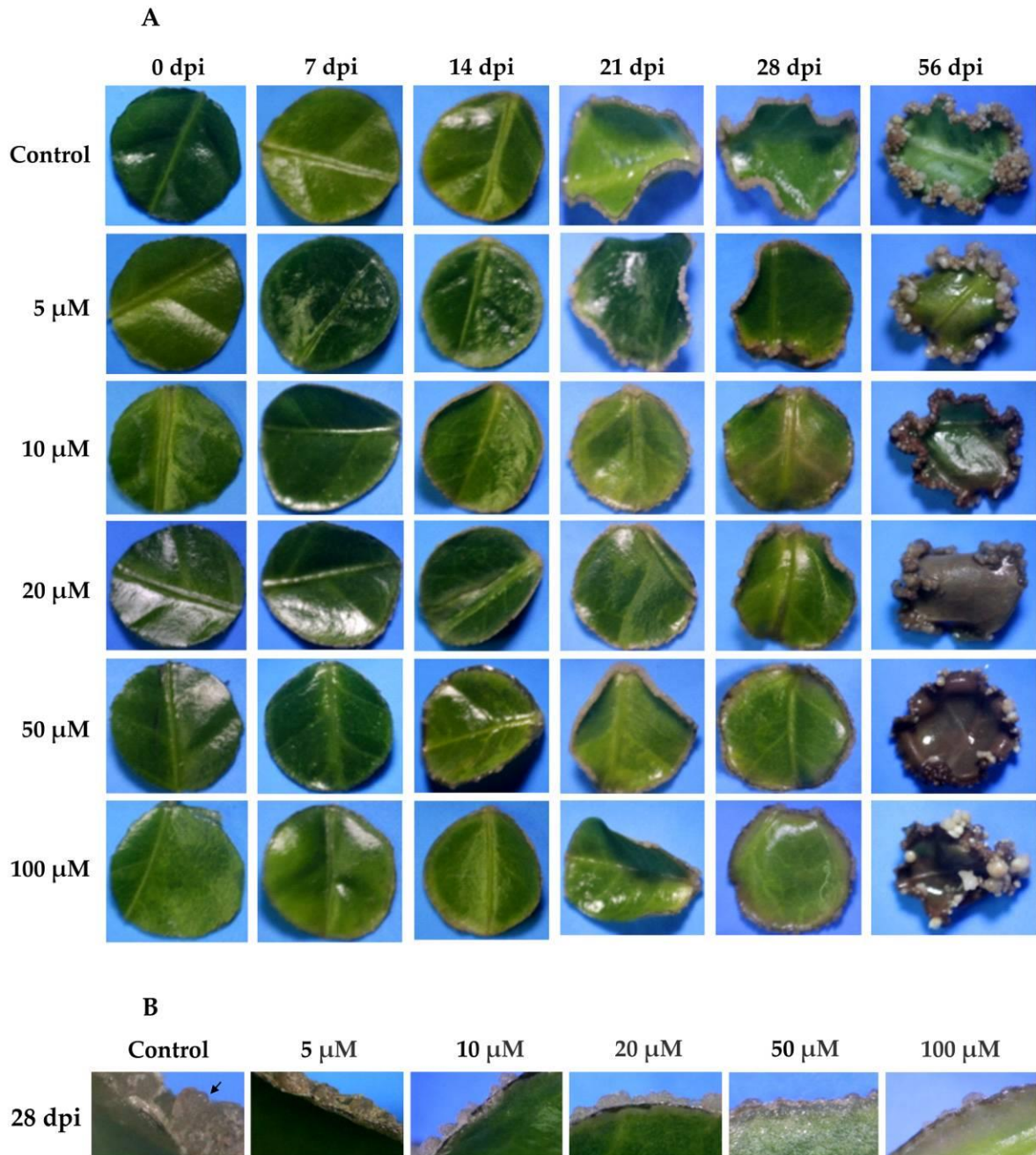


Figure 12 Effect of yucasin during the induction of SE in *C. canephora*. **A**, Different concentrations of yucasin were applied exogenously (5, 10, 20, 50, and 100 μM) to the pre-treatment medium. The effect of yucasin was documented every seven days until 28 dai and then on day 56 dai of SE. **B**, A comparison of the effect of yucasin 28 dai for all the yucasin concentrations. Note the abundance of proembryogenic mass on the control, as well as the presence of proembryos (black arrow).

The presence of free IAA decreased significantly after the explants were transferred to the SE induction medium (**Figure 2.3**). However, this small amount of IAA is very important for the induction of the embryogenic process. When yucasin was added, this small amount disappeared and the embryogenic process did not take place (**Figure 2.9**).

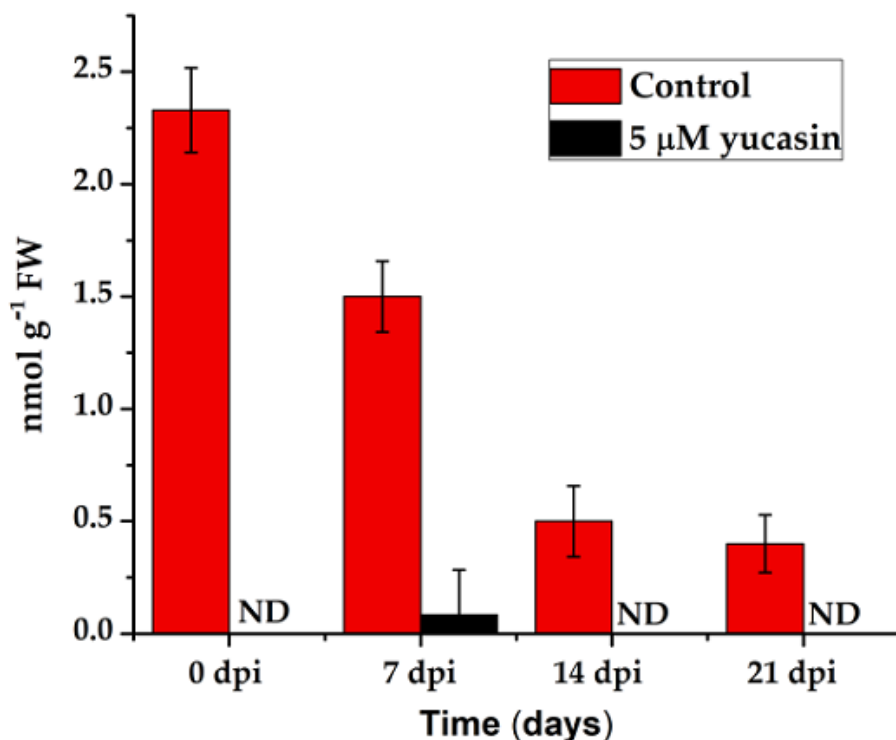


Figure 13 Quantification of the IAA endogenous content in leaf explants of *C. canephora* treated with 5 μM yucasin. Samples were collected at 0, 7, 14, and 21 days after SE induction. The bars over the columns represent the mean value ± standard error of three independent experiments. ND = not detected.

Quantification of the number of embryos produced 56 dai showed a significant decrease in the number of embryos produced by the explants exposed to the yucasin inhibitor (**Figure 2.10**). In the presence of the inhibitor, only globular-shape embryos were formed. The decrease varied from 72 to 94% of the control. Even the lower concentration of the inhibitor produced a sharp decrease in the number of embryos. In the presence of 10 μM-

100 μM of yucasin, the number of globular embryos was less than 40 embryos per flask, in comparison with 300 globular embryos per flask for the control (**Figure 2.10**).

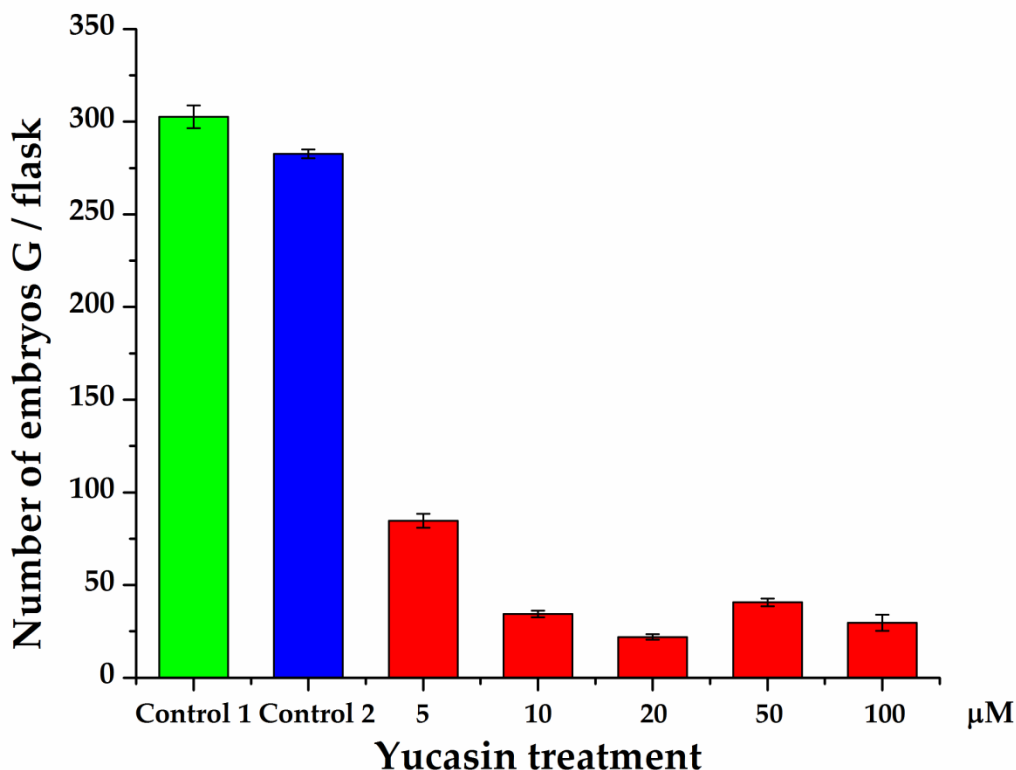


Figure 14 Effect of yucasin on the production of somatic embryos during the induction process in *C. canephora*. Only globular-stage embryos were formed after 56 days, so the comparison was limited to the number of globular embryos formed throughout SE induction. The data are the results of three independent biological experiments; the bars represent the standard error.

2.4.5 Restoration of somatic embryogenesis by exogenous addition of IAA

To confirm that the effect seen on somatic embryo production was due to the inhibition of IAA biosynthesis as a result of yucasin treatment, we added 1.0 μM of IAA to the medium of induction of the SE containing the explants treated previously with 100 μM yucasin-induction medium. Twenty-eight days after the exogenous addition of IAA, the embryogenic process inhibited by the yucasin was restored (**Figure 2.11A**). It is possible

to see all the stages of development after the addition of exogenous IAA (**Figure 2.11B,C**). In contrast, the samples treated with yucasin but not exogenous IAA did not produce embryos, beyond the few globular embryos already present at the beginning of the experiment (**Figure 2.11D-E**). The somatic embryos produced after the addition of the exogenous IAA are entirely normal, and the somatic embryos reached the cotyledonar stage (**Figure 2.11F**). The production of somatic embryos in the induction medium containing yucasin + exogenous IAA was more than 77% higher than the control without yucasin (**Figure 2.11G**).

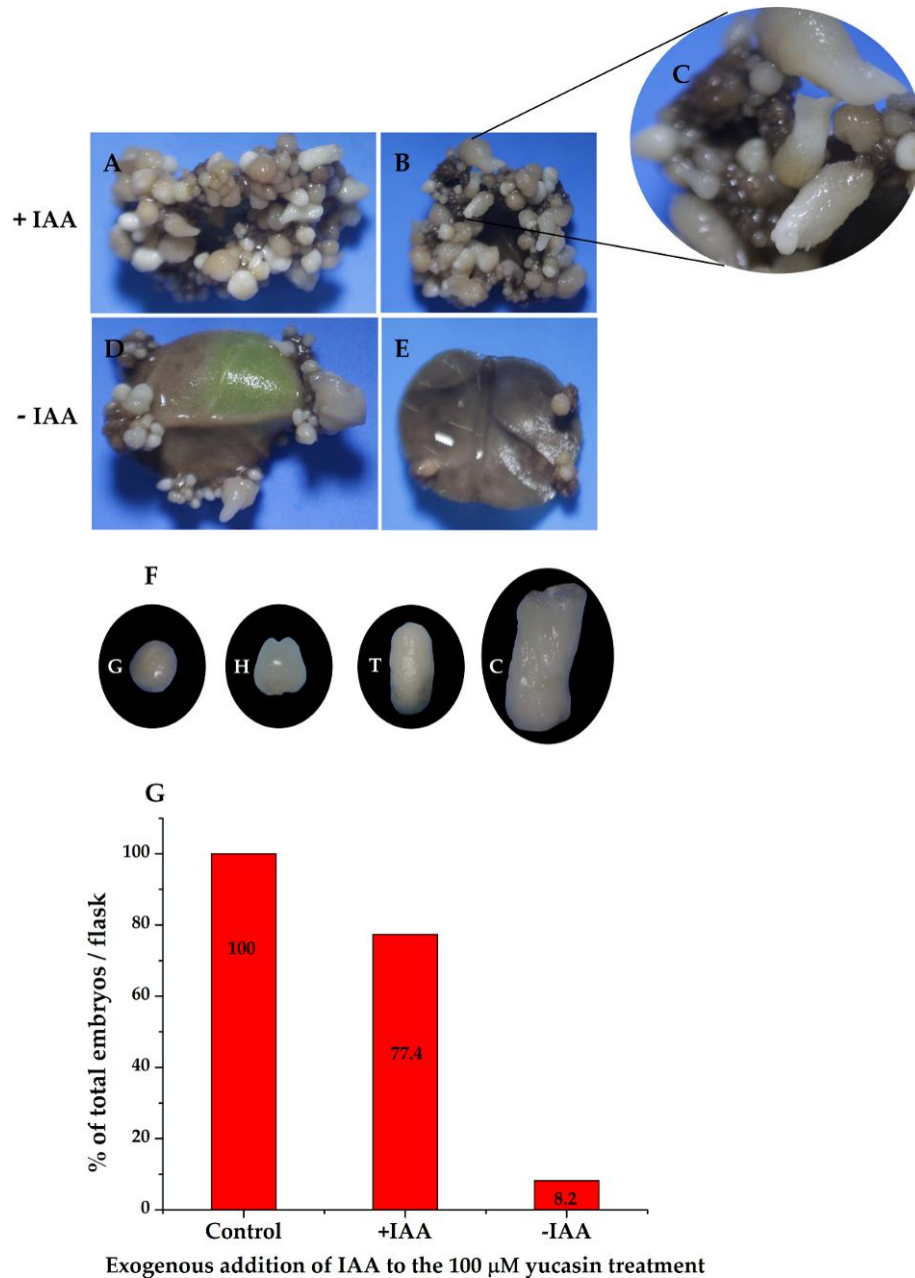


Figure 15 The exogenous addition of IAA restores somatic embryogenesis in explants previously treated with 100 μ M yucasin. A and B, restoration of somatic embryogenesis by exogenous application of IAA to explants treated with 100 μ M yucasin. C, close-up shows the presence of somatic embryos at different stages of development. D and E, explants in the presence of 100 μ M yucasin. F, different development stages of somatic embryos after four weeks in the presence of exogenous IAA. G, the total percentage of embryos formed in

flasks with and without IAA.

2.5 Discussion

Several biochemical and genetic studies of SE have been reported, including *A. thaliana* (Wójcikowska *et al.*, 2016), *Brassica napus* (Kumar *et al.*, 2016), *Medicago truncatula* (Rose, 2019), *Coffea* spp. (Nic-Can *et al.*, 2013; Loyola-Vargas *et al.*, 2016) and many other species (Loyola-Vargas *et al.*, 2016; Pais, 2019; Aguilar-Hernández and Loyola-Vargas, 2018). However, the mechanism by which somatic cells change their genetic program and become somatic embryos is not yet fully understood.

SE is a complex process and is highly regulated. In this work, we focused on IAA biosynthesis mediated by YUCs. It has been reported that auxin transport (Petrášek and Friml, 2009; Benková *et al.*, 2003) and signaling plays an essential role during the entire life cycle of plants including embryogenesis (Nonhebel, 2015; de Vega-Bartol *et al.*, 2013; Méndez-Hernández *et al.*, 2019).

In this study, we showed that *CcYUC*-mediated IAA biosynthesis is required during the SE induction process in *C. canephora*. Histological analysis showed that at the beginning of the proliferation of the proembryogenic mass 21 dai, the embryogenic cells appeared near the vascular tissue (**Figure 2.2 D**). The formation of embryogenic structures was observed from 28 dai onwards. By 56 dai, all of the different development stages of the somatic embryos of *C. canephora* were present (**Figure 2.1**). These data are in line with the well-documented fact that mesophyll cells located near vascular bundles of leaves are the first to divide (Berthouly, 1996; Santana-Buzzy *et al.*, 2007). These cells produce up to fivefold more proteins than non-embryogenic cells (Tahara *et al.*, 1995). The embryogenic cells are characterized as small, isodiametric, and densely cytoplasmic. These cells then undergo a series of successive divisions to give rise to a somatic embryo (Quiroz-Figueroa *et al.*, 2002).

The increases of IAA signal during the pre-treatment period (Ayil-Gutiérrez *et al.*, 2013) (**Figure 2.3B**) could be due to *de novo* biosynthesis. The increase in the expression of *CcYUC1*, *CcYUC1-putative*, *CcYUC4*, and *CcYUC-Like* during the pre-treatment support this assumption (**Figure 2.5**). Consistent with this hypothesis, qRT-PCR expression analysis of the *CcYUC* genes during the SE induction process showed that most (5/8) of

the *CcYUCs* encoded in the genome were transcriptionally active at the beginning of the SE induction. The transcript levels on day zero were congruent with the free IAA signal found in the explants in the induction medium. The *YUC* genes family encodes flavin monooxygenase enzymes for the biosynthesis of IAA from IPyA (Stepanova et al., 2011). Biochemical and genetic studies indicate that plants use Trp as a substrate, which is converted to IPyA as an intermediary for the production of IAA (Mashiguchi et al., 2011).

In situ hybridization has determined *YUC1* and *YUC4* expression at the apical meristem and primordia of young leaves during organogenesis in *A. thaliana* (Cheng et al., 2006; Liu et al., 2014; Chen et al., 2016). These genes are activated quickly after wounding (within 4 hours), suggesting that these two genes participate in the production of endogenous auxin in leaf explants (Chen et al., 2016). In this same model, the overexpression of *YUC* genes increases the endogenous content of IAA in young leaves. The mutation of the *YUC* genes produces a drastic decrease in the content of IAA (Mashiguchi et al., 2011; Woodward and Bartel, 2005; Kasahara, 2015). Similarly, in maize, *yuc* mutations have been shown to cause a reduction of IAA levels and disturb the vegetative development (Bernardi et al., 2012).

In *A. thaliana*, the inhibition of *YUC* genes prevents the expression of *WOX11*, resulting in the blocking of rooting (Chen et al., 2016). This labour is divided among the different *YUC* genes. *YUC1* and *YUC4* are expressed suddenly in response to wounding after detachment in both light and dark conditions and promote auxin biogenesis in both mesophyll and competent cells (Chen et al., 2016). These two genes are also expressed at the beginning of the induction of the SE in *C. canephora* (**Figure 2.5**), suggesting a similar role in both species. However, the inactivation of a single *YUC* gene does not cause developmental defects, due to the redundant function between *YUC* genes in *A. thaliana* (Chen et al., 2006; 2007). Therefore, we used a specific inhibitor to block the function of YUC enzymes in *C. canephora*. Yucasin inhibits the activity of YUC enzymes and suppresses the effect of the high-auxin phenotype of *YUC* overexpression found in *A. thaliana* (Tsugafune et al., 2017). The results shown in **figures 2.8** reveal that the inhibition of the IAA biosynthesis (**Figure 2.9**) strongly affected the progress of the SE in *C. canephora*. The immunolocalization of IAA in *C. canephora* explants treated with the

inhibitor (**Supplementary material S6**) shows no signal in the explants exposed to yucasin (**Supplementary material S6C, G**).

The exogenous addition of IAA to explants treated with yucasin restored the SE process (**Figure 2.10**). These results reveal that the YUC-mediated biosynthesis of the auxin IAA is critical for SE in *C. canephora*. The IPyA pathway is highly conserved in land plants; however, and since the IAA can be synthesized through five different routes, one of them independent of tryptophan (from indole-3-glycerol phosphate (Sitbon et al., 2000; Wang et al., 2015), a contribution to the IAA pool from some of the other four routes cannot be ruled out.

In this study, we used different concentrations of yucasin (5, 10, 20, 50 y 100 μ M). We showed that yucasin inhibited the production of somatic embryos in explants of *C. canephora* after (**Figure 2.10**). The action of IAA occurs in its free form and acts in the nucleus to carry out the expression of auxin response genes (Gallei et al., 2020). Different concentrations of this auxin may give rise to various physiological processes [64]. Its synthesis and distribution in tissue determine the action of auxin; mainly by its polar transport during SE in *A. thaliana* (Petrášek and Frim, 2009; Petrášek et al., 2011). During zygotic embryogenesis, IAA is regulated by its biosynthesis and spatio-temporal localization through specific carriers of auxin PIN (pin-formed) and ABCB (ATP-binding cassette protein subfamily B (Zazimalová et al., 2007; Krecek et al., 2009).

On the other hand, the IAA found in treatments with 100 μ M yucasin was possibly due to two factors: first, the release of IAA through hydrolysis of IAA-conjugates. Conjugation plays a central role in the homeostasis of the IAA (Woodward and Bartel, 2005; Korasick et al., 2013), and this reaction catalyzed by the Gretchen Hagen 3 enzymes (GH3) family of acyl acid-amido synthetases (Westfall et al., 2010). The IAA found in this work in explants with yucasin could be the result of IAA-Leu-resistant (IRL) enzyme activity (Rampey et al., 2004). In the absence of de novo biosynthesis of IAA (by the inhibition of yucasin), the IAA conjugates hydrolyze to leave it in its free form (Bartel and Fink, 1995). IAA metabolism depends on which amino acid is attached; for example, the conjugation of IAA with alanine or leucine results in a form that is stored but can be easily hydrolyzed (LeClere et al., 2002). Auxin conjugates are hydrolyzed to release IAA to maintain intracellular homeostasis in tissues in response to environmental conditions (Quint and

Gray, 2006). Recently, hydrolysis of aspartic (IAA-asp) and glutamic (IAA-glu) conjugates were reported in strawberry plants to provide free IAA for fruit growth (Tang et al., 2006). The second factor that could explain the presence of IAA in explants treated with yucasin is the existence of an alternate route to produce IAA (Woodward and Bartel, 2005). Indole-3-acetaldehyde (IAAld) has been proposed as an intermediary in the IAA biosynthesis pathway, since some bacteria produce IAA from IPyA using IAAld as an intermediary (Patten and Glick, 1996). However, there is not enough evidence for this theory. Therefore, IAAld is unlikely to participate in the IPyA pathway (Mashiguch et al., 2011). Another auxiliary route in the biosynthesis of IAA is from indole-3-acetaldoxime (IAOX) (Sugawara et al., 2009). CYP79B2 and CYP79B3 catalyze the conversion of Trp to IAOx (Mikkelsen et al., 2015; Zhao et al., 2002). However, it has been reported that the IAOx pathway is specific to *Brassicaceae* plants, because *CYP79B* genes are very limited in these species (Sugawara et al., 2009).

However, many questions remain unanswered about the de novo biosynthesis of IAA during the SE induction process. Several factors are implicated in the induction, including alteration of the cell wall composition, changes in growth regulators, genetic expression, and epigenetic regulations (De-la-Peña et al., 2015). Furthermore, although it is believed that the predominant route in auxin synthesis is from IPyA, the molecular mechanisms that regulate biosynthesis at the transcriptional level and protein level are unknown (Eklund et al., 2015).

In summary, the data in this research suggest that the pre-treatment of the coffee plantlets produces an increase in the level of IAA. This increase is due to de novo biosynthesis, and the presence of IAA at the beginning of the induction of SE in *C. canaphora* is indispensable for the process to begin.

Author Contributions: conceptualization, V.M.L.V.; methodology, M.A.U.C., C.P.H., R.M.G.A., L.B.-A. V.A.-H.; formal analysis, V.M.L.V., V.A.-H.; investigation, M.A.U.C.; resources, V.M.L.V.; writing—original draft preparation, M.A.U.C.; writing—review and editing, V.M.L.V.; supervision, V.M.L.V.; project administration, V.M.L.V.; funding acquisition, V.M.L.V.

Funding: This research was supported by Consejo Nacional de Ciencia y Tecnología CONACYT grant (Grant 1515)

Acknowledgments: We would like thank Angela Ku-Gonzalez for her technical support in the confocal microscope and to Irma Angelica Jiménez-Ramírez for her support in histology.

Conflicts of Interest: The authors declare no conflict of interest.

Abbreviations

DAI	Days after induction
IAA	Indole-3-acetic acid
IPA	Indole-3-pyruvic acid
Kin	Kinetin
NAA	Naphthalenacetic acid
SE	Somatic embryogenesis
Trp	Tryptophan

2.4.7 SUPPLEMENTARY MATERIAL

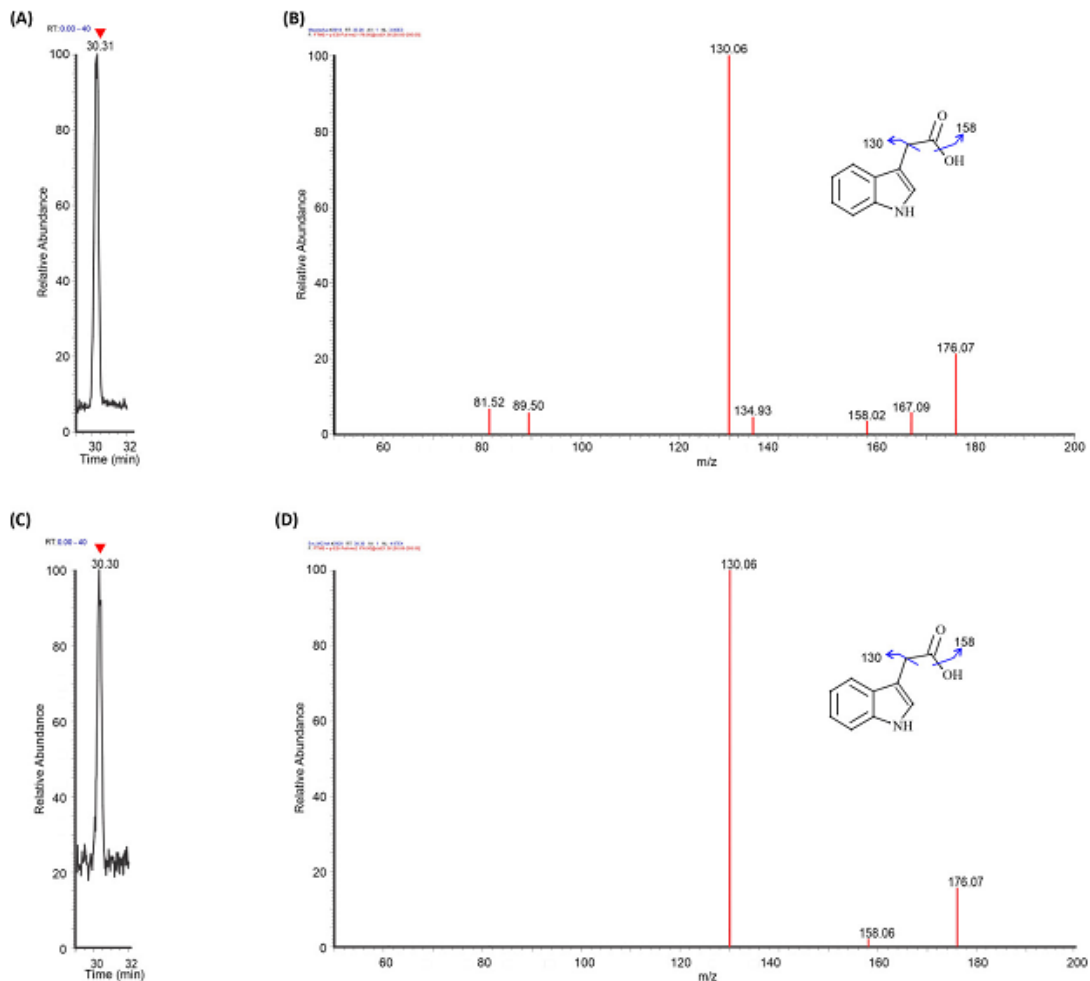


Figure S1. Chromatograms and fragmentation pattern obtained for indole-3-acetic acid by LC-MS/MS. (A and B) Chromatograms and fragmentation pattern for standard. (C and D) Chromatograms and fragmentation pattern obtained from pre-induced leaf samples without yucasin inhibitor. Red arrowheads in chromatograms indicate the retention time for indole-3-acetic acid.

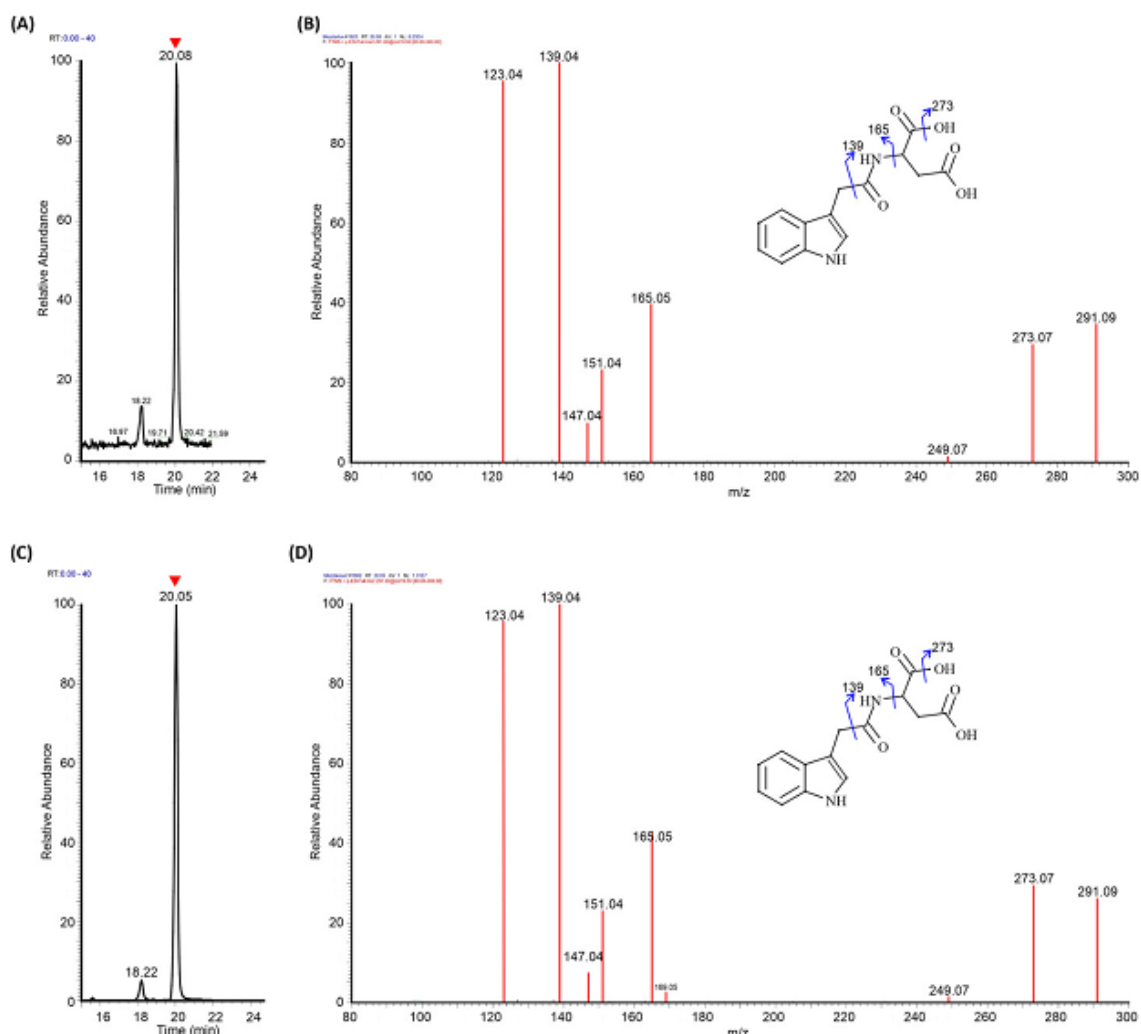


Figure S2. Chromatograms and fragmentation pattern obtained for indole-3-acetyl-L-aspartic acid by LC-MS/MS. (A and B) Chromatograms and fragmentation pattern for standard. (C and D) Chromatograms and fragmentation pattern obtained from pre-induced leaf samples without yucasin inhibitor. Red arrowheads in chromatograms indicate the retention time for indole-3-acetyl-L-aspartic acid.

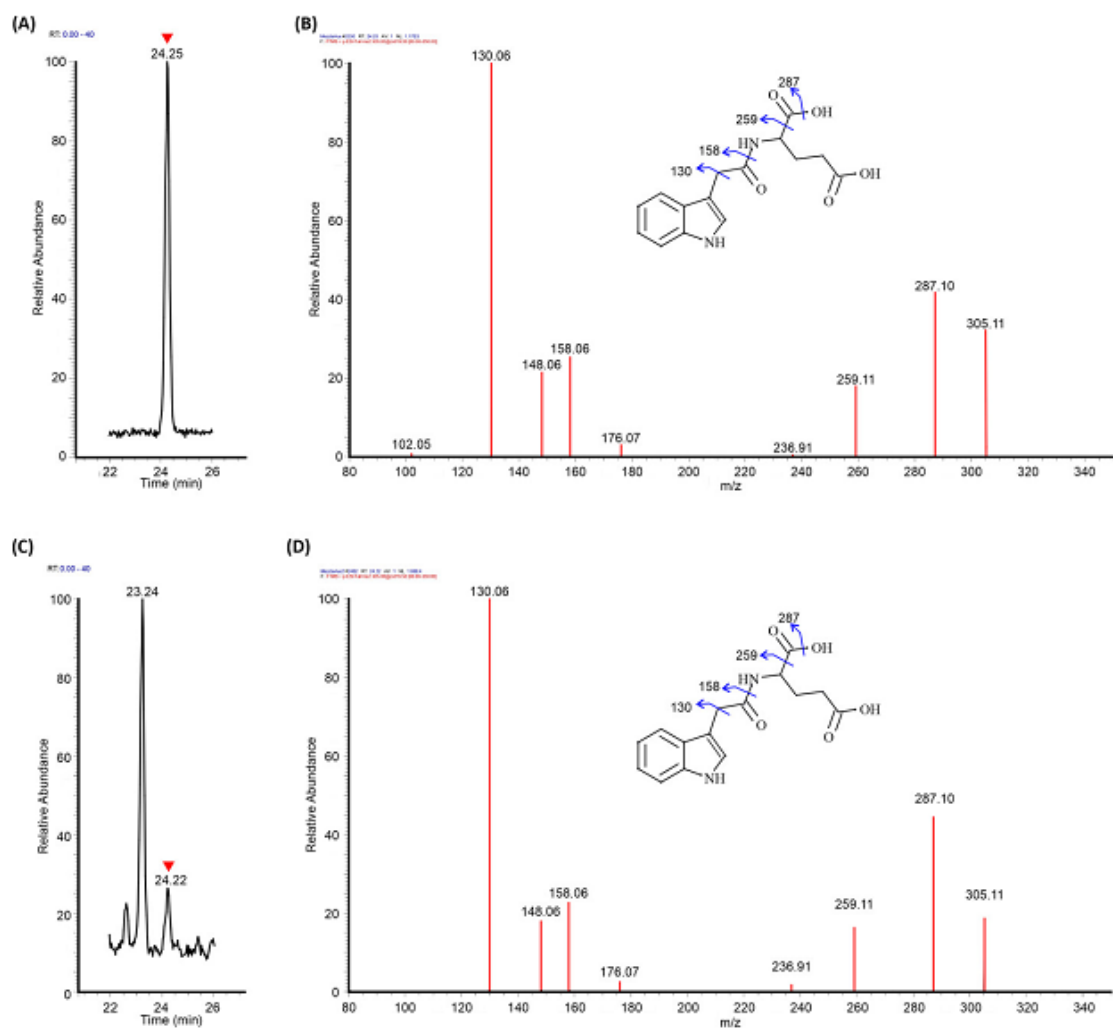


Figure S3. Chromatograms and fragmentation pattern obtained for indole-3-acetyl-L-glutamic acid by LC-MS/MS. (A and B) Chromatograms and fragmentation pattern for standard. (C and D) Chromatograms and fragmentation pattern obtained from pre-induced leaf samples without yucasin inhibitor. Red arrowheads in chromatograms indicate the retention time for indole-3-acetyl-L-glutamic acid.

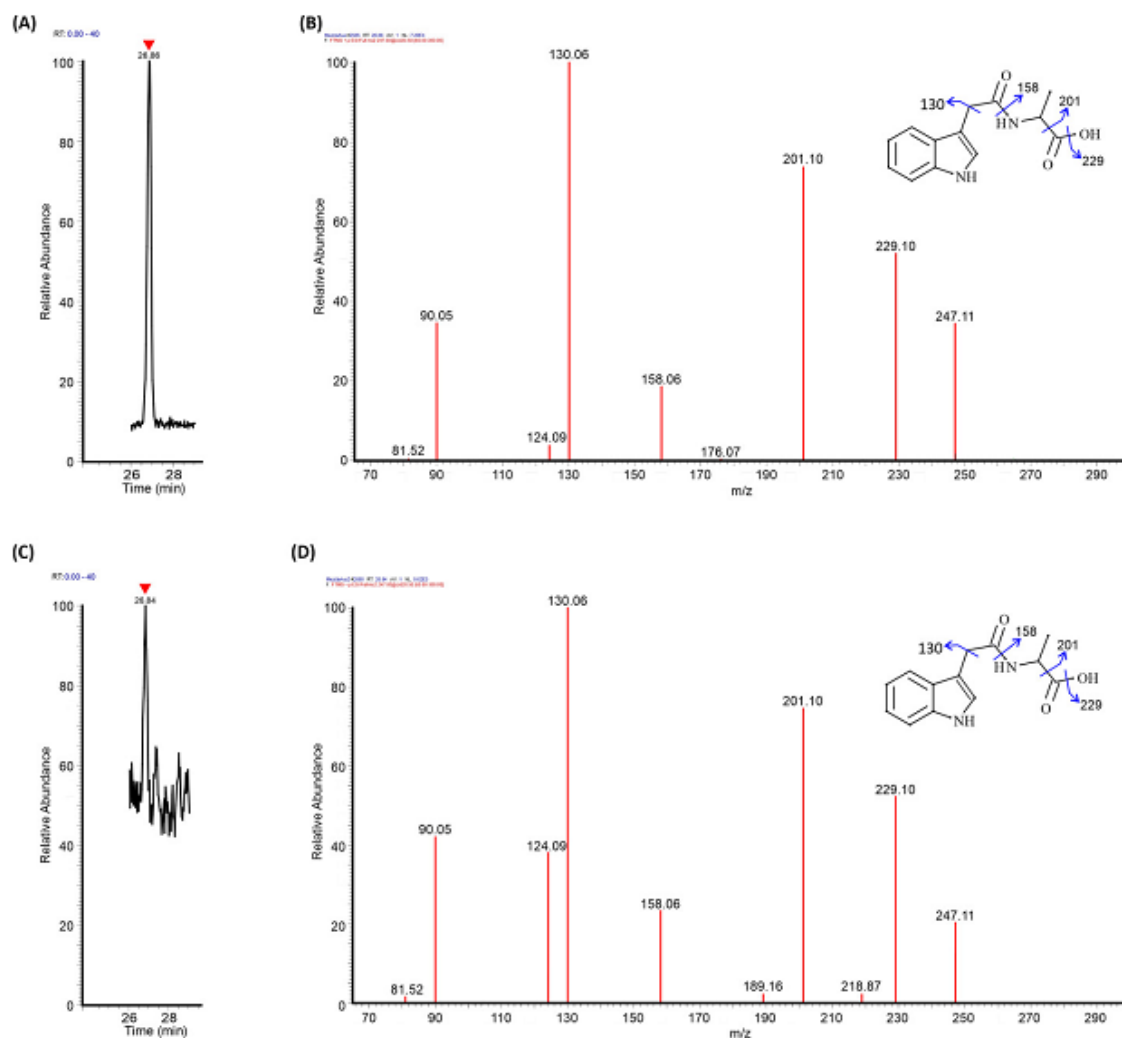


Figure S4. Chromatograms and fragmentation pattern obtained for indole-3-acetyl-L-alanine by LC-MS/MS. (A and B) Chromatograms and fragmentation pattern for standard. (C and D) Chromatograms and fragmentation pattern obtained from pre-induced leaf samples without yucasin inhibitor. Red arrowheads in chromatograms indicate the retention time for indole-3-acetyl-L-alanine.

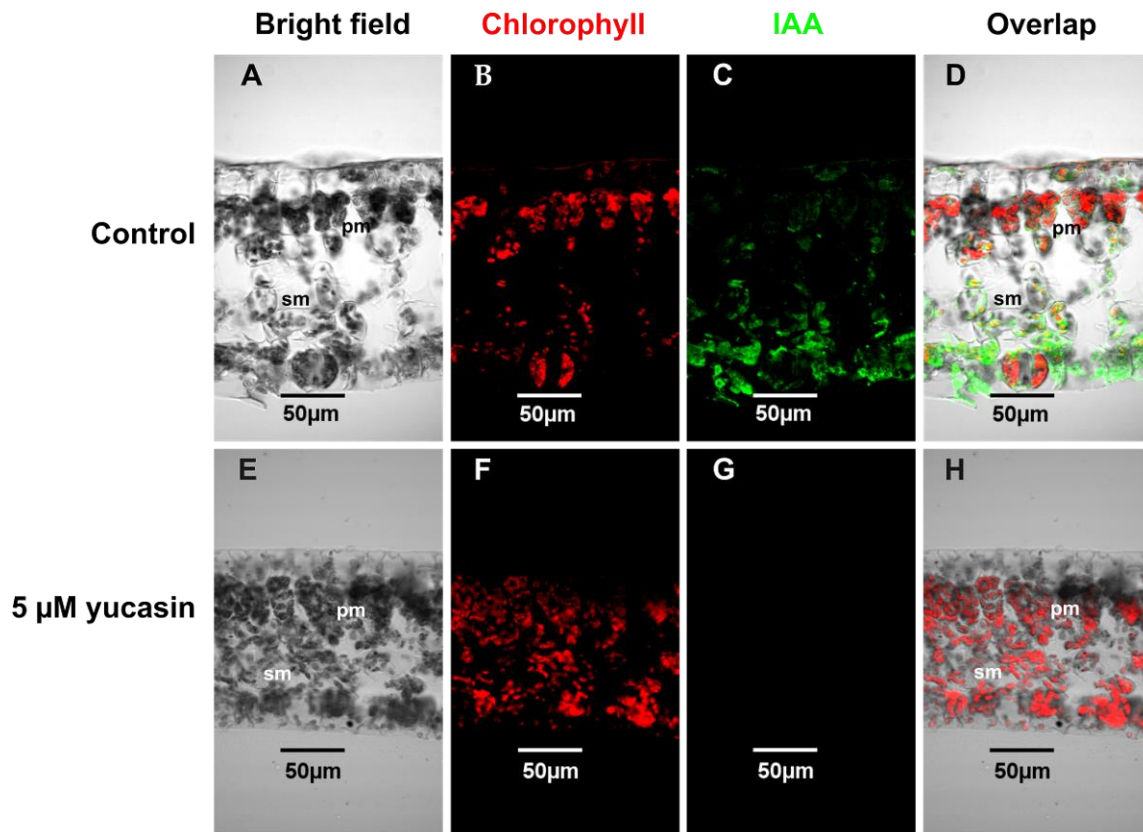


Figure S6. Immunolocalization of free IAA in *C. canephora* explants treated with 5 µM yucasin. Confocal images of longitudinal sections of leaf explants of induction day (D0). Panel **A** and **E** bright field. **B** and **F** chlorophyll autofluorescence (red). **C** and **G** visualization of IAA by the Alexa 488 chromophore bonded to the antibody that recognizes the antibody-IAA (green). **D** and **H** overlapping of the chlorophyll and IAA confocal images. Note that on the day of induction, there is not IAA signal in the explants treated with 5 µM yucasin.

CHAPTER III

Identification, analysis, and modeling of the YUCCA protein family in genome-wide of *Coffea canephora*

Miguel A. Uc-Chuc¹, Ángela F. Ku-González¹, Irma A. Jiménez-Ramírez¹ and Víctor M. Loyola-Vargas^{1,*}

- 1 Unidad de Bioquímica y Biología Molecular de Plantas, Centro de Investigación Científica de Yucatán, A.C. Calle 43 No. 130 x 32 y 344 Col. Chuburná de Hidalgo, Mérida C.P. 97205, México; miguel.uc@cicy.mx (M.A.U.-C.); angela@cicy.mx (A.F.K.-G.); irma.jimenez@cicy.mx (I.A.J.-R.)

* Correspondence: vmloyola@cicy.mx

Article in review. Proteins.

Abstract: Auxins are involved in almost every aspect of plant growth and development processes, from embryogenesis to senescence. Indole-3-acetic acid (IAA) is the main known natural auxin, which is synthesized by enzymes TRYPTOPHAN AMINOTRANSFERASE OF ARABIDOPSIS (TAA) and YUCCA (YUC) of flavin-containing monooxygenases family (FMO) from the tryptophan-dependent pathway. In the present study, genome-wide identification and comprehensive analysis of the YUC-proteins family were conducted in *Coffea canephora*. A total of 10 members of the *CcYUC* genes family were identified in *C. canephora*. Phylogenetic analysis revealed that the *CcYUC* protein family was evolutionary conserved, and they were formed into four groups. On the other hand, bioinformatics analysis predicted a hydrophobic transmembrane helix (TMH) for a *CcYUC* (YUC10) member only. Isoelectric point (pI), molecular weight (Mw), signal peptide, subcellular localization, and phosphorylation sites were predicted for *CcYUC* proteins. YUCs enzymes require the prosthetic group flavin adenine dinucleotide (FAD) and the cofactor nicotinamide adenine dinucleotide phosphate (NADPH) for their enzymatic activity. Therefore, we include the molecular docking for *CcYUC2*-FAD-NADPH-IPyA and the yucasin. Yucasin is a specific inhibitor for YUC activity. The docking results showed FAD and NADPH binding at the big and small domain sites, respectively, in *CcYUC2*. IPyA poses very close to FAD and the big domain, and yucasin competes for the same site as IPA blocking IAA production.

Keywords: auxin; *Coffea canephora*; IPyA; YUCCA; FMO; yucasin; Docking

3.1. Introduction

Flavin-containing monooxygenases (FMO) display a spectrum of key physiological roles. FMO enzymes are widespread in nature and perform a wide variety of redox reactions, including hydroxylation, reduction, monooxygenation, DNA repair, and cellular signaling (Macheroux et al., 2011). In plants, the YUCCA protein family (YUC) belongs to a class of FMO exclusively involved in auxin biosynthesis (Zhao et al., 2001). Auxin is one of the most important growth regulators mediating signals endogenous to control plant growth and development (Bingsheng et al., 2019).

It is of vital importance to know exactly where auxin is synthesized in plants. It has long been held that auxin is synthesized in young developing leaves. However, it is now known that auxin can be synthesized in many different plant tissues (Chandler, 2009). At the cellular level, the most investigated and accepted pathway for auxin biosynthesis is from the tryptophan-dependent route (Trp) through two enzymatic steps involved tryptophan aminotransferases of arabidopsis (TAA) and YUC flavin-containing monooxygenases (Zhao, 2014). In the TAA/YUC-route, TAA enzymes convert Trp to indole-3-pyruvic acid (IPyA). Then, YUC proteins use IPyA to produce Indole-3-acetic acid (IAA) (Zhao, 2014). IAA is the main known natural auxin, synthesized by TAA/YUC rout (Zhao, 2014). The IAA has a similar structure to the Trp amino acid and is a weak organic acid with an indole ring and an acid carboxyl function (Friml et al., 2003; Paque and Weijers, 2016). In plants, different auxin concentrations affect cell division, differentiation, phyllotaxis, organogenesis, and embryogenesis (Cheng et al., 2006; Cheng et al., 2007; Grones and Friml, 2015; Paque and Weijers, 2016).

It has been reported that during embryogenesis, auxin biosynthesis is to play a critical role because previous studies have shown that auxin biosynthesis is dynamic during embryogenesis (Ribnicky et al., 2002; Ayil-Gutiérrez et al., 2013). Overexpression of *YUC1*, *YUC2*, *YUC4*, and *YUC6* genes increases auxin production in *Arabidopsis thaliana* seedlings (Cheng et al., 2006). Experimental evidence demonstrated that YUC functions as the rate-limiting step of the IPyA pathway, indicating that YUC plays a crucial role in developmental processes regulated by cellular auxin levels (Tsugafune et al., 2017). The

TAA/YUC pathway is also highly conserved throughout the plant kingdom (Stepanova et al., 2011). Auxin biosynthesis through YUCs has been demonstrated in several model species, including *Arabidopsis thaliana* (Dai et al., 2013), *Zea mays* (Gallavotti et al., 2008) *Oryza sativa*, (Mashiguchi et al., 2011; Brumos et al., 2013; Kakei et al., 2017) and *Brachypodium distachyon* (Pacheco et al., 2013).

The redundant function of the proteins YUC has been reported. For example, both *YUC1* and *YUC4* are expressed in discrete groups of cells throughout embryogenesis. Their expression patterns overlap with *YUC10* and *YUC11* during embryogenesis (Cheng et al., 2007). On the other hand, single or double mutants do not affect development, unlike the quadruple mutants of *yuc1 yuc4 yuc10 yuc11* fail to develop a hypocotyl and a root meristem (Cheng et al., 2007). Reverse genetics approaches are useful for studying the functionality of YUCs; however, the use of specific inhibitors outweighs the redundant function. Yucasin is a powerful specific YUC enzyme inhibitor and has been used successfully in several studies (Nishimura et al., 2014; Chen et al., 2016).

Recently, we reported the pattern of expression of *CcYUC1*, *CcYUC3*, *CcYUC4*, *CcYUC6*, and *CcYUC10* during somatic embryogenesis in *Coffea canephora* embryogenesis (Uc-Chuc et al., 2020). Through a pharmacological study, we found that the CcYUC family carries out IAA auxin biosynthesis and that de novo auxin biosynthesis is crucial for somatic initiation embryogenesis (Uc-Chuc et al., 2020).

Despite the great effort that scientific research has provided a clearer picture in the last decade of the enzymes involved in auxin biosynthesis, several questions regarding this process's biochemical mechanisms and subcellular localization have not been elucidated. There are few reported studies in maize and Arabidopsis of auxin biosynthetic activity can be found in microsomal fractions (Kriechbaumer et al., 2015; 2016), and some of auxin biosynthetic proteins showed endoplasmic reticulum (ER)-localization, due to transmembrane helix (TMH) (Kriechbaumer et al., 2016). Eleven members of the *AtYUCs* family have been found to exist in *A. thaliana*, of which *AtYUC4.2* is a splice variant located on the ER in flower (Kriechbaumer et al., 2012). Similarly, *AtYUC5*, *AtYUC8*, and *AtYUC9* were localized in the ER of the root, the rest of the *AtYUC* proteins in the cytosol (Poulet and Kriechbaumer, 2017).

This research presents a deep characterization of CcYUC proteins, based on a phylogenetic and bioinformatic analysis that includes predicting TMH, signal peptide, subcellular localization, phosphorylation sites, modeling, and docking molecular; besides, we performed an auxin immunolocalization assay in explants from in *Coffea canephora*.

Our results suggest that the CcYUCs proteins family are highly conserved and participate in the IAA auxin biosynthesis pathway through the IPyA intermediate in *C. canephora*. We report the prediction of some members of the CcYUC family localized in ER and mitochondria while the majority located in the cytoplasm. The molecular docking study shows the prosthetic group FAD and cofactor NADPH in the large and small domain within the CcYUC2 protein. IPyA binds very closely to FAD, and the yucasin inhibitor competes for the same IPyA binding site.

3.2 Materials and methods

3.2.1 Searching of CcYUC proteins in *C. canephora*

The CcYUCs protein family sequence was obtained from the *C. canephora* genome available online at Coffee Genome Hub (Denoëud et al., 2014 <http://coffee-genome.org/>). Each sequence of the YUC proteins was downloaded in the fasta format. A blast was performed using the NCBI database to verify that the downloaded sequences belong to the FMO. YUC orthologs of other plant species were also downloaded from the NCBI database. This was carried out to find out if there is a phylogenetic relationship with other plant species.

3.2.2 Multiple- sequence alignments and phylogenetic tree construction

Multiple sequence alignment was carried out with MUSCLE software using default parameters. The amino-acid sequence corresponding to CcYUCs families in *C. canephora* was studied for conserved motif analysis. The phylogenetic tree was constructed using the neighbour-joining method with MEGA 7.0 software. The unrooted tree was generated through 1000 bootstrap values for the reliability of the tree.

3.2.3 Prediction of isoelectric point, molecular mass, transmembrane helix, subcellular localization, signal peptide, and phosphorylation sites in CcYUCs proteins in *C. canephora*

Theoretical isoelectric point (pI) and molecular weight (MW) were predicted using the Compute pI/MW tool on the ExPASy server (http://web.expasy.org/compute_pi/). Transmembrane helix (TMH) was analyzed on the TMHMM Server v2.0 (<http://www.cbs.dtu.dk/services/TMHMM-2.0/>) and signal peptide prediction we use SignalP 3.0 (<http://www.cbs.dtu.dk/services/SignalP-3.0/>). The subcellular localization of selected proteins was predicted on the PSORTII (<https://psort.hgc.jp/form2.html/>) and to predicted phosphorylation sites with NetPhosYeast 1.0 Server (<http://www.cbs.dtu.dk/CBS/services/NetPhosYeast/>).

3.2.4 Building of three-dimensional structures (3D), modelling and molecular docking of selected CcYUCs proteins in *C. canephora*.

Nine sequences of *C. canephora* CcYUCs proteins were selected to predict 3D structures (table 4). Each 3D structure was built using the SWISS-MODEL software, accessible via the ExPASy web server (<https://swissmodel.expasy.org/>). Best predicted models were evaluated by Global Model Quality Estimation (GMQE) was assessed after model building using QMEAN global score. The Chimera MatchMaker tool (Pettersen *et al.*, 2004) was used to compare the homology modeling structure of the nine CcYUCs proteins. UCSF Chimera 1.14 software was used to model and visualize the built 3D structures (Pettersen *et al.*, 2004).

Molecular docking experiments were carried out to evaluate the binding properties of FAD, NADPH, IPyA, and yucasin to the predicted CcYUC2 structural model, using the DockThor server (<https://dockthor.lncc.br/v2/>) and HDock server (<http://hdock.phys.hust.edu.cn/>) (Yan *et al.*, 2017; 2020). We chose the 3D structure of CcYUC2 to do molecular docking because it was the model with the highest predicted quality. The DockThor scoring function is based on the MMFF94S force field (de Magalhães *et al.*, 2014). Force field-based functions consist of a sum of energy terms from a classical force field, usually considering the protein-ligand complex's interaction energies and the internal ligand energy. In contrast, the solvation energy can be computed by continuum solvation models

(Guedes, et al., 2018). Standard docking mode was performed using the FAD, NADPH, IPyA, and yucasin PDB structures. The 3D structures of IPyA, FAD, NADPH, and yucasin were built from the molecular formula using the structure edition tool option built structure of the UCSF Chimera 1.14 software. The molecular formulas were downloaded at PubChem <https://pubchem.ncbi.nlm.nih.gov/>. A grid box with blind molecular docking was used to define the docking region. This was done because we do not know the binding sites of the cofactors and the ligand. The parameters are referred to as defaults in DockThor, and the structures with positional root mean square deviation (RMSD) o up to 3 Å were clustered together. All results were analyzed using UCSF Chimera 1.14 Molecular Graphics Systems (Pettersen et al., 2004).

3.2.5 Plant material

C. canephora plantlets were propagated and maintained in MS inorganic culture medium [(Murashige and Skoog 1962) (Phyto Technology Laboratories, M524)] without growth regulators under *in vitro* photoperiod conditions 16/8 h ($150 \mu \text{mol m}^{-2} \text{s}^{-1}$) at $25 \pm 2 \text{ }^\circ\text{C}$. The MS medium contains 29.6 μM thiamine-HCl (Sigma, T3902), 550 μM myo-inositol (Sigma, I5125), 0.15 μM L-cysteine hydrochloride hydrate (Sigma, C8277), 16.24 μM nicotinic acid (Sigma, N4126), 87.64 mM sucrose, and 0.25% (w/v) Culture Gel TM Type I-Bio Tech Grade (Phyto 418 Technology Laboratories, G434), to pH 5.8.

3.2.6 Yucasin treatment

The ES system developed in our laboratory consists of two phases (Quiroz-Figueroa et al., 2006): a pre-treatment stage and then induction. In the pre-treatment, a batch of plantlets *in vitro* was selected and placed in a semisolid medium. The culture medium used was MS medium with 0.54 μM NAA (Sigma N1145) and 2.32 μM Kin (Sigma K0753-5G), for fourteen days under photoperiod conditions (16 h light/8 h dark) at $25 \pm 2 \text{ }^\circ\text{C}$. Yucasin, an inhibitor of the YUC protein function in the auxin biogenesis pathway, [5-(4-chlorophenyl)-4H-1, 2, 4-triazole-3-thiol (Santa Cruz Biotechnology, 233161)] was added to the pre-treatment medium at concentrations at 5 μM . DMSO was added as a control. For the induction, leaves two and three were used. The leaf explants were cut into circles of approximately 0.25 cm in diameter and transferred in 250 mL flasks with 50 mL of auxin-free Yasuda liquid medium (Yasuda et al., 1985) supplemented with 5 μM BA (Phyto

Technology Laboratories, B800). The cultures were incubated in the dark at 25 ± 2 °C and shaking (100 rpm) for 56 days (Quiroz-Figueroa et al., 2006). Samples were taken of induction day for IAA localization. The experiments were performed in biological triplicate.

3.2.7 IAA immunolocalization in leaves explant of *C. canephora*

The plant tissues were fixed in FAA solution [10% formaldehyde (Fischer BioReagents, BP531), 5% acetic acid (Sigma, 695092), and 50% ethanol (Meyer, 0390)] for 72 h in dark conditions at 4 °C. A gradient of sucrose (10, 20, 30%) was made to embed the samples in a PB buffer [10 mM sodium phosphate dibasic (Sigma, S3264) and 2 mM potassium phosphate monobasic (Sigma, P5655)], pH 7.2 (adjusted with NaOH 1 N). The samples were embedded in a Leica tissue freezing medium (Leica Biosystem, Code 14020108926) at -26 °C. The blocks were sectioned at 10 µm with a cryostat (Leica Biosystem CM1950) with low profile blades (Thermo Scientific, 1407060).

Immunolocalization was performed with slight modifications of the protocols previously reported for Ni-can et al. (2013) and Márquez-López et al. (2018). We eliminated paraffin use in this method and replaced it with the Leica tissue freezing medium (Leica Biosystem, Code 14020108926) to embed the tissues. In short, the slides with sample tissue (previously rinsed with 0.1% poly-L-lysine in H₂O) were washed three times with sterile distilled water to remove excess Leica tissue freezing medium, then washed three times with the PB buffer, pH 7.2 (adjusted with NaOH 1 N). Sections were blocked with 3% bovine serum albumin (BSA, Sigma, A2153) in PB for 1 h at 4 °C. After three rinsings with PB, sections were incubated overnight with anti-IAA mouse monoclonal antibody (Sigma, A0855) diluted 1:100 in 1% BSA in PB buffer. After three rinses with PB buffer, sections were incubated for 3 h in darkness with Alexa Fluor 488-labeled anti-mouse IgG antibody (Invitrogen, A-11001) diluted 1:100 in PB. After three washes with PB buffer, the tissue sections were treated with 10 µL of Vectashield mounting medium and DAPI to stain the nuclei of plant cells (Vector Laboratories, H-1200) and stored in the dark for 1 h at 4 °C. The images were obtained using a confocal laser scanning microscope (Olympus, FV1000 SW) and the FV10 ASW 3.1 viewer software. The IAA signal was detected using an excitation wavelength of 488 nm; the emission wavelength was 520 nm. The DAPI staining signal was detected using the excitation wavelength of 405 nm; the emission wavelength was 461 nm.

3.3 Results

3.3.1 Identification of the CcYUC protein family in *C. canephora*

To identify the CcYUC in *C. canephora*, we first performed a genome-wide analysis. The genome was downloaded from the Coffee Genome Hub page (<http://coffee-genome.org/>). The *C. canephora* genome is made up of 11 chromosomes (Denoeud et al., 2014), 130,503 coding sequences (CDS), 25,574 protein-coding genes, 25,573 mRNA, and 25,574 proteins (**Figure 3.1A**).

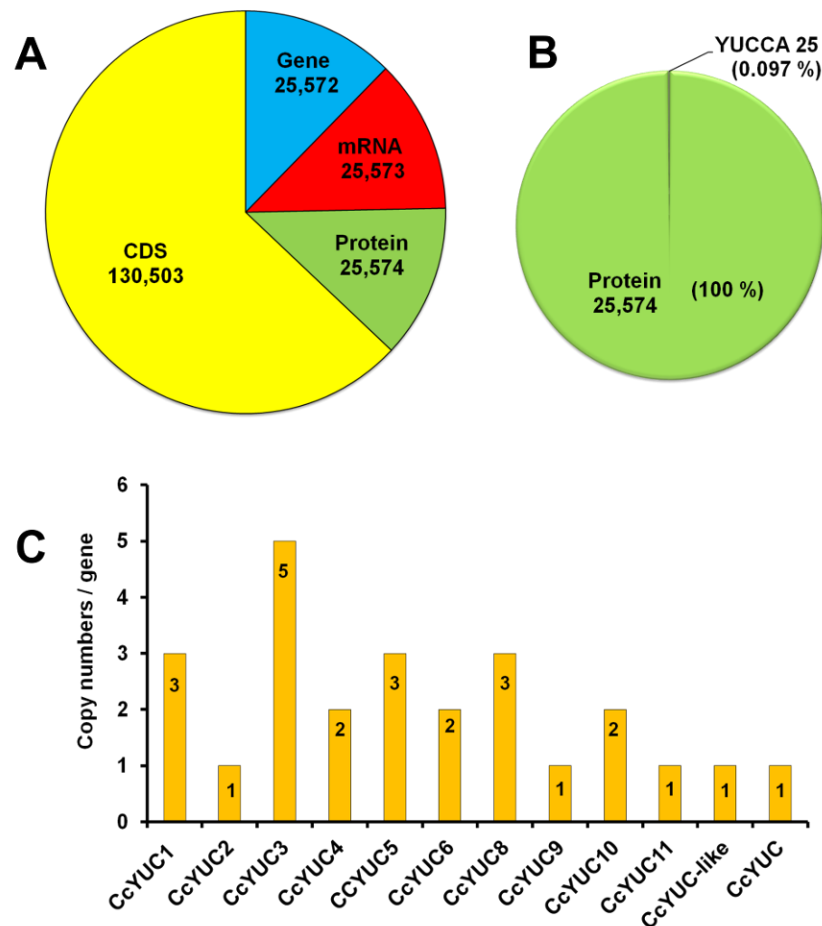


Figure 16 *C. canephora* genome analysis. **A**) cake graph representing the number of CDS coding sequences, genes, mRNAs, and proteins found in the genome. **B**, **C**; percentage and total numbers of CcYUC proteins in the genome, respectively.

A total of 10 members of the CcYUC genes family were identified in the *C. canephora* genome. CcYUC genes were named from CcYUC1 to CcYUC11 [CcYUC1 (three copies), CcYUC2 (one copy), CcYUC3 (five copies), CcYUC4 (two copies), CcYUC5 (three copies), CcYUC6 (two copies), CcYUC8 (three copies), CcYUC9 (one copy), CcYUC10 (two copies), and CcYUC11 (one copy)] (**Figure 3.1C**). We also found two unidentified CcYUC genes, CcYUC-Like and CcYUC. If we group all the copies, we get 25 CcYUC in total. This corresponds to 0.97% of the protein in the entire *C. canephora* genome (**Figure 3.1B**).

3.3.2 Phylogenetic analysis and identification of motifs in CcYUC proteins

We downloaded the protein sequences from the Coffee Genome Hub page (<http://coffee-genome.org/>). Among all the CcYUC copies (**Figure 3.1C**), we found 8 copies that encode peptides less than 200 amino acids length. We discarded those copies because the CDSs produce trick sequences, and it could be pseudogenes. Then, sixteen copies in total were selected for analysis (**Table 3**).

To identify conserved CcYC proteins' conserved regions, multiple alignments were performed using the AtYUC1 (AT4G32540) sequence of *A. thaliana* as reference. As expected, the CcYUC proteins' family members exhibited similar conserved regions. The most highlight characteristics of the FMO are the motif binding FAD and NADPH, which indicated that they might have a close evolutionary relationship (**Figure 3.2**). The protein FMO plus the prosthetic group (FAD) and the cofactor (NADPH) in its 4 α -hydroperoxy flavin forms are crucial to carrying out the enzymatic activity (Ziegler, 1993; Dai et al., 2013).

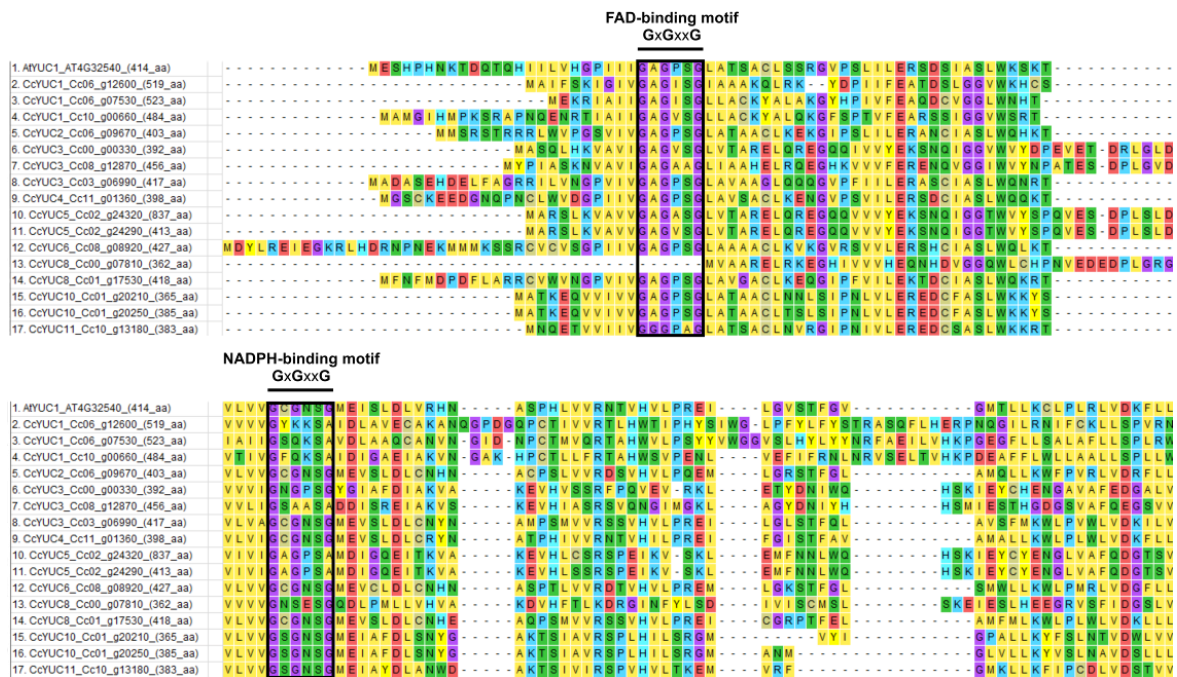


Figure 17 Alignments of multiple sequences of CcYUC proteins family in *C. canephora*. The sequences were aligned using the algorithm MUSCLE (Multiple Sequence Comparison by Log-Expectation) alignment tools with default parameters. The multiple conserved motifs FAD and NADPH are labeled with black boxes.

The sixteen CcYUC proteins of *C. canephora* can be grouped into four different groups (**Figure 3.3**). Five proteins comprise the first group: two copies CcYUC3, two copies CcYUC5 and, one copy CcYUC8. Group two consists of three copies of CcYUC1. The other groups are CcYUC2, 3, 4, 6, 8, and CcYUC10, 11 (**Figure 3.3**). The results of the phylogenetic tree show that CcYUC could have a redundant function in *C. canephora*.

To simplify the analysis of CcYUC proteins in *C. canephora*, we select a copy of each gene and analyze them to research whether there is a phylogenetic relationship with the AtYUC of *Arabidopsis* (**Figure 3.4**). The phylogenetic tree of these proteins shows the same topology to the tree in figure 2. CcYUC2-AtYUC2 they share the 63%, CcYUC6-AtYUC6 the 68%, CcYUC4-AtYUC4 the 58% but 99% with AtYUC1. Although CcYUC1-CcYUC5 comprises the same group with AtYUC10-AtYUC11 and CcYUC10-CcYUC11, they are far apart phylogenetically. The closest phylogenetically are CcYUC3-AtYUC3 with 98% and CcYUC8-AtYUC8 with 99% (**Figure 3.4**).

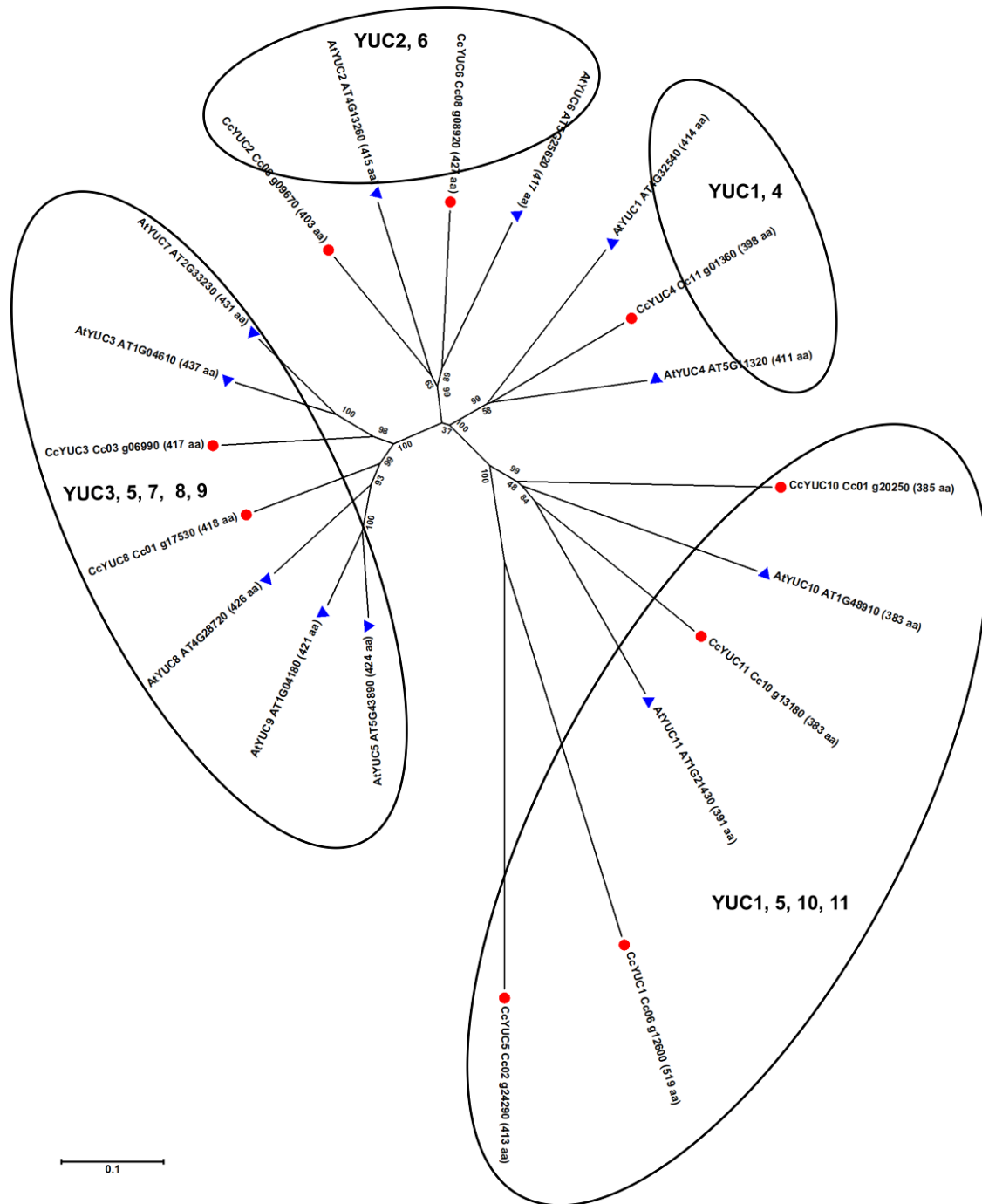


Figure 19 Phylogenetic tree of CcYUC/AtYUC proteins family of the *C. canephora* and *A. thaliana*. Phylogenetic unrooted tree created using the Neighbor-joining statistical method. The number of Bootstrap replications was 5000. The evolutionary distances were computed using the p-distance method. CcYUC of *C. canephora* is marked with red circles, and

AtYUC of *A. thaliana* is marked with blue triangles. The unrooted phylogenetic tree was constructed with MEGA 7.0.

3.3.3 Bioinformatics analysis of CcYUC proteins in *C. canephora*

In silico analysis of CcYUC proteins suggested to be involved in *C. canephora* auxin biosynthesis was carried out. In *A. arabidopsis*, ER-localized and cytosol YUC proteins were reported (Kriechbaumer et al., 2016). In this analysis, the prediction for transmembrane helix and the isoelectric point was included for the CcYUC proteins of *C. canephora*.

The CcYUC proteins selected for this study are shown in **Table 3**. This analysis predicted potential hydrophobic trans-membrane helix (TMH) for CcYUC10 Cc01_g20210 y CcYUC10 Cc01_g20250 (**Table 3**). According to the algorithm TMHMM, both copies of CcYUC10 (Cc01_g20210 and Cc01_g20250) could feature an N-terminal (TMH) between amino acid (aa) 7 and 29 for membrane insertion with the C-terminus facing the cytosol (**Figure 3.5**). In *A. thaliana*, the isoform YUC4.1 was shown to possess a C-terminal TMH with the enzymatic N-terminus facing the cytosol (Kriechbaumer et al., 2012). Not TMH was found in the other CcYUC proteins. In monocots, all proteins in rice and maize feature TMH. In *Musa acuminata*, with the largest number of proteins from the YUC3-7-8-5-9 group, five out of ten feature a predicted TMH. The eudicotyledons group comprises YUC3-7 in *Vitis vinifera*, *Prunus persica*, and *Theobroma cacao* mainly features predicted TMH (Poulet and Kriechbaumer, 2017). The question arose from these data: did CcYUC proteins at some point in evolution lose their TMH, or are they acquired new characteristics? To answer this question, a deeper analysis is required.

On the other hand, the theoretical isoelectric point (pI) and molecular weight (Mw) ranged from 5.92 to 9.26 (average pI = 7.68) and from 39.94 kDa to 95.40 kDa (average Mw = 50.51 kDa), respectively. The detailed information of each CcYUC protein is listed in Table 1, including the gene identifier (ID) in the genome database, the length of the amino-acid sequence, chromosomal location, chromosome position, and TMH predicted.

Table 3. CcYUC family in *C. canephora* used in this study.

Gene Name	ID	Chromosome Localization	Chromosome Position	Protein Length (aa)	pI	MW (kDa)	Trans Membrane Helix (TMH)
CcYUC1	Cc06_g12600	6	10261037..10264096	519	6.14	59.49	0
CcYUC1	Cc06_g07530	6	6035217..6037513	523	8.40	58.91	0
CcYUC1	Cc10_g00660	10	576441..578982	484	8.30	55.31	0
CcYUC2	Cc06_g09670	6	7837742..7840348	403	9.08	44.79	0
CcYUC3	Cc00_g00330	0	547028..549948	392	6.63	44.45	0
CcYUC3	Cc08_g12870	8	28112764..28116360	456	6.42	51.83	0
CcYUC3	Cc03_g06990	3	6115473..6117425	417	8.84	46.75	0
CcYUC4	Cc11_g01360	11	4890835..4893603	398	8.83	44.24	0
CcYUC5	Cc02_g24320	2	21362458..21369747	837	5.92	95.40	0
CcYUC5	Cc02_g24290	2	21335380..21338780	413	6.07	47.29	0
CcYUC6	Cc08_g08920	8	23420828..23423817	427	9.26	47.12	0
CcYUC8	Cc00_g07810	0	64311280..64317805	362	8.12	41.22	0
CcYUC8	Cc01_g17530	1	34801637..34803126	418	8.75	47.05	0
CcYUC10	Cc01_g20210	1	36877928..36879827	365	7.56	39.94	1
CcYUC10	Cc01_g20250	1	36909931..36911809	385	7.57	42.42	1
CcYUC11	Cc10_g13180	10	22975906..22977533	383	7.07	42.00	0

Note. The table shows the protein length in **aa** amino acids. Prediction **pI** isoelectric point and molecular mass in **kDa** using Compute pI/MW tool. For the TMH transmembrane helix, TMHMM server v 2.0 was used.

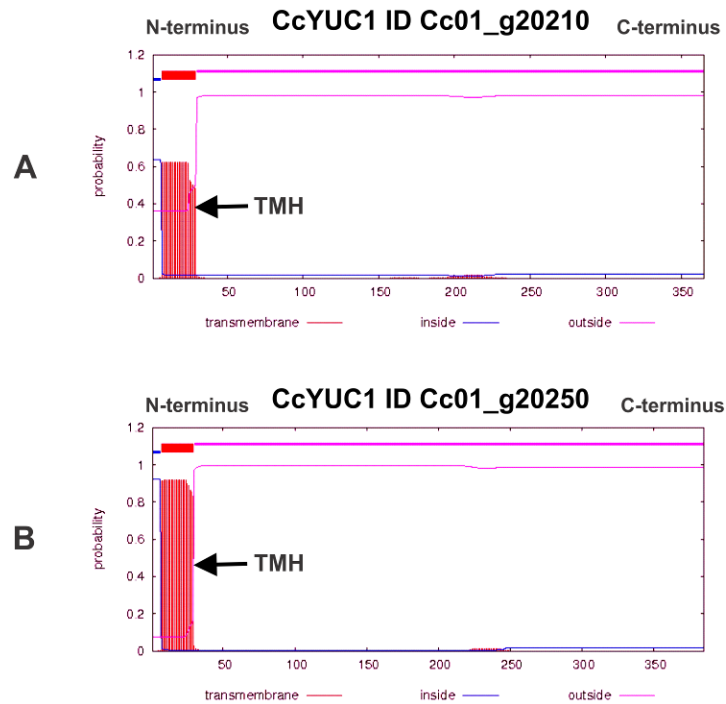


Figure 20 Predicted transmembrane helix (TMH) in the amino acid sequence of A) CcYUC10 Cc01_g20210 and B) CcYUC Cc01_g 20250 auxin biosynthetic proteins in *C. canephora*. Black arrows show the TMH.

Previous reports showed that the Arabidopsis AtYUC4 gene encodes two major splice isoforms resulting in AtYUC4.2 (Kriechbaumer et al., 2012). Besides, it was documented auxin biosynthetic activity can be found in microsomal fractions show in ER localization (Kriechbaumer *et al.*, 2015a), and later the subcellular location of the YUC proteins in the ER was reported (Kriechbaumer et al., 2016).

Therefore, for a more detailed analysis of the CcYUC proteins in *C. canephora*, we include predicting the signal peptide and subcellular localization (**Table 4**). Using the prediction algorithm SignalP 3.0 CcYUC1 (two copies), CcYUC2, CcYUC3 (two copies), CcYUC5 (two copies), and CcYUC10 (two copies) are indicated to possess an N-terminal signal peptide. The most likely cleavage site between aa varies by each CYUC protein (**Table 4**).

The prediction of subcellular localization was performed using the PSORTII program. The prediction showed that more than half of the analyzed CcYUCs proteins were located in the cytoplasm. However, CcYUC2, CcYUC4, and CcYUC5's subcellular localization were mitochondria, ER, and extracellular region, respectively (**Table 4**). Although the subcellular

localization of auxin biosynthetic pathway proteins has been reported in the cytoplasm and ER (Sparkes et al., 2006; Kriechbaumer et al., 2016), there is no experimental evidence of subcellular localization in the mitochondria and the extracellular region; therefore it might suggest other regulatory implications of auxin.

Table 4. The table below shows the prediction of signal peptide, most likely cleavage site, and subcellular location of CcYUCs enzymes in *C. canephora*.

Enzyme Name	ID	Signal Peptide	The most likely cleavage site between aa	Cleavage sequence (-)	Subcellular Localization
CcYUC1	Cc06_g12600	Yes	20 and 21	AAA-KQ	Cytoplasmic
CcYUC1	Cc06_g07530	Yes	23 and 24	ALA-KG	Cytoplasmic
CcYUC1	Cc10_g00660	-	-	-	-
CcYUC2	Cc06_g09670	Yes	28 and 29	ATA-AC	Mitochondrial
CcYUC3	Cc00_g00330	Yes	21 and 22	VTA-RE	Extracellular, including cell wall
CcYUC3	Cc08_g12870	Yes	22 and 23	IAA-HE	Cytoplasmic
CcYUC3	Cc03_g06990	-	-	-	Cytoplasmic
CcYUC4	Cc11_g01360	-	-	-	Endoplasmic Reticulum
CcYUC5	Cc02_g24320	Yes	20 and 21	VTA-RE	Extracellular, including cell wall
CcYUC5	Cc02_g24290	Yes	20 and 21	VTA-RE	Extracellular, including cell wall
CcYUC6	Cc08_g08920	-	-	-	Cytoplasmic
CcYUC8	Cc00_g07810	-	-	-	Cytoplasmic
CcYUC8	Cc01_g17530	-	-	-	-
CcYUC10	Cc01_g20210	Yes	21 and 22	ATA-AC	Cytoplasmic
CcYUC10	Cc01_g20250	Yes	21 and 22	ATA-AC	Cytoplasmic
CcYUC11	Cc10_g13180	-	-	-	Cytoplasmic

Note. To do this, SignalP 3.0 and PSORTII programs were used. (-) cleavage sequence; -, not found.

Posttranslational modifications such as phosphorylation are related to signalling activities and regulatory mechanisms (Juarez-Escobar et al., 2020). There are no reports of posttranslational modification in YUC proteins; therefore, we include predicting phosphorylation sites of CcYUC proteins in *C. canephora*. The NetPhosYeast 1.0 server predicted phosphorylation sites on all selected proteins. **Table 5** lists the analyzed CcYUC proteins, the sequence, and position of the phosphorylated aa. Mostly serine was the phosphorylated aa, and the numbers of phosphorylation sites; it was different from each analyzed protein (**Figure 3.6**). The phosphorylation of an aa residue can cause a conformational change in the protein structure affecting its function. Phosphorylation can control the activity, structure, and cellular location of a protein (Juarez-Escobar et al., 2020).

Table 5. Information on the phosphorylation sites of the selected CcYUCs enzymes in *C. canephora*.

Enzyme	Phosphorylated aa position	Sequence	Protein	Phosphorylated aa position	Sequence
CcYUC1 (519 aa)	36 S	EATDSLGGV	CcYUC2 (403 aa)	3 S	--MMSRSTR
	45 S	WKHCSYRST		111 S	NTVVS AEFD
	53 T	TKLQTPRCD		275 S	LELKSI TGK
	71 S	QRDNSSFPT		280 T	ITGKTPVLD
	143 S	QTSESDTVE		343 S	GKNLSSEED
	285 S	CKLLSPVRN		344 S	KNLSSEEDG
	478 S	ISTFSINHT		378 S	LLGTSMDAR
	505 S	AEAFSPYCS			
509 S	SPYCSQDYQ				
CcYUC3 (417 aa)	5 S	MADASEHDE	CcYUC4 (398 aa)	3 S	--MGSCKEE
	51 S	LERASCIAS		49 S	ILERSDCIA
	114 S	RFNESVQSA		169 S	VRHTSVYKS
	117 S	ESVQSAKYD		175 S	YKSGSEFQD
	135 S	TVVASDNSE		266 T	KRPKTGPIQ
	271 S	IKRPSTGPL		278 T	ATGKTPVLD
	284 T	TEGKTPVLD		376 S	LGTASDAVK
	378 S	RRGLSGASF			
	381 S	LSGASFDAI			
	408 S	QGALSLANR			
	414 T	ANRRTCKS-			
417 S	RTCKS----				
CcYUC5 (413 aa)	4 S	-MARSLKVA	CcYUC6 (427 aa)	63 S	VLERSHCIA
	46 S	TWVYSPQVE		130 S	QSVVSAEYD
	51 S	PQVESDPLS		223 S	NHNASPTLV
	55 S	SDPLSLDPK		243 S	LKNLSGKTP
	83 S	LMGFSDYPF		294 S	MLGKSTFGL
	144 S	ESRRSTCDE		297 T	LSGKTPVLD

	145 T	SRRSTCDEL		316 S	DIKVSPGIQ
	150 S	CDELSSSEE		326 S	LRPLSAEFV
	152 S	ELSSSEEIF		395 S	LLGASMDAK
	179 S	PGIKSWPGK		417 S	SKHFSYFAR
	187 S	KQIHSHNYR		423 S	FARPSSLQS
	227 S	EVHLSSRSP		424 S	ARPSSLQS-
	230 S	LSSRSPEIK		427 S	SSLQS----
	266 S	QDGTVAAD			
	292 T	NDVTIDEN			
	315 S	APGLSFVGL			
CcYUC8 (418 aa)	132 S	VKTVSTNGS	CcYUC10 (385 aa)	104 S	RSVESAQYD
	136 S	STNGSARSD		123 S	RNLGSSDPE
	139 S	GSARSDVEY		124 S	NLGSSDPEE
	273 S	LKRPSLGPL		173 S	KNGKSYENK
	286 T	TKGKTPVLD		187 S	GSGNSGMEI
	299 S	EKIRSGEIN		208 S	IAVRSPLHI
	357 S	GFPKSPFPN		284 S	QKIKSGEIQ
	380 S	RRGLSGASA		295 S	PAVASLGGN
	383 S	LSGASADAT		374 S	LDAQSIAND
	416 S	RRCISQF--			
CcYUC11 (383 aa)	41 S	DCSASLWKK			
	105 S	VESASFDVT			
	122 S	KNALSGAIE			
	204 S	IVIRSPVHV			
	263 T	LKNMTGQSP			
	266 S	MTGQSPVID			
	328 S	KDGTSLFNE			

Note. NetPhosYeast 1.0 Server was used to predict phosphorylation sites. **S**, serine; **T**, tyrosine; **aa**, amino acids.

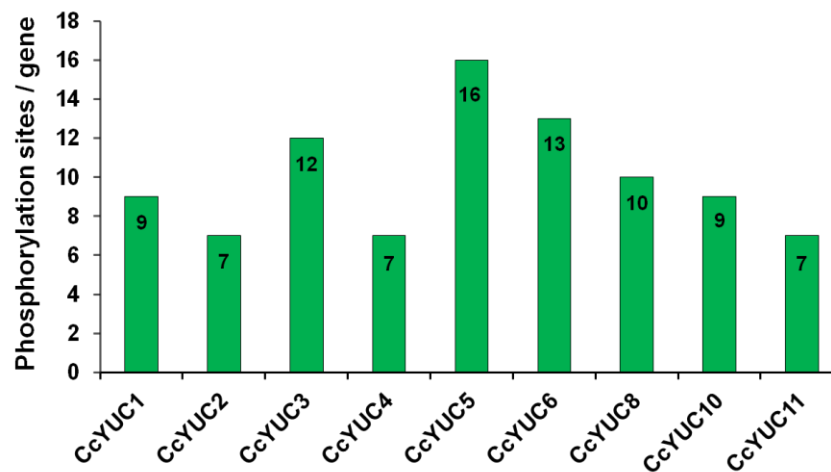


Figure 21 Prediction of CcYUC protein phosphorylation sites in *C. canephora*. The NetPhosYeast 1.0 server was used to predict the phosphorylation sites of nine CcYUC proteins.

3.3.4 3D structure prediction and modelling of the CcYUC proteins family

For further insight on the CcYUC proteins in *C. canephora*, we performed 3D structure prediction of nine CcYUC proteins and the modeling with UCSF Chimera 1.14 software (**Figure 3.7**). The aa sequences of the nine CcYUC proteins were submitted to SWISS-MODEL to predict their 3D structure by homology. All models of the predicted CcYUC proteins are homo-dimers, which comprise chains A and B (**Figure 3.7**). Each chain has, on average, between 15 α -helices and 13 β -strands. CcYUC1 and CcYUC2 were the proteins with the most β -strands, 19 and 16, respectively (**Figure 3.8A-3.8B**).

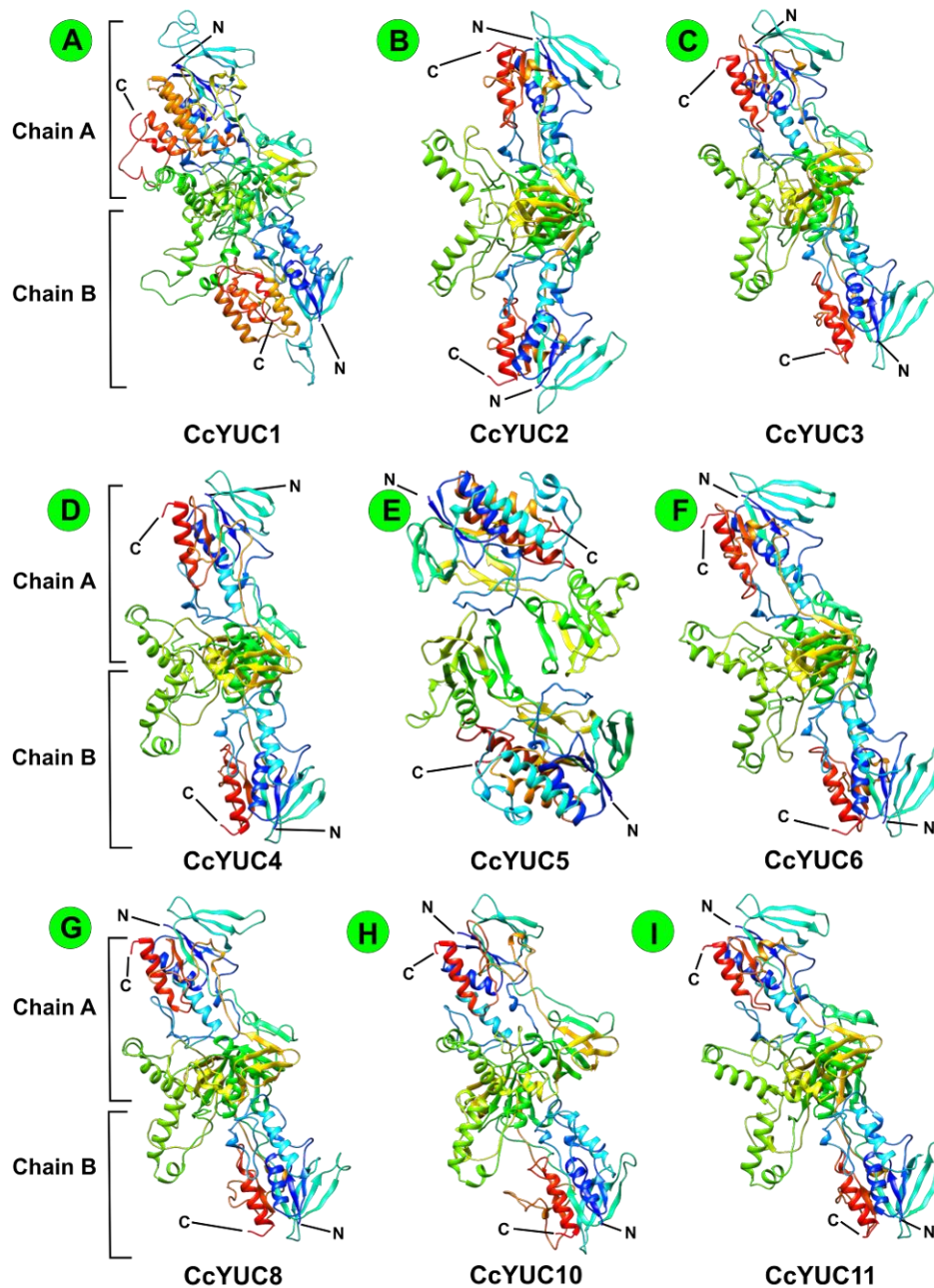


Figure 22 Homology predictions of the 3D structures of nine CcYUC proteins in *C. canephora*. The models built are **A)** CcYUC1, **B)** CcYUC2, **C)** CcYUC3, **D)** CcYUC4, **E)** CcYUC5, **F)** CcYUC6, **G)** CcYUC8, **H)** CcYUC10 and **I)** CcYUC11.

The CcYUC protein family in *C. canephora* is composed of two structural domains (**Figure 3.8**). In CcYUC2, residues 151–330 form a small structural domain, with the remainder of

the polypeptide chain forming the big domain. A channel is present between these two domains, which corresponds to the pocket. An 84-residue-long polypeptide chain segment in a predominantly random coil configuration with three α -helices minor secondary structure elements occurs in the interface between the two domains (**Figure 3.8B**). However, these random coil configuration segments varied for each CcYUC protein as well as the number of residues. Crystallographic studies done with FMO of *Schizosaccharomyces pombe* indicate that this configuration provides stability with the overall domain organization (Eswaramoorthy et al., 2006). The small domain was similar to that reported by Eswaramoorthy et al., 2006. The small domain consists of a five-stranded parallel β -sheet flanked by a three-stranded antiparallel β -sheet and three to four α -helix (**Figure 3.8**).

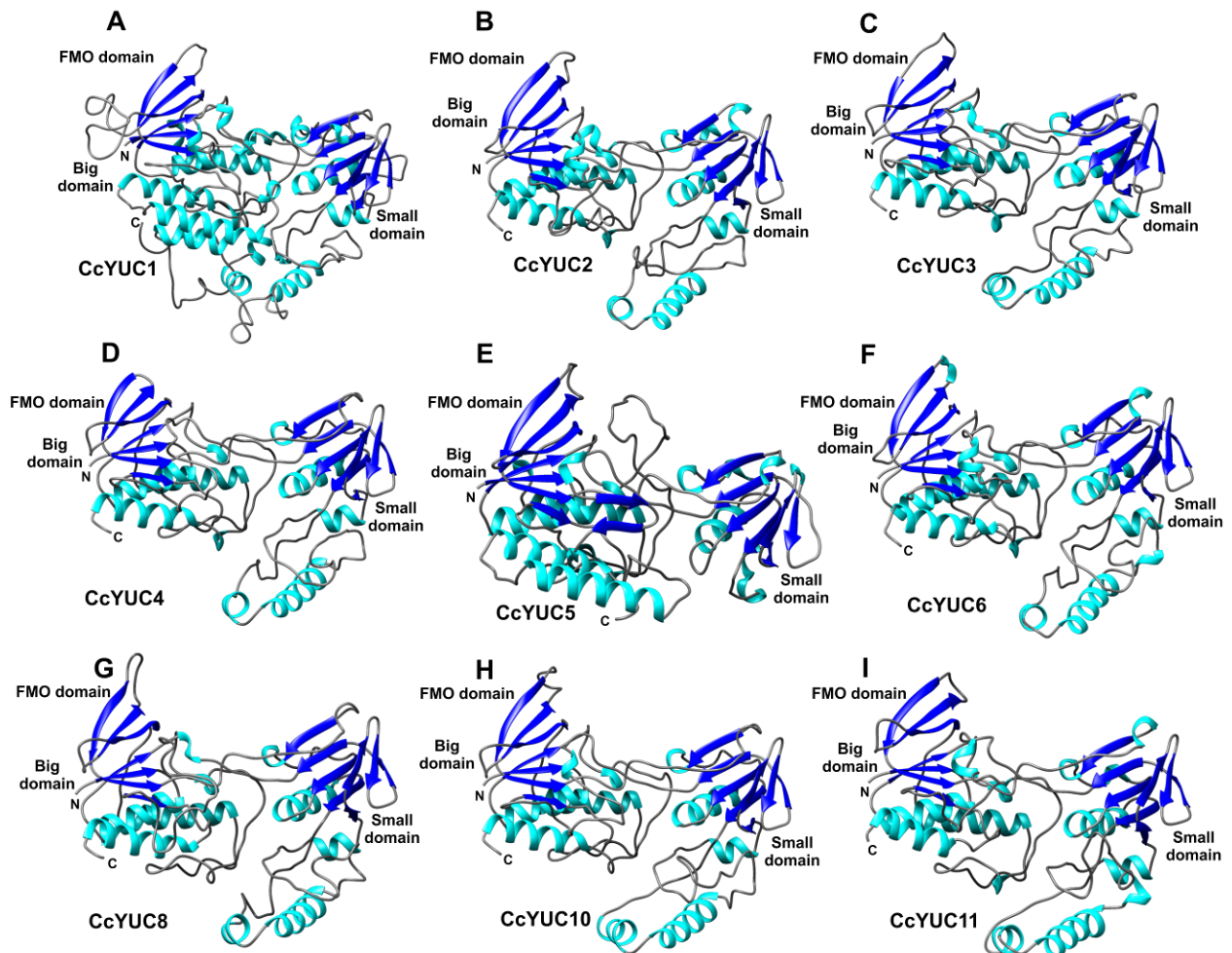


Figure 23 Modeling of the 3D structures of nine proteins of the CcYUC family in *C. canephora*. CcYUC proteins are formed by the big domain and the small domain. The FMO domain is located in the big domain. **D**, CcYUC1; **B**, CcYUC2; **C**, CcYUC3; **D**, CcYUC4; **E**, CcYUC5; **F**, CcYUC6; **G**, CcYUC8; **H**, CcYUC10; **I**, CcYUC11. All images were generated using the UCSF Chimera 1.14 software.

The FMO domain is located in the big domain and consists of a four-stranded parallel β -sheet flanked by a three-stranded antiparallel β -sheet on one side and six α -helices on the other (Eswaramoorthy et al., 2006). All CcYUC 3D structures analyzed in this study have the FMO domain (**Figure 3.8**). However, the FMO domain of CcYUC1 is formed up of a three-stranded parallel β -sheet; that is, it lacks a β -strand (**Figure 3.8A**). The other eight CcYUC proteins conserve a four-stranded parallel β -sheet (**Figure 3.8B-I**).

On the other hand, we aligned CcYUC1-2-3-4-5-6-8-10-11 from *C. canephora* in their homo-dimeric shape (**Figure 3.9**). The result showed that CcYUC5 did not align with the rest of the analyzed CcYUC proteins (**Figure 3.9A**). In CcYUC1, both polypeptide chains (A and B) overhang a helical length. Besides, CcYUC1 protein architecture highlights out in size concerning the aligned CcYUC proteins. We performed the alignment again without including CcYUC1 and CcYUC5; the result showed that CcYUC2-3-4-6-8-10-11 share very similar structures (**Figure 3.9B**). The alignment presented in **Figure 3.9B** showed that seven (CcYUC2-3-4-6-8-10-11) of nine CcYUC proteins are highly conserved in 3D structure.

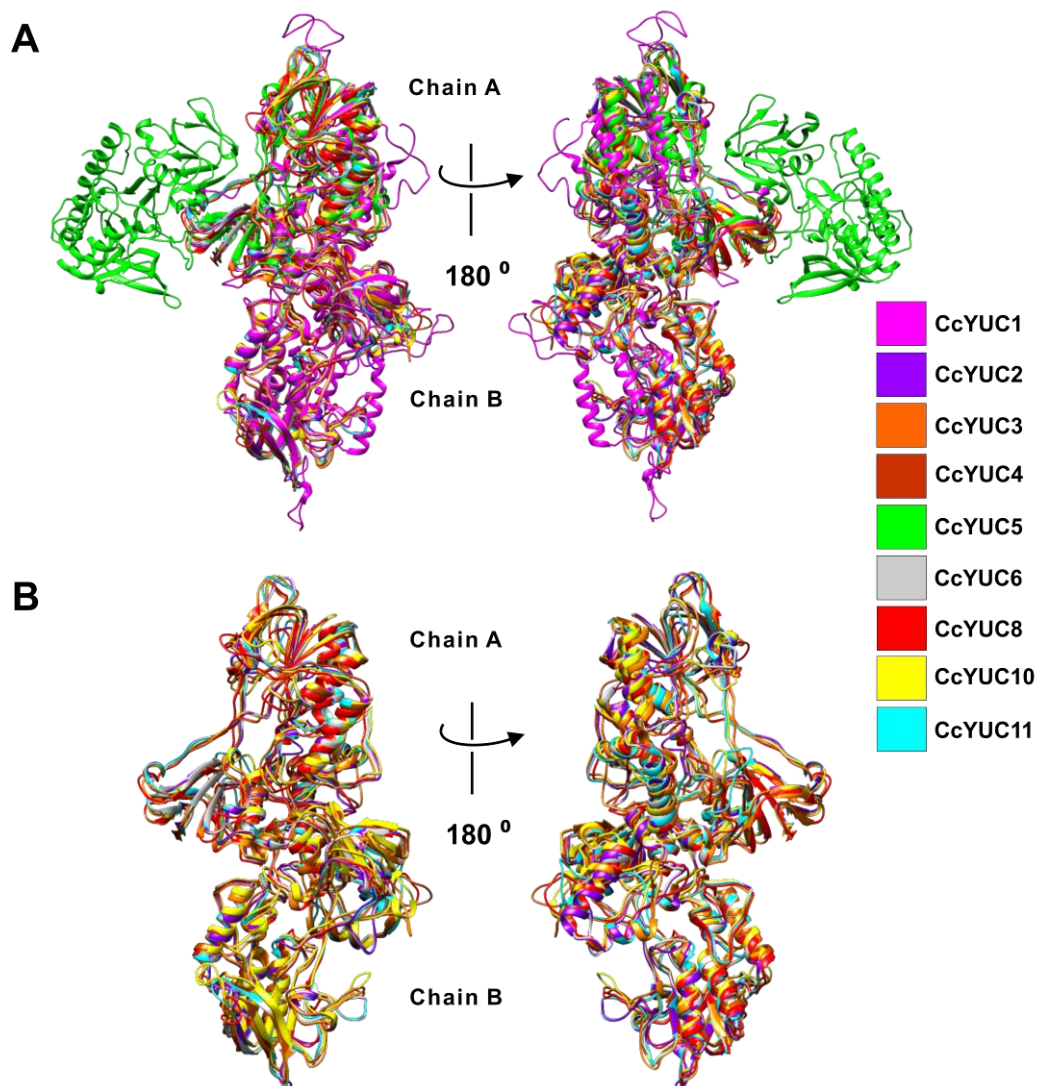


Figure 24 Alignment of the CcYC proteins family in *C. canephora*. **A**, multiple alignments of CcYUC1-2-3-4-5-6-8-10-11. **B**, multiple alignments without CcYUC1 and CcYUC5. The images were generated using UCSF Chimera 1.14 software.

To investigate whether the proteins CcYUC of *C. canephora* are involved in the auxin biosynthesis pathway, it was necessary to perform multiple alignments of the A chains of the proteins CcYUC1-2-3-4-5-6-8-10-11 for identity to FAD and NADPH binding motifs. FAD and NADPH binding motifs are located in the big and small domains, respectively (**Figure 6A-B, 6C-D**). The FAD-binding motifs are highly conserved in the nine proteins

analyzed (**Figure 3.10B**). However, the NADPH-binding motif it was only present in seven CcYUC proteins [CcYUC2-3-4-6-8-10-11] (**Figure 3.10D**) except CcYUC1 and CcYUC5. The alignment between CcYUC 1 and CcYUC5 showed that they share a 22.6% similarity (**Figure 3.10E**). Although the CcYUC1 and CcYUC5 proteins lack the NADPH-binding sequence, CcYUC1 has a structure similar to the NADPH-binding motif (**Figure 3.10F**). It is possible that the CcYUC5 protein has lost the function of auxin synthesis because they lack sequence and structure to the NADPH-motif (**Figure 3.10G**), or it has acquired some unknown function. For this, it is necessary to carry out laboratory experiments to support it. However, these bioinformatic data suggest that the CcYUC proteins have maintained the sequences and structures corresponding to FAD and NAPH throughout evolution. Accordingly, they conserve the function of auxin biosynthesis, except CcYUC5.

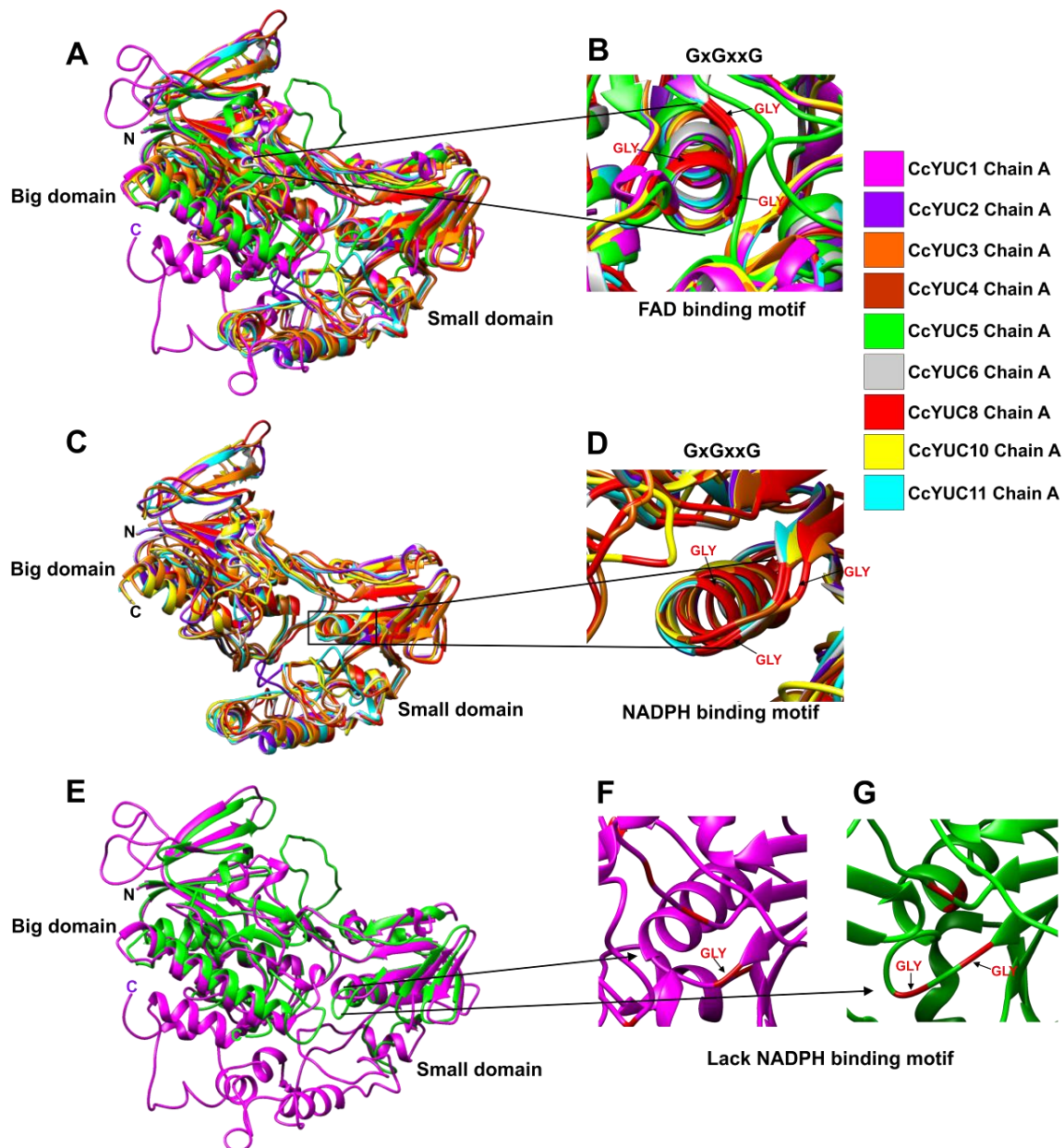


Figure 25 Alignment and identification of FAD and NADPH motifs of CcYUC proteins in *C. canephora*. A-B, alignment and identification of the FAD-binding motif of nine (CYUC1-2-3-4-5-6-8-10-11) CcYUC proteins. C-D, alignment, and identification of the NADPH-binding motifs without CcYUC1, and CcYUC5. E, alignment of CcYUC1, and CcYUC5. F-G, CcYUC1 lacks the FAD motif but retains structure, and CcYUC5 lacks sequence and structure to the NADPH-binding motif. All images were generated using the UCSF Chimera 1.14 software.

3.3.5 Molecular docking

The most conserved route in plants to produce IAA is through IPrA (Zhao et al., 2001). In this pathway, members of the YUC protein family catalyze the last step of conversion from IPrA to IAA (Kakei et al., 2015). To synthesize IAA, YUC enzymes require the FAD prosthetic group and NADPH cofactor for their catalytic function (Nishimura et al., 2017). Although IPrA is its substrate, there are not crystallographic studies showing the binding site. In this study, we also include yucasin. Yucasin has been reported to be a specific inhibitor of YUC protein activity (Nishimura et al., 2014). However, it is unknown is the site of binding in the proteins YUC. That is why we carry out the docking experiment using FAD, NADPH, IPrA, and yucasin as substrates for the CcYUC2 protein of *C. canephora*. Data such as molecular formula, molecular weight, and 2D structure of FAD, NADPH, IPrA, and yucasin were downloaded at PubChem (**Table 4**).

The docking site was located in the cleft formed between the big and small domains (**Figure 3.11B**). FAD is close to nucleotide-binding motif Gly19, Ala20, Gly21, Pro22, Ser23, and Gly24 located in the first strand–turn– helix motif is at the core of the big domain. The residues Gly24, Trp51, Glu148, Asn149, Lys231, Lys279, Thr280, Pro281, Gly368, Thr370, Gly373, Leu374, and Thr377, interact physically with prosthetic group FAD (**Figure 3.11A**). The adenine nucleotide makes hydrogen-bonding contacts with Gly24 of this motif. In total, 13 residues directly interact with FAD through 23 Hydrogen bonds (**Table 4**). IPrA was located near to the flavin of the prosthetic group FAD close small domain (Figure 3.11B-C). Two hydrogen bonds are formed between IPrA and the CcYUC2 protein (**Figure 3.11C and Table 6**). The Ser192 and Asn191 residues interact directly with the amino and carboxyl groups of IPrA; a third hydrogen bond is formed between the carboxyl of IPrA and Hydrogen 17 of FAD (**Figure 3.11C**). The NADPH cofactor is bound to the second nucleotide-binding motif, Gly188, Cys189, Gly190, Asn191, Ser192, and Gly193, which is located at the strand–turn– helix motif within the small domain (**Figure 3.11D**). The anime group of the NADPH cofactor's adenine interacts with Gly269 and Lys279 residues of the CcYUC2 protein. In contrast, the skeleton close to nicotinamide makes two hydrogen-bonding contacts with Asn191 residue of this motif (**Figure 3.11D**). In short, the interaction of the CcYUC2-NADPH complex is given by 12 hydrogen bonds (**Table 6**).

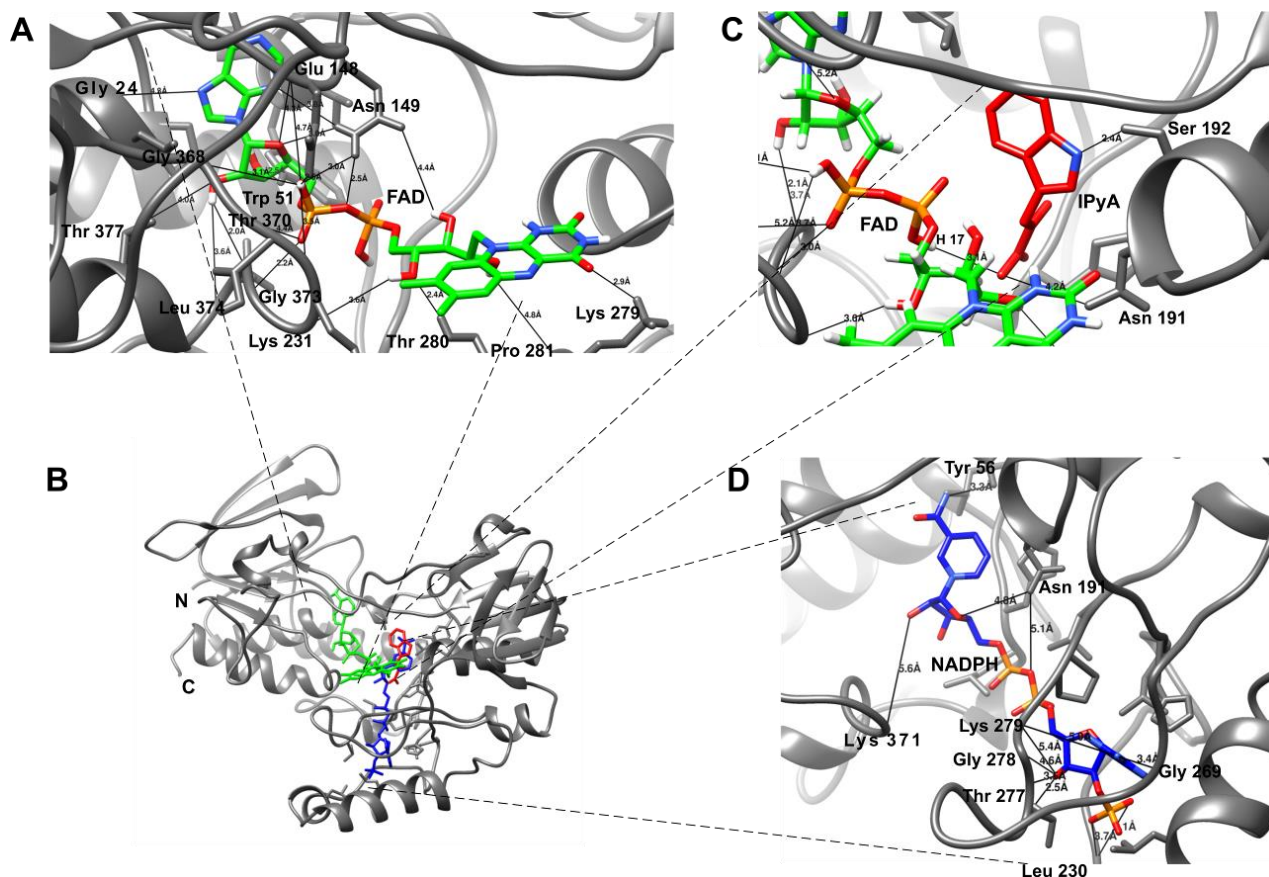
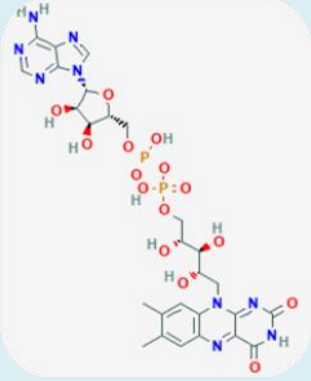
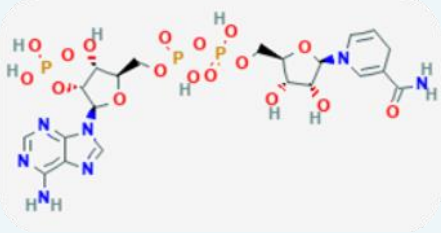
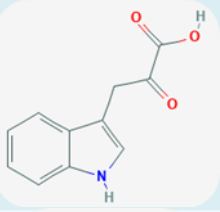
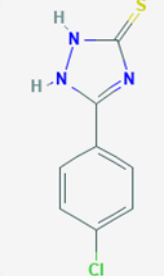


Figure 3.11 CcYUC2–FAD–NADPH–IPA complexes. B, Ribbon diagram derived from the structure of CcYUC2 with FAD A; IPyA C, and NADPH D coloured in green, red, and blue, respectively. All images were generated using the UCSF Chimera 1.14 software.

It has been reported that FAD appears strongly bound to the enzyme FMO, whereas NADPH appears weaker bound in a superficial (Eswaramoorthy et al., 2006). Although there is a difference between the number of hydrogen bonds between CcYUC2-FAD and CcYUC2- NADPH complex, it is understandable that hydrogen bonds are one of the forces that maintain the binding during the protein-substrate complex and provides stability in the protein complex as shown in CcYUC2-IPyA with only two hydrogen bonds (**Figure 3.11C**).

Table 6. Hydrogen bonding interactions between FAD-NADPH-IPyA and Yucasin with residues of the CcYUC2 protein in *C. canephora*.

Ligand	Molecular Formula	Molecular Weight (g/mol)	2D Structure	Residues	H-bond
FAD	$C_{27}H_{33}N_9O_{15}P_2$	785.5		Gly24 Trp51 Glu 48 Asn149 Lys231 Lys279 Thr280 Pro281 Gly368 Thr370 Gly373 Leu374 Thr377	23
NADPH	$C_{21}H_{30}N_7O_{17}P_3$	745.4		Tyr56 Asn191 Leu230 Lys239 Gly269 Thr277 Gly278 Lys371	12
IPyA	$C_{11}H_9NO_3$	203.19		Asn191 Ser192	2
Yucasin	$C_8H_6ClN_3S$	211.67		Tyr56 Ser192	3

Note. The molecular mass of IPyA and yucasin are similar.

3.3.6 Immunolocalization and inhibition of IAA biosynthesis

To confirm that the CcYUC proteins family is involved in the IAA biosynthesis pathway in *C. canephora*, we used yucasin, a specific inhibitor of YUC proteins' functional activity

(Nishimura et al., 2014). Biochemical and genetic studies indicate that plants use Trp as a substrate, converted to IPyA as an intermediary for IAA auxin biosynthesis (Mashiguchi et al., 2011). TAA enzymes convert Trp to IPyA by removing the amino group (Stepanova et al., 2008; 2008; Yamada et al., 2009). Then, the YUC enzymes synthesize IAA using IPyA as a substrate through an oxidative decarboxylation process (Mashiguchi et al., 2011) (**Figure 3.12A**).

On the other hand, Nishimura and colleagues reported that yucasin strongly inhibits YUC1 recombinant protein activity against the substrate IPyA in a competitive manner (Nishimura et al., 2014). The yucasin inhibitor pose in the docking showed that it competes for the same site that IPyA (**Figure 3.12B**). Yucasin interacts with the Tyr56 and Ser192 residues (**Table 6**) of the small domain in the same IPyA binding cavity (**Figure 3.12B**). Also, yucasin is similar in structure and molecular mass to IPyA (**Table 6**); therefore, yucasin can easily bind to CcYUC2, causing enzyme activity inhibition. In this study, we provide a bioinformatics approach to molecular docking between CcYUC2-yucasin. These data suggest that yucasin may inhibit the functional activity of all CcYUC proteins family in *C. canephora*.

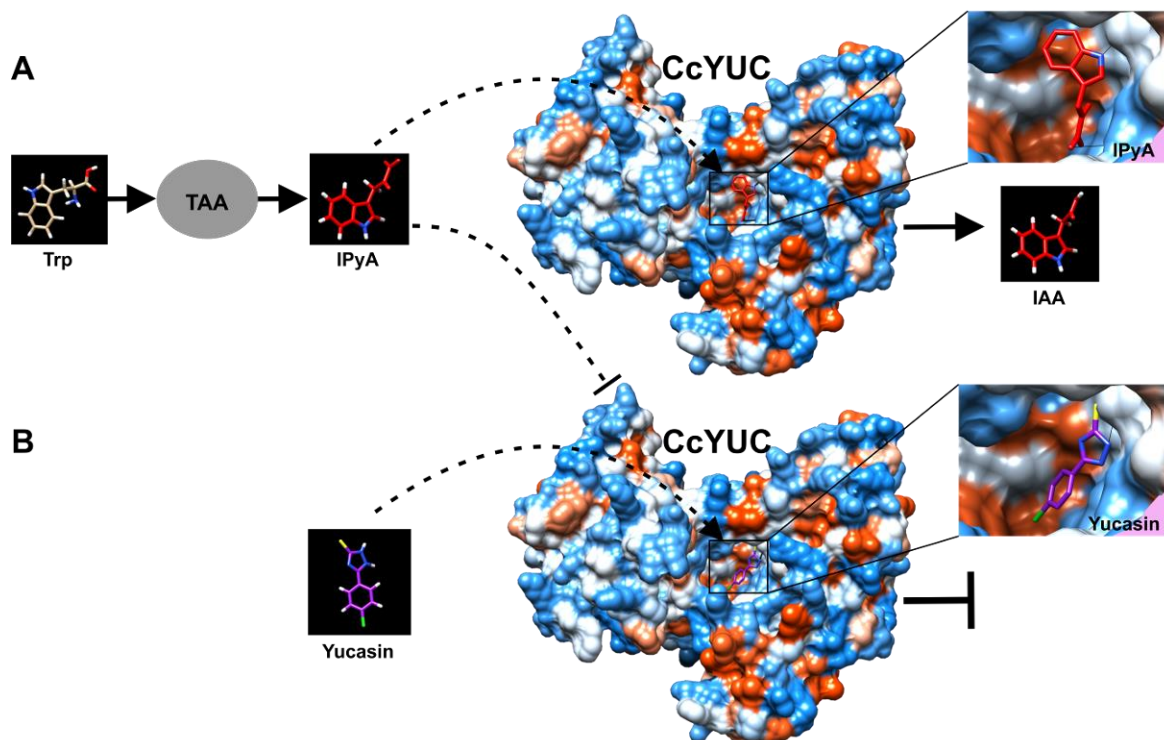


Figure 3.12 Trp-Dependent IAA biosynthesis mechanism and YUC protein functional activity inhibition by yucasin in *C. canephora*. A, the first step is the removal of the amino group from the Trp substrate by the TAA aminotransferases to produce IPyA. The second step is the oxidative decarboxylation of IPyA catalyzed by the CcYUC family to produce IAA. B, yucasin competes with IPyA by the same pocket for inhibiting auxin biosynthesis. A-B, representation of the surface hydrophobicity of the CcYUC-IPA-yucasin complex. In red, the hydrophobic surface and blue, the hydrophilic surface indicate that CcYUC has uneven electrostatic charge distribution.

To examine whether yucasin directly inhibits the conversion of IPyA to IAA by CcYUC, it was necessary to investigate the endogenous location of IAA in foliar explants and second the effect of yucasin. For it, we added 5 μM of yucasin to *C. canephora* seedlings for fourteen days in MS culture medium (pre-treatment with 0.54 μM NAA and 2.32 μM Kin). Next, we select the leaves to generate circular explants of 0.25 cm. The explants were then transferred to an auxin-free medium supplemented with 5 μM benzyladenine (BA). We used an anti-IAA mouse monoclonal primary antibody specific for free IAA and an Alexa Fluor 488-labeled anti-mouse IgG expand secondary antibody.

Immunolocalization assays showed a signal marked of free IAA in explants without yucasin (**Figure 3.13C**). Further, endogenous accumulation was observed at specific sites, such as in the nuclei of mesophyll cells (**Figure 3.13D**). These results suggesting biosynthesis and endogenous accumulation of free IAA in leaf tissue. While in yucasin-treated explants, IAA production was inhibited (**Figure 3.13G; 3.13H**). We recently reported that IAA biosynthesis is necessary for somatic embryogenesis and its inhibition severely affects embryonic process induction in *C. canephora* (Uc-Chu et al., 2020). Additionally, we report the expression of some members of the CcYUC family during the somatic embryogenesis induction process in *C. canephora* (Uc-Chu et al., 2020). The data provided in this study demonstrate that IAA biosynthesis is through the IPyA intermediary and is, in turn, catalyzed by the CcYUC family of proteins in *C. canephora*.

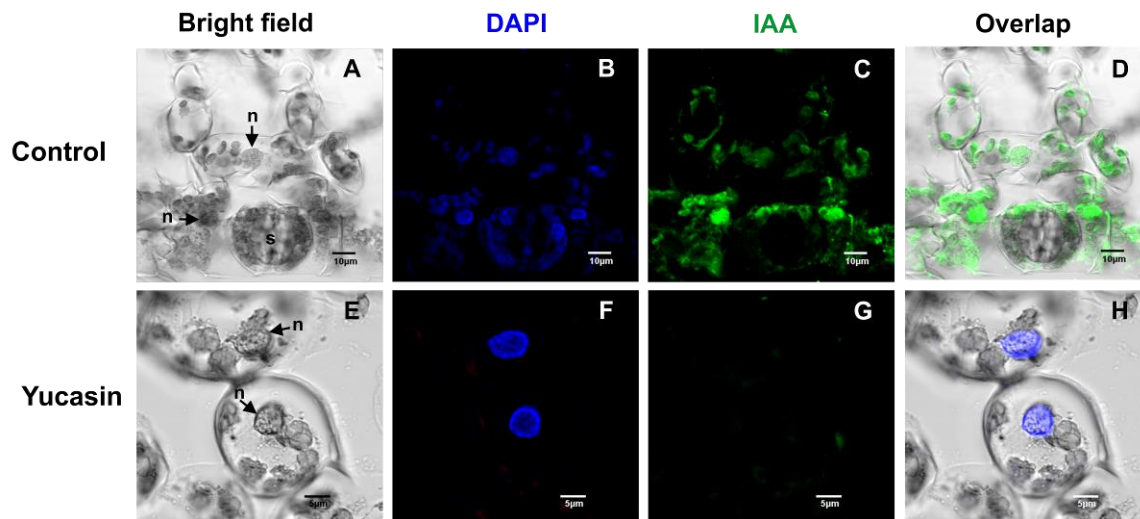


Figure 26 Endogenous immunolocalization of free IAA in leaf explants of *C. canephora*. Confocal microscopy images of cross-sections of leaf explants. Explants treated with (+) and without (-) yucasin. (**A-E**), Bright field; (**B-F**), nuclei staining with blue DAPI; (**C-G**), free IAA signal in green and (**D-H**), merge. Note that panel **C** shows an accumulation of free IAA and panel **G** there is no signal of free IAA due to the action of yucasin. Nucleus **n** and stoma **s**.

3.4 Discussion

Auxin is an essential molecule that controls almost every aspect of plant growth and development. IAA, the most studied nature auxin, is extremely potent because controlling many aspects of plant growth and development, despite its relatively simple chemical

structure. IAA has been found in all plant tissues and controls vascular differentiation, cell division, cell expansion, cell differentiation, organogenesis, and embryogenesis (Quint et al., 2006; Cheng et al., 2006; Cheng et al., 2007; Grones and Friml, 2015; Paque and Weijers, 2016).

Genetic and biochemical studies demonstrate that IAA is mainly synthesized from Trp via IPyA by two-step reactions involving TAA/YUC enzymes (Zhao, 2014). This work presents a deep characterization based on a phylogenetic and bioinformatic analysis of CcYUC proteins in *C. canephora*. We found ten members of the CcYUCs gene family of flavin-containing monooxygenases. We found several copies of the CcYUC genes, such as three copies for CcYUC1-CcYUC3-CcYUC5 and up to five copies of CcYUC3. In total, were 25 copies that encode for YUC-FMO (**Figure 3.1**); surprisingly, only 0.097% corresponds to the total proteins involved in auxin biosynthesis in the *C. canephora*. In Arabidopsis, there are 11 YUC genes for auxin biosynthesis (Cheng et al. 2006, Cheng et al. 2007), 14 in *Medicago truncatula* (Wang et al., 2019), 22 in *Glycine max* (Wang et al., 2017), 14 in *Oryza sativa* (Woo et al., 2007), 14 in *Zea may* (Li et al., 2015) and 6 in *Solanum lycopersicum* (Expósito-Rodríguez et al., 2007). This indicates that the YUC orthologs have been diversified and conserved in plants, including *C. canephora*.

It has been mentioned that the presence of membrane anchoring via TMH in YUC could already be found early on in evolution in mosses (Poulet and Kriechbaumer, 2017). In this study, we found the presence of TMH only in CcYUC10; this could indicate that the rest of the CcYUC lost the TMH to specialize in specific sites because most of the CcYUC showed the presence of having signal peptide sequence. That is possible, thanks to distribution from gene duplications (Poulet and Kriechbaumer, 2017). However, the prediction of CcYUC2 localization in mitochondria remains to be clarified, although the activity of auxin biosynthesis enzymes has already been reported in the ER and cytoplasm (Kriechbaumer et al., 2015). Previous studies have shown that one of the Arabidopsis *AtYUC4* genes exists in two major splice isoforms. *AtYUC4.2* features a C-terminal hydrophobic transmembrane domain (TMD). This TMD was shown to be inserted into the ER membrane, with the remainder of the protein facing the cytosol (Kriechbaumer et al., 2012).

On the other hand, alignment amino acid sequences of the analyzed CcYUC proteins presented the FAD and NADPH binding motifs (**Figure 3.2**). However, CcYUC5 and CcYUC1 lack the NADPH-binding motif, although, in CcYUC1, the three-dimensional structure of the NADPH-binding motif is perfectly preserved (**Figure 3.10F**). YUC proteins have been reported to require FAD and NADPH to generate IAA (Nishimura et al., 2017); therefore, it is possible that CcYUC5 did not participate in IAA biosynthesis or lost the function of producing IAA throughout its evolutionary duplication. Other group members can replace the inability of CcYUC5 to synthesize IAA by the redundant function that exists between the YUC family members (Cheng et al., 2007). CcYUC proteins family in *C. canephora* was grouped in four different groups similar to that reported in *A. thaliana* (Poulet and Kriechbaumer, 2017). Orthologs of *A. thaliana* YUCs genes have been analyzed in various plant species, including tomato, maize, and rice, and appear to be involved in the auxins biosynthesis (Expósito-Rodríguez et al., 2007; Yamamoto et al., 2007).

Additionally, the multiple alignments of the 3D structures of the CcYUC proteins suggest that all the proteins selected for this study are highly conserved (**Figure 6B, 6D**) except YUC5, mentioned earlier (**Figure 3.10G**). However, all CcYUCs proteins in *C. canephora* conserved the FMO domain. Several kinds of FMOs have been described in all kingdoms of life (Schlenk, 1998; Schlaich, 2007; Huijbers et al., 2014). All these enzymes share biochemical, mechanistic, and sequence features. However, they present differences regarding substrate specificity and catalyzed reactions. FMOs use the electrophilic flavin C4 α -hydroperoxide to oxygenate a wide spectrum of organic compounds (Schlenk, 1998). Previous studies suggest that some FMOs do not require the target substrate's presence for the reduction of the FAD by NADPH (Cashman, 2005). Instead, the enzyme-bound NADPH cofactor reacts with molecular oxygen to form the unstable C4 α -hydroperoxyflavin intermediate, which is now primed to function as either an oxygenase (Ziegler, 1993). So far, plant YUC proteins are exclusively involved in auxin biosynthesis using IPyA as a substrate (Zhao et al., 2001). However, some FMO has been associated with systemic acquired resistance (SAR) against pathogens (Mishina and Zeier, 2006).

In summary, auxin biosynthesis via the YUCCA pathway is very well conserved in *C. canephora*. Besides, CcYUC proteins not only are exclusively cytosolic but also could be

linked to the ER-membrane. Interestingly auxin transporters of the PIN family and can also be found in the ER (Kriechbaumer et al., 2015). Furthermore, various networks between auxin and ethylene signaling have been described in the ER (Grefen et al., 2008). Auxin biosynthesis could be regulated by subcellular compartmentation between the cytosol and ER; without forgetting the possible phosphorylation regulation. Furthermore, the use of the yucasin inhibitor is specific to block the catalytic function of YUCs (**Figures 3.12B; 3.13G**); therefore, we can use it to study auxin activity biosynthesis in plants.

ACKNOWLEDGEMENTS

M.A.U.-C. gratefully acknowledges a scholarship from CONACyT for graduate studies.

CONFLICT OF INTEREST

The authors declare no conflict of interest.

AUTHOR CONTRIBUTIONS

M.A.U.-C., A.F.K.-G., and I.A.J.-R., performed the experiments; investigation, M.A.U.-C; writing—original draft preparation, M.A.U.-C; writing—review and editing, V.M.L.-V; funding acquisition, supervision, project administration, editing, review and approval of the manuscript.

Funding: This research was supported by Consejo Nacional de Ciencia y Tecnología CONACYT (Grant FC-1515).

CHAPTER IV

General discussion

Plants rely on diverse endogenous signaling molecules to drive their development and responses to the environment. One of these signaling molecules, IAA auxin, impacts nearly every aspect of plant growth and development, including shoot growth, branching, root growth, cell division, cell expansion, cell differentiation, organogenesis, and embryogenesis (Ribnicky et al., 2002; Quint et al., 2006; Cheng et al., 2006; 2007; Grones and Friml, 2015; Paque and Weijers, 2016). However, the molecular mechanism that regulates auxins' biosynthesis during the somatic embryogenesis induction process remains unknown.

This work shows that IAA auxin biosynthesis is critical at the beginning of SE in *C. canephora* explants (**Figure 3.1**). Furthermore, the results indicate an accumulation of an auxin gradient, and its location in the cell nucleus is central to embryogenic fate. Previous studies have shown that an auxin maximum is required for root meristem maintenance (Nicholas et al., 2018); auxin homeostasis models rely on the coordination of auxin biosynthesis, both in shoot tissues and root tissues, and its cell-to-cell transport via influx and efflux carriers to generate these auxin maxima.

The existence of auxin biosynthesis and the transcriptional activation of auxin biosynthesis genes in wounded foliar explants in *A. thaliana* were reported (Chen et al., 2007; 2016). Similar results were found with the auxin biosynthesis genes CcYUCs in foliar explants of *C. canephora* (**Figure 1.5**). Furthermore, using 3-¹⁴C-Trp, yucasin treatment, and molecular docking suggests de novo auxin biosynthesis via the TAA-YUC pathway using IPyA as a substrate.

Taken together, these results suggest that local auxin biosynthesis in the leaves explants is necessary for the ES in *C. canephora*. The contribution of the leaves explants-derived IPyA biosynthesis pathway is consistent with work showing that auxin biosynthetic pathways are active in the leaves explants during embryogenesis and de novo root organogenesis in Arabidopsis (Chen et al., 2016). On the other hand, a redundant function

of the *YUCs* genes in *C. canephora* is possible, as previously reported in other plant models.

Finally, we found that the *CcYUCs* gene family is highly conserved in our study model and belongs to the enzymes with functional FMO activity. The bioinformatic analysis predicted the subcellular localization sites of the *CcYUC* proteins and the binding sites of the FAD-NADPH-IPyA substrates and the inhibitor yucasin with the *CcYUC2* protein. Few subcellular localization studies have been carried out; however, the existence of auxin biosynthesis proteins in the cytosol and the ER-membrane compartments has been confirmed (Kriechbaumer et al., 2015; (Kriechbaumer et al., 2016). The enzymatic activity of the *CcYUC* proteins is highly dependent on the FAD prosthetic group and the NADPH cofactor (Nishimura et al., 2014). The results obtained in this study showed the presence of FAD and NADPH binding sites in most of the *CcYUCs* proteins analyzed; except *CcYUC5*, which lacks the motif binding NADPH.

Auxin biosynthesis and metabolism have been of interest to the plant community since its discovery. Whereas advances have been made in understanding some points of the homeostasis of auxin, the molecular mechanisms involved in the initiation of embryogenesis are unknown. This doctoral study provides an important advance in understanding the onset of SE in the *C. canephora* model. The leading actor, auxin IAA.

In this work, we provide solid experimental evidence to answer the biological question generated, and at the same time, we check the hypothesis raised. Besides, all the aims of the work were met. Consequently, this work is vital for future generations who are about to tackle the wonderful and complex world of somatic embryogenesis of plants.

CHAPTER V**5.1 CONCLUSIONS**

Auxin is involved in almost every aspect of plant growth and development processes, from embryogenesis to senescence. In this study, we demonstrate that the auxin IAA is crucial during the SE induction process in *C. canephora*. The data presented describe the expression of the CcYUCs genes on day zero of the SE induction process. The location of free IAA on day zero is consistent with gene expression analysis, suggesting de novo biosynthesis of IAA. Also, exogenous application of yucasin inhibited IAA synthesis and blocked SE. In conclusion, the expression levels, the location of IAA and the yucasin inhibitor's use in this investigation provide valuable information for understanding IAA biosynthesis during the SE induction process in *C. canephora*.

IAA is the main known natural auxin, synthesized by TAA and YUC enzymes of the FMO family from the Trp-dependent pathway. In the present work, genome-wide identification and comprehensive analysis of the YUC-proteins family were conducted in *C. canephora*. A total of 10 members of the CcYUC genes family were identified in *C. canephora*. Phylogenetic analysis revealed that the CcYUC proteins family was evolutionary conserved, and they were formed into four groups. On the other hand, the bioinformatic analysis predicted a hydrophobic transmembrane helix (TMH) for a CcYUC (YUC10) member only.

PERSPECTIVES

Based on the results and conclusions presented in this work, future work prospects are oriented in the following directions.

1. In the foreground would be the works to complete the characterization aspects shown *in silico* of the CcYUC proteins. Specifically, the post-translational modifications and subcellular localization of the CcYUC proteins could be studied through mass spectrometry and transmission electron microscopy, respectively.
2. In the background, analyze the expression pattern of the transcription factors *WOXs*, *WIND1* using qRT-PCR. Furthermore, it would be interesting to determine the expression of *IRL* and *GH3* in leaf explants treated with the yucasin inhibitor.
3. Another interesting point to complete would be the enzymatic activity of the proteins CcYUC1 and CcYUC5 because the bioinformatics results suggest that both proteins do not have the binding motifs to NADPH; however, CcYUC1 preserves the binding structure to NADPH.

BIBLIOGRAPHIC REFERENCES

- Adamowski M, Friml J (2015) PIN-dependent auxin transport: Action, regulation, and evolution. *Plant Cell* 27: 20-32.
- Aguilar-Hernández V, Loyola-Vargas VM (2018) Advanced Proteomic Approaches to Elucidate Somatic Embryogenesis. *Front. Plant Sci.* 9, 9, doi:10.3389/fpls.2018.01658.
- Anthony F, Bertrand B, Lashermes P, Charrier A (1997) La biologie moléculaire en appui a l'amélioration génétique du caféier arabica. *Plantations, Recherche, Développement* 6: 369-377.
- Arroyo-Herrera A, Ku-Gonzalez A, Canche-Moo R, Quiroz-Figueroa FR, Loyola-Vargas VM, Rodriguez-Zapata LC, Burgeff-D'Hondt C, Suárez-Solis VM, Castaño E (2008) Expression of WUSCHEL in *Coffea canephora* causes ectopic morphogenesis and increases somatic embryogenesis. *Plant Cell Tiss Org* 94: 171-180, doi.org/10.1007/s11240-008-9401-1.
- Axel Poulet and Verena Kriechbaumer (2017) Bioinformatics Analysis of Phylogeny and Transcription of TAA1YUC Auxin Biosynthetic Genes, *Int. J. Mol. Sci.* 2017, 18, 1791, doi:10.3390/ijms18081791.
- Ayil-Gutiérrez B, Galaz-Ávalos RM, Peña-Cabrera E, Loyola-Vargas VM (2013) Dynamics of the concentration of IAA and some of its conjugates during the induction of somatic embryogenesis in *Coffea canephora*. *Plant Signal. Behav.* 8, e26998, doi:10.4161/psb.26998.
- Bai B, Su YH, Yuan J, Zhang XS (2013) Induction of somatic embryos in *Arabidopsis* requires local YUCCA expression mediated by the down-regulation of ethylene biosynthesis. *Mol Plant* 6: 1247-1260.
- Balzan S, Johal GS, Carraro N (2014) The role of auxin transporters in monocots development. *Front. Plant Sci.* 5, 393, doi:10.3389/fpls.2014.00393.

-
- Barbosa ICR, Hammes UZ, Schwechheimer C (2018) Activation and polarity control of PIN-FORMED auxin transporters by phosphorylation. *Trends in Plant Scienc.* 23 (6):523-538.
- Barbosa IC, Zourelidou M, Willige BC, Weller B, Schwechheimer C. (2014) D6 PROTEIN KINASE activates auxin transport-dependent growth and PIN-FORMED phosphorylation at the plasma membrane. *Dev Cell.*29(6):674-685, doi:10.1016/j.devcel.2014.05.006.
- Bartel B, and Fink GR (1995) ILR1, an amidohydrolase that releases active indole-3-acetic acid from conjugates. *Science* 268, 1745–1748.
- Baudino S, Hansen S, Brettschneider R, Hecht VrF, Dresselhaus T, Lo+êrz H, Dumas C, Rogowsky PM (2001) Molecular characterisation of two novel maize LRR receptor-like kinases, which belong to the SERK gene family. *Planta* 213: 1-10.
- Bertrand B, Nuñez C, Sarah JL (2000) Disease complex in coffee involving *Meloidogyne arabicida* and *Fusarium oxysporum*. *Plant Pathol* 49: 383-388.
- Berthouly M, Michaux-Ferriere NM (1996) High frequency somatic embryogenesis in *Coffea canephora*. *Plant Cell, Tissue Organ Cult. (PCTOC)* 44, 169–176, doi:10.1007/bf00048196.
- Bernardi J, Lanubile A, Li QB, Kumar D, Kladnik A, Cook SD, Ross JJ, Marocco A, Chourey PS (2012) Impaired auxin biosynthesis in the defective endosperm18 mutant is due to mutational loss of expression in the *ZmYuc1* gene encoding endosperm-specific YUCCA1 protein in maize. *Plant Physiol*, 160, 1318–28, doi:10.1104/pp.112.204743.
- Benkova E, Michniewicz M, Sauer M, Teichmann T, Seifertová D, Jürgens G, Friml J (2003) Local, Efflux-Dependent Auxin Gradients as a Common Module for Plant Organ Formation. *Cell*, 115, 591–602, doi:10.1016/s0092-8674(03)00924-3.

-
- Bennett T and Leyser O (2014) The Auxin Question: A Philosophical Overview. In: Zažímalová E., Petrášek J., Benková E. (eds) Auxin and Its Role in Plant Development. Springer, Vienna. 3-19, doi.org/10.1007/978-3-7091-1526-8_1.
- Bingsheng Lv, Zhenwei Yan, Huiyu Tian, Xiansheng Zhang, and Zhaojun Ding (2019) Local Auxin Biosynthesis Mediates Plant Growth and. Trends in Plants Science, Vol 24, Issue 1, doi.org/10.1016/j.tplants.2018.10.014.
- Boutillier K, Offringa R, Sharma VK, Kieft H, Ouellet T, Zhang L, Hattori J, Liu C, Van Lammeren AAM, Miki BLA, Custers JBM, Van Lookeren-Campagne MM (2002) Ectopic expression of BABY BOOM triggers a conversion from vegetative to embryonic growth. Plant Cell 14: 1737-1749.
- Brumos J, Alonso JM, Stepanova AN (2013) Genetic aspects of auxin biosynthesis and its regulation. Physiol. Plant. 151, 3–12, doi:10.1111/ppl.12098.
- Cashman JR (2005) some distinctions between flavin-containing and cytochrome P450 monooxygenases. Biochem Biophys Res Commun 338(1):599-604. doi: 10.1016/j.bbrc.2005.08.009.
- Chandler JW (2009) Local auxin production: a small contribution to a big field. BioEssays 31(1):60-70, doi: 10.1002/bies.080146.
- Chen L, Tong J, Xiao L, Ruan Y, Liu J, Zeng M, Huang H, Wang JW, Xu L (2016) YUCCA-mediated auxin biogenesis is required for cell fate transition occurring during de novo root organogenesis in Arabidopsis. J. Exp. Bot. 67, 4273–84, doi:10.1093/jxb/erw213.
- Cheng Y, Dai X, and Zhao Y (2006) Auxin biosynthesis by the YUCCA flavin monooxygenases controls the formation of floral organs and vascular tissues in Arabidopsis. Genes Dev. 20, 1790–1799.

-
- Cheng Y, Dai X, and Zhao Y (2007) Auxin synthesized by the YUCCA flavin monooxygenases is essential for embryogenesis and leaf formation in *Arabidopsis*. *Plant Cell*. 19, 2430–2439.
- Chugh A, Khurana P (2002) Gene expression during somatic embryogenesis – recent advances. *Curr Sci* 83: 715-730.
- Cohen JD, Hu WS, Ribnicky DM, Cooke TJ (2002) An auxin surge following fertilization in carrots: a mechanism for regulating plant totipotency. *Planta*, 214, 505–509, doi:10.1007/s004250100639.
- Cook SD (2019) An historical review of phenylacetic acid. *Plant and Cell Physiology*. 60 (2): 243–254, <https://doi.org/10.1093/pcp/pcz004>.
- Cook SD, Nichols DS, Smith J, Chourey PS, McAdam EL, Quittenden L, Ross JJ (2016) Auxin biosynthesis: Are the indole-3-acetic acid and phenylacetic acid biosynthesis pathways mirror images? *Plant Physiol* 171: 1230-1241.
- Costanzo E, Trehin C. and Vandenbussche M (2014) The role of WOX genes in flower development. *Annals of Botany* 114: 1545–1553, doi:10.1093/aob/mcu123.
- Dai X, M ashiguchi K, Chen Q, Kasahara H, Kamiya Y et al. (2013) The biochemical mechanism of auxin biosynthesis by an *Arabidopsis* YUCCA flavin-containing monooxygenase. *J. Biol. Chem.* 288:1448–57.
- Dejonghe W, and Russinova E (2014) Target identification strategies in plant chemical biology. *Front. Plant Sci.* 5, 352, doi: 10.3389/fpls.2014.00352.
- De-La-Peña C, Nic-Can GI, Galaz-Ávalos RM, Avilez-Montalvo R, Loyola-Vargas VM (2015) The role of chromatin modifications in somatic embryogenesis in plants. *Front. Plant Sci.* 6, 383, doi:10.3389/fpls.2015.00635.
- Denoeud F, Carretero-Paulet L, Dereeper A, Droc G, Guyot R, Pietrella M, Zheng C, Alberti A, Anthony F, Aprea G et al. (2014) The coffee genome provides

- insight into the convergent evolution of caffeine biosynthesis. *Science*, 345, 1181–1184, doi:10.1126/science.1255274.
- de Vega-Bartol JJ, Simões M, Lorenz WW, Rodrigues AS, Alba R, Dean JF, Miguel CM (2013) Transcriptomic analysis highlights epigenetic and transcriptional regulation during zygotic embryo development of *Pinus pinaster*. *BMC Plant Biol* 13: 1-21.
- De Vega J, Santos RR, Simões M, Miguel CM (2013) Normalizing gene expression by quantitative PCR during somatic embryogenesis in two representative conifer species: *Pinus pinaster* and *Picea abies*. *Plant Cell Rep.* 32, 715–729, doi:10.1007/s00299-013-1407-4.
- Dudits D, Bögre L, Györgyey J (1991) Molecular and cellular approaches to the analysis of plant embryo development from somatic cells in vitro. *J. Cell Sci.*, 99, 473–482.
- Eklund DM, Ishizaki K, Flores-Sandoval E, Kikuchi S, Takebayashi Y, Tsukamoto S, Hirakawa Y, Nonomura M, Kato H, Kouno M, Bhalerao RP, Lagercrantz U, Kasahara H, Kohchi T, Bowman JL (2015) Auxin produced by the indole-3-pyruvic acid pathway regulates development and gemmae dormancy in the liverwort *Marchantia polymorpha*. *Plant Cell* 27: 1650-1669.
- Etienne H (2005) Somatic embryogenesis protocol: Coffee (*Coffea arabica* L. and *C. canephora* P.). In S Jain, P Gupta, eds, *Protocol for Somatic Embryogenesis in Woody Plants*. Forestry Sciences, vol 77. Springer, Dordrecht, doi.org/10.1007/1-4020-2985-3_14.
- Expósito-Rodríguez M, Borges AA, Borges-Pérez A, Hernández M and Pérez JA (2007) Cloning and biochemical characterization of ToFZY, a tomato gene encoding a flavin monooxygenase involved in a tryptophan-dependent auxin biosynthesis pathway. *J. Plant Growth Regul.* 26, 329–340.

- Feng S and Jacobsen SE (2011) Epigenetic modifications in plants: an evolutionary perspective. *Curr. Opin. Plant Biol.* 14, 179–186, doi:10.1016/j.pbi.2010.12.00.
- Florez SL, Erwin RL, Maximova SN, Gultinan MJ, Curtis WR (2015) Enhanced somatic embryogenesis in *Theobroma cacao* using the homologous BABY BOOM transcription factor. *BMC Plant Biol* 15: 1-13.
- Fuentes-Cerda C, Monforte-González M, Méndez-Zeel M, Rojas-Herrera R, Loyola-Vargas VM (2001) Modification of the embryogenic response of *Coffea arabica* by the nitrogen source. *Biotechnol. Lett.* 23, 1341–1343, doi:10.1023/a:1010545818671.
- Furutani M, Vernoux T, Traas J, Kato T, Tasaka M and Mitsuhiro A (2006) PINFORMED1 and PINOID regulate boundary formation and cotyledon development in *Arabidopsis* embryogenesis. *Development* 131:5021-5030.
- France Denoeud, Lorenzo Carretero-Paulet, Alexis Dereeper, et al. (2014) The coffee genome provides insight into the convergent evolution of caffeine biosynthesis, *science*, vol 345 issue 620.
- Friml J, Vieten A, Sauer M, Weijers D, Schwarz H, Hamann T, Offringa R, Jurgens G (2003) Efflux-dependent auxin gradients establish the apical-basal axis of *Arabidopsis*. *Nature* 426: 147-153.
- Gaj M, Zhang S, Harada J, Lemaux P (2005) Leafy cotyledon genes are essential for induction of somatic embryogenesis of *Arabidopsis*. *Planta* 222: 977-988.
- Gallavotti A, Barazesh S, Malcomber S, Hall D, Jackson D, Schmidt RJ, McSteen P (2008) *sparse inflorescence1* encodes a monocot-specific *YUCCA*-like gene required for vegetative and reproductive development in maize. *Proc Natl Acad Sci (USA)* 105: 15196-15201.

-
- Gallei M, Luschnig C, Friml J (2020) Auxin signalling in growth: Schrödinger's cat out of the bag. *Curr. Opin. Plant Boil.* 53, 43–49, doi:10.1016/j.pbi.2019.10.003.
- Grefen C, Stadele K, Ruzicka K, Obrdlík P, Harter K, Horak J (2008) Subcellular localization and in vivo interactions of the *Arabidopsis thaliana* ethylene receptor family members. *Molecular Plant* 1, 308–320.
- Grones P and Friml J (2015) Auxin transporters and binding proteins at a glance. *J Cell Sci* 128: 1-7, doi: 10.1242/jcs.159418.
- Guo F, Liu C, Xia H, Bi Y, Zhao C, Zhao S, Hou L, Li F, Wang X (2013) Induced expression of AtLEC1 and AtLEC2 differentially promotes somatic embryogenesis in transgenic tobacco plants. *PLoS ONE* 8: e71714.
- He W, Brumos J, Li H. et al. (2011) A small-molecule screen identifies l-kynurenine as a competitive inhibitor of TAA1/TAR activity in ethylene-directed auxin biosynthesis and root growth in *Arabidopsis*. *Plant Cell*, 23, 3944–3960.
- Huijbers MM, Montersino S, Westphal AH, Tischler D, van Berkel WJ (2014) Flavin dependent monooxygenases. *Arch Biochem Biophys.* 544:2–17, doi:10.1016/j.abb.2013.12.005.
- Hull AK, Vij R, Celenza JL (2000) *Arabidopsis* cytochrome P450s that catalyze the first step of tryptophan-dependent indole-3-acetic acid biosynthesis. *Proc. Natl. Acad. Sci. USA* 97, 2379–2384, doi:10.1073/pnas.040569997.
- Ivanova A, Velcheva M, Denchev P, Atanassov A, Van Onckelen HA (1994) Endogenous hormone levels during direct somatic embryogenesis in *Medicago falcata*. *Physiol Plant* 92: 85-89.
- Jia W, Li B, Li S, et al., (2016) Mitogen-Activated Protein Kinase Cascade MKK7-MPK6 Plays Important Roles in Plant Development and Regulates Shoot Branching by Phosphorylating PIN1 in *Arabidopsis*. *PLoS*

Biol.14(9):e1002550. Published 2016 Sep 12,
doi:10.1371/journal.pbio.1002550.

Jiménez VM (2001) Regulation of in vitro somatic embryogenesis with emphasis on to the role of endogenous hormones. *Rev Bras Fisiol Veg* 13: 196-223.

John W. Chandler (2009) Local auxin production: a small contribution to a big field. *BioEssays* 31:60–70, doi 10.1002/bies.080146.

Jorin-Novo, J.V., Komatsu S, Weckwerth W, Wienkoop S (eds.) (2020) *Plant Proteomics: Methods and Protocols*, *Methods in Molecular Biology*, vol. 2139, ©Springer Science Business Media, LLC, part of Springer Nature, doi.org/10.1007/978-1-0716-0528-8_14.

Junker A, Mönke G, Rutten T, Keilwagen J, Seifert M, Thi TMN, Renou JP, Balzergue S, Viehöver P, Hähnel U, Ludwig-Müller J, Altschmied L, Conrad U, Weisshaar B, Bäumlein H (2012) Elongation-related functions of LEAFY COTYLEDON1 during the development of *Arabidopsis thaliana*. *Plant J* 71: 427-442.

Kakei Y, Nakamura A, Yamamoto M, Ishida Y, Yamazaki C, et al. (2017) Biochemical and chemical biology study of rice OsTAR1 revealed that tryptophan aminotransferase is involved in auxin biosynthesis; identification of a potent OsTAR1 inhibitor, pyruvamine2031. *Plant Cell Physiol.* 58:598–606.

Kakei Y, Yamazaki C, Suzuki M, Nakamura A, Sato A, Ishida Y, Kikuchi R, Higashi S, Kokudo Y, Ishii T, Soeno K and Shimada Y (2014) Small-molecule auxin inhibitors that target YUCCA are powerful tools for studying auxin function. *The Plant Journal* 84, 827–837, doi: 10.1111/tpj.13032.

Kakei Y, Yamazaki C, Suzuki M, Nakamura A, Sato A, Ishida Y, Kikuchi R, Higashi S, Kokudo Y, Ishii T, Soeno K and Shimada Y (2015) Small-molecule auxin

-
- inhibitors that target YUC CA are powerful tools for studying auxin function. *The Plant Journal*. 84, 827–837, doi: 10.1111/tpj.13032.
- Kasahara H (2015) Current aspects of auxin biosynthesis in plants. *Biosci. Biotechnol. Biochem.* 80, 34–42, doi:10.1080/09168451.2015.1086259.
- Kleine-Vehn J, Huang F, Naramoto S, Zhang J, Michniewicz M, Offringa R, Friml J (2009) PIN auxin efflux carrier polarity is regulated by PINOID kinase-mediated recruitment into GNOM-independent trafficking in Arabidopsis. *Plant Cell* 21: 3839-3849.
- Korasick DA, A Enders T, Strader LC (2013) Auxin biosynthesis and storage forms. *J. Exp. Bot.*, 64, 2541– 2555, doi:10.1093/jxb/ert080.
- Křeček P, Skůpa P, Libus J, Naramoto S, Tejos R, Friml J, Zazimalova E (2009) The PIN-FORMED (PIN) protein family of auxin transporters. *Genome Boil.* 10, 249, doi:10.1186/gb-2009-10-12-249.
- Kriechbaumer, V.; Seo, H.; Park, W.J.; Hawes, C. (2015) Endoplasmic reticulum localization and activity of maize auxin biosynthetic enzymes. *Plant Physiol.* 169, 1933–1945.
- Kriechbaumer V, Botchway SW, Slade SE, Knox K, Frigerio L, Oparka K, Hawes C. (2015b) Reticulomics: Protein-protein interaction studies with two plasmodesmata-localized reticulon family proteins identify binding partners enriched at plasmodesmata, endoplasmic reticulum, and the plasma membrane. *Plant Physiology* 169, 1933–1945.
- Kriechbaumer V, Botchway SW and Hawes C (2016) Localization and interactions between Arabidopsis auxin biosynthetic enzymes in the TAA/YUC-dependent pathway. *Journal of Experimental Botany*, Vol. 67, No. 14 pp. 4195–4207, doi:10.1093/jxb/erw19.

- Kriechbaumer V, Wang P, Hawes C, Abell BM (2012) Alternative splicing of the auxin biosynthesis gene YUCCA4 determines its subcellular compartmentation. *Plant J.* 70, 292–302.
- Korasick D, Enders T A and Strader L C (2013) Auxin biosynthesis and storage forms. *J. Exp. Bot.* 64, 2541–2555.
- Kumar P and Srivastava DK (2015) Biotechnological applications in in vitro plant regeneration studies of broccoli (*Brassica oleracea* L. var. *italica*), an important vegetable crop. *Biotechnol. Lett.*, 38, 561–571, doi:10.1007/s10529-015-2031-x.
- LeClere S, Tellez R, Rampey RA, Matsuda SPT, Bartel B (2002) Characterization of a Family of IAA-Amino Acid Conjugate Hydrolases from *Arabidopsis*. *J. Boil. Chem.* , 277, 20446–20452, doi:10.1074/jbc.m111955200.
- Ledwon A, Gaj M (2009) LEAFY COTYLEDON2 gene expression and auxin treatment in relation to embryogenic capacity of *Arabidopsis* somatic cells. *Plant Cell Rep* 28: 1677-1688.
- Liu J, Sheng L, Xu Y, Li J, Yang Z, Huang H, Xu L (2014) WOX11 and 12 Are Involved in the First-Step Cell Fate Transition during de Novo Root Organogenesis in *Arabidopsis*. *Plant Cell*, 26, 1081–1093, doi:10.1105/tpc.114.122887.
- Li W, Zhao X, Zhang X (2015) Genome-wide analysis and expression patterns of the YUCCA genes in maize. *J. Genet. Genom*, 42, 707–710.
- Liu X, Hegeman AD, Gardner G, Cohen JD (2012) Protocol: High-throughput and quantitative assays of auxin and auxin precursors from minute tissue samples. *Plant Methods*, 8, 31, doi:10.1186/1746-4811-8-31.
- 79 Lotan T, Ohto M, Matsudaira YK, West MAL, Lo R, Kwong RW, Yamagishi K, Fischer RL, Goldberg RB, Harada JJ (1998) *Arabidopsis* LEAFY

COTYLEDON1 is sufficient to induce embryo development in vegetative cells. *Cell* 93: 1195-1205.

Loyola-Vargas VM, Ochoa-Alejo N (2012) Plant cell culture protocols. Methods in molecular biology. Vol. 877. Human Press, Berlin Heidelberg, pp 1-430.

Loyola-Vargas VM and Ochoa-Alejo N (2016) Somatic Embryogenesis. An Overview. In *Somatic Embryogenesis: Fundamental Aspects and Applications*; Springer: Berlin/Heidelberg, Germany; pp. 1–8.

Loyola-Vargas VM, Avilez-Montalvo JR, Aviles-Montalvo RN, Márquez-López RE, Galaz-Ávalos RM, Mellado-Mojica E (2016) Somatic Embryogenesis in *Coffea* spp. In *Somatic Embryogenesis: Fundamental Aspects and Applications*; Springer: Berlin/Heidelberg, Germany,; pp. 241–266.

Lyuqin Chen, Jianhua Tong, Langtao Xiao, Ying Ruan, Jingchun Liu, Minhuan Zeng, Hai Huang, Jia-Wei Wang, and Lin Xu (2016) YUCCA-mediated auxin biogenesis is required for cell fate transition occurring during de novo root organogenesis in *Arabidopsis*. *Journal of Experimental Botany*, Vol. 67, No. 14 pp. 4273–4284, doi:10.1093/jxb/erw213.

Macheroux P, Kappes B, Ealick SE (2011) Flavogenomics a genomic and structural view of flavin dependent proteins, *FEBS J.* 278; 2625–2634.

Magnani E, Jiménez-Gómez JM, Soubigou-Taconnat L, Lepiniec L, Fiume E (2017) Profiling the onset of somatic embryogenesis in *Arabidopsis*. *BMC Genomics* 18: 998.

Márquez-López RE, Pérez-Hernández C, Ku-González Ángela, Galaz-Ávalos RM, Loyola-Vargas VM (2017) Localization and transport of indole-3-acetic acid during somatic embryogenesis in *Coffea canephora*. *Protoplasma*, 255, 695–708, doi:10.1007/s00709-017-1181-1

-
- Mashiguchi K, Tanaka K, Sakai T, et al. (2011) The main auxin biosynthesis pathway in Arabidopsis. *Proc. Nat. Acad. Sci. USA.* 108:18512–18517.
- Ma Q, Zhou W, Zhang P (2015) Transition from somatic embryo to friable embryogenic callus in cassava: dynamic changes in cellular structure, physiological status, and gene expression profiles. *Front. Plant Sci.* 6, 986, doi:10.3389/fpls.2015.00824.
- Méndez-Hernández HA, Ledezma-Rodríguez M, Avilez-Montalvo RN, Juárez-Gómez YL, Skeete A, Avilez-Montalvo J, De-La-Peña C, Loyola-Vargas VM (2019) Signaling Overview of Plant Somatic Embryogenesis. *Front. Plant Sci.*, 10, 77, doi:10.3389/fpls.2019.00077.
- Michalczyk L, Cooke TJ, Cohen JD (1992) Auxin levels at different stages of carrot somatic embryogenesis. *Phytochemistry* 31: 1097-1103.
- Michniewicz M, Zago MK, Abas L, Weijers D, Schweighofer A, Meskiene I, Heisler MG, Ohno C, Zhang J, Huang F, Schwab R, Weigel D, Meyerowitz EM, Luschnig C, Offringa R, Friml J (2007) Antagonistic regulation of PIN phosphorylation by PP2A and PINOID directs auxin flux. *Cell* 130: 1044-1056.
- Mijangos-Cortés J and Loyola-Vargas VM (2004) Somatic embryogenesis: A valuable alternative for propagating selected robusta coffee (*Coffea canephora*) clones. *Vitr. Cell. Dev. Boil. - Anim.*, 40, 95–101, doi:10.1079/ivp2003486.
- Mikkelsen MD, Hansen CH, Wittstock U, et al. (2000) Cytochrome P450 CYP79B2 from Arabidopsis catalyzes the conversion of tryptophan to indole-3-acetaldoxime, a precursor of indole glucosinolates and indole-3-acetic acid. *J. Biol. Chem.* 275:33712–33717, doi:10.1074/jbc.m001667200.

- Mishina TE and Zeier J (2006) The Arabidopsis flavin-dependent monooxygenase FMO1 is an essential component of biologically induced systemic acquired resistance. *Plant Physiol.* 141(4):1666–1675.
- Murashige T and Skoog F (1962) A Revised Medium for Rapid Growth and Bio Assays with Tobacco Tissue Cultures. *Physiol. Plant.*, 15, 473–497, doi:10.1111/j.1399-3054.1962.tb08052.x.
- Nishimura T, Matano N, Morishima T, Kakinuma C, Hayashi Ki, Komano T, Kubo M, Hasebe M, Kasahara H, Kamiya Y, Koshiba T (2012) Identification of IAA transport inhibitors including compounds affecting cellular PIN trafficking by two chemical screening approaches using maize coleoptile systems. *Plant Cell Physiol* 53: 1671-1682.
- Nagashima A, Uehara Y and Sakai T (2008) The ABC subfamily B auxin transporter AtABCB19 is involved in the inhibitory effects of N-1-naphthylphthalamic acid on the phototropic and gravitropic responses of Arabidopsis hypocotyls. *Plant Cell Physiol.* 49, 1250 –1255.
- Naramoto S (2017) Polar transport in plants mediated by membrane transporters: focus on mechanisms of polar auxin transport. *Curr. Opin. Plant Boil.* 40, 8–14, doi:10.1016/j.pbi.2017.06.012.
- Nic-Can GI, Lopez-Torres A, Barredo-Pool F, Wróbel K, Loyola-Vargas VM, Rojas-Herrera R and De-La-Peña C (2013) New Insights into Somatic Embryogenesis: LEAFY COTYLEDON1, BABY BOOM1 and WUSCHEL-RELATED HOMEODOMAIN4 Are Epigenetically Regulated in Coffea canephora. *PLoS ONE*, 8, e72160, doi:10.1371/journal.pone.0072160.
- Nishimura T, Hayashi Ki, Suzuki H, Gyohda A, Takaoka C, Sakaguchi Y, Matsumoto S, Kasahara H, Sakai T, Kato Ji, Kamiya Y, Koshiba T (2014) Yucasin is a potent inhibitor of YUCCA, a key enzyme in auxin biosynthesis. *Plant J* 77: 352-366.

-
- Nolasco M (1985) *Café y sociedad en México*. Centro de Ecodesarrollo, México, pp 1-454.
- Nonhebel HM (2015) Tryptophan-Independent Indole-3-Acetic Acid Synthesis: Critical Evaluation of the Evidence. *Plant Physiol.* 169, 1001–1005, doi:10.1104/pp.15.01091.
- Oochi A, Hajny J, Fukui K, Nakao Y, Gallei M, Quareshy M, Takahashi K, Kinoshita T, Harborough SR, Kepinski S, Kasahara H, Napier R, Friml J, Hayashi K (2019) *Plant Physiology*. 180:1152–1165.
- Pacheco-Villalobos D, Sankar M, Ljung K, Hardtke CS (2013) Disturbed local auxin homeostasis enhances cellular anisotropy and reveals alternative wiring of auxin-ethylene crosstalk in *Brachypodium distachyon* seminal roots. *PLOS Genet.* 9:e1003564.
- Pais MS (2019) Somatic Embryogenesis Induction in Woody Species: The Future After OMICs Data Assessment. *Front. Plant Sci.* 10, 240, doi:10.3389/fpls.2019.00240.
- Patten CL, Glick BR (1996) Bacterial biosynthesis of indole-3-acetic acid. *Can. J. Microbiol.* 42:207–220.
- Paque S and Weijers D (2016) Auxin: the plant molecule that influences almost anything. *BMC Biology* 14: 1-5.
- Peer WA, Blakeslee JJ, Yang H, Murphy AS (2011) Seven Things We Think We Know about Auxin Transport. *Mol. Plant.* 4, 487–504, doi:10.1093/mp/ssr034.
- Petrášek J and Friml J (2009) Auxin transport routes in plant development. *Development*, 136, 2675–2688, doi:10.1242/dev.030353.

- Petrášek J, Malínská K, Zazimalova E (2010) Auxin Transporters Controlling Plant Development. In *Ion Channels and Plant Stress Responses*; Springer: Berlin/Heidelberg, Germany; 7:255–290.
- Petrášek J, Malínská K, Zazimalová E (2011) Auxin transporters controlling plant development transporters and pumps in plant signaling. In M Geisler, K Venema, eds, *Transporters and pumps in plant signaling*. Springer, Berlin Heidelberg 255-290.
- Phillips KA, Skirpan AL, Liu X, Christensen A, Slewinski TL, Hudson C, Barazesh S, Cohen JD, Malcomber S, McSteen P (2011) vanishing tassel2 encodes a grass-specific tryptophan aminotransferase required for vegetative and reproductive development in maize. *Plant Cell*. 23(2):550-66, doi: 10.1105/tpc.110.075267.
- Pierik RLM (1990) Rejuvenation and micropropagation. In HJJ Nijkamp, LHW Van der Plas, J Van Aartrijk, eds, *Progress in plant cellular and molecular biology*, Ed 1. Kluwer Academic Publishers, The Netherlands, pp 91-101.
- Priyono, Florin B, Rigoreau M, Ducos JP, Sumirat U, Mawardi S, Lambot C, Broun P, Pétiard V, Wahyudi T, Crouzillat D (2010) Somatic embryogenesis and vegetative cutting capacity are under distinct genetic control in *Coffea canephora* Pierre. *Plant Cell Rep* 29: 343-357.
- Qian T, Peng Y, Tillmann M, Cohen JD, Slovin JP (2019) Indole-3-acetylaspartate and indole-3-acetylglutamate, the IAA-amide conjugates in the diploid strawberry achene, are hydrolyzed in growing seedlings. *Planta*, 249 (4):1073-1085.
- Quintana-Escobar AO, Nic-Can GI, Avalos RMG, Loyola-Vargas VM, Góngora-Castillo E (2019) Transcriptome analysis of the induction of somatic embryogenesis in *Coffea canephora* and the participation of ARF and Aux/IAA genes. *PeerJ*, 7, e7752, doi:10.7717/peerj.7752.

- Quint M and Gray WM (2006) Auxin signaling. *Curr Opin Plant Biol.* 9(5):448–53.
- Quiroz-Figueroa F, Méndez-Zeel M, Saavedra AL, Loyola-Vargas VM (2001) Picomolar concentrations of salicylates induce cellular growth and enhance somatic embryogenesis in *Coffea arabica* tissue culture. *Plant Cell Rep.* 20, 679–684, doi:10.1007/s002990100386.
- Quiroz-Figueroa F, Fuentes-Cerda C, Rojas-Herrera R, Loyola-Vargas VM (2002) Histological studies on the developmental stages and differentiation of two different somatic embryogenesis systems of *Coffea arabica*. *Plant Cell Rep.* 20, 1141–1149, doi:10.1007/s00299-002-0464-x.
- Quiroz-Figueroa F, Monforte-González M, Galaz-Ávalos RM, Loyola-Vargas VM, Vázquez-Flota F (2005) Direct Somatic Embryogenesis in *Coffea canephora*. In *Plant Cell Culture Protocols*; Springer: Berlin/Heidelberg, Germany; Volume 318, pp. 111–118.
- Quiroz-Figueroa F, Rojas-Herrera R, Galaz-Ávalos RM, Loyola-Vargas VM (2006) Embryo production through somatic embryogenesis can be used to study cell differentiation in plants. *Plant Cell Tissue Organ Cult. (PCTOC)*, 86, 285–301, doi:10.1007/s11240-006-9139-6.
- Rashotte AM, Poupart J, Waddell CS, Muday GK (2003) Transport of the two natural auxins, indole-3-butyric acid and indole-3-acetic acid, in *Arabidopsis*. *Plant Physiol* 133: 761-772.
- Rampey RA, LeClere S, Kowalczyk M, Ljung K, Sandberg G, Bartel B (2004) A Family of Auxin-Conjugate Hydrolases That Contributes to Free Indole-3-Acetic Acid Levels during *Arabidopsis* Germination¹. *Plant Physiol.* 135, 978–988, doi:10.1104/pp.104.039677.
- Ribnicky DM, Cohen JD, Hu WS, and Cooke TJ (2002) An auxin surge following fertilization in carrots: A mechanism for regulating plant totipotency. *Planta* 214: 505–509.

-
- Robert H, Grones P, Stepanova AN, Robles LM, Lokerse AS, Alonso JM, Weijers D, Friml J (2013) Local auxin sources orient the apical-basal axis in *Arabidopsis* embryos. *Curr Biol* 23: 2506-2512.
- Rodríguez-Sanz, H, Solís MT, López MF, Gómez-Cadenas A, Risueño MC Testillano PS (2015) Auxin Biosynthesis, Accumulation, Action and Transport are Involved in Stress-Induced Microspore Embryogenesis Initiation and Progression in *Brassica napus*. *Plant Cell Physiol.* 56, 1401–1417, doi:10.1093/pcp/pcv058.
- Rodríguez-Sanz H, Manzanera JA, Solís MT, Gómez-Garay A, Pintos B, Risueño MC, Testillano PS (2014) Early markers are present in both embryogenesis pathways from microspores and immature zygotic embryos in cork oak, *Quercus suber* L. *BMC Plant Biol* 14: 224.
- Rojas-Herrera R, Quiroz-Figueroa FR, Sánchez-Teyer F, Loyola-Vargas VM (2002) Molecular analysis of somatic embryogenesis: An overview. *Physiol Mol Biol Plants* 8: 171-184.
- Rose RJ (2019) Somatic Embryogenesis in the *Medicago truncatula* Model: Cellular and Molecular Mechanisms. *Front. Plant. Sci.* 10, 267, doi:10.3389/fpls.2019.00267.
- Rupps A, Raschke Juliane, Rümmler Martin, Linke Bettina, Zoglauer Kurt, (2016) Identification of putative homologs of *Larix decidua* to BABYBOOM (BBM), LEAFY COTYLEDON1 (LEC1), WUSCHEL-related HOMEODOMAIN-BOX2 (WOX2) and SOMATIC EMBRYOGENESIS RECEPTOR-like KINASE (SERK) during somatic embryogenesis *Planta*; 243(2):473-88, doi: 10.1007/s00425-015-2409-y.
- Santana N, Gonzalez ME, Valcarcel M, Canto-Flick A, Hernández MM, Fuentes-Cerda FJ, Barahona F, Mijangos-Cortes J, Loyola-Vargas VM (2004) Somatic embryogenesis: A valuable alternative for propagating selected robusta coffee (*Coffea canephora*) clones. *Vitr. Cell. Dev. Boil. - Anim.* 40, 95–101, doi:10.1079/ivp2003486.

-
- Santana-Buzzy N, Rojas-Herrera R, Galaz-Ávalos RM, Ku-Cauich JR, Mijangos-Cortés J, Gutiérrez-Pacheco LC, Canto A, Quiroz-Figueroa F, Loyola-Vargas VM (2007) Advances in coffee tissue culture and its practical applications. *Vitr. Cell. Dev. Boil. - Anim.*, 43, 507–520, doi:10.1007/s11627-007-9074-1.
- Schlauch NL (2007) Flavin-containing monooxygenases in plants: looking beyond detox. *Trends Plant Sci.* 12(9):412–418, doi: 10.1016/j.tplants.2007.08.009.
- Schlenk D (1998) Occurrence of flavin-containing monooxygenases in non-mammalian eukaryotic organisms. *Comp Biochem Physiol C Pharmacol Toxicol Endocrinol.* 121(1–3):185– 95.
- Schoof H, Lenhard M, Haecker A, Mayer KFX, Jürgens G, Laux T (2000) The stem cell population of Arabidopsis shoot meristems is maintained by a regulatory loop between the CLAVATA and WUSCHEL genes. *Cell* 100: 635-644.
- Sitbon F, Åstot C, Edlund A, Crozier A, Sandberg G (2000) The relative importance of tryptophan-dependent and tryptophan-independent biosynthesis of indole-3-acetic acid in tobacco during vegetative growth. *Planta*, 211, 715–721, doi:10.1007/s004250000338.
- Sparkes IA, Runions J, Kearns A, Hawes C. (2006) Rapid, transient expression of fluorescent fusion proteins in tobacco plants and generation of stably transformed plants. *Nature Protocols* 1, 2019 -2025.
- Stepanova AN, Robertson-Hoy J, Yun J, Benavente LM, Xie D, Dolezal K, Schlerentz A, Jurgens G and Alonso JA (2008) TAA1-Mediated Auxin Biosynthesis Is Essential for Hormone Crosstalk and Plant Development. *Cell* 133, 177–191, doi 10.1016/j.cell.2008.01.047.
- Stepanova A N, Yun J, Robles LM, Novak O, He W, et al. (2011) The Arabidopsis YUCCA1 flavin monooxygenase functions in the indole-3-pyruvic acid branch of auxin biosynthesis. *Plant Cell* 23:3961–73.

-
- Stone SL, Kwong LW, Yee KM, Pelletier J, Lepiniec L, Fischer RL, Goldberg RB, Harada JJ (2001) Leafy cotyledon encodes a B3 domain transcription factor that induces embryo development. *Proc Natl Acad Sci (USA)* 98: 11806-11811.
- Subramaniam Eswaramoorthy, Jeffrey B. Bonanno, Stephen K. Burley, and Subramanyam Swaminathan (2006) Mechanism of action of a flavin-containing monooxygenase. *Proceedings of the National Academy of Sciences of the United States of America*. 103 (26) 9832-9837, doi.org/10.1073/pnas.0602398103.
- Sugawara S, Mashiguchi K, Tanaka K, Hishiyama S, Sakai T, Hanada K, Kinoshita-Tsujimura K, Yu H, Dai X, Takebayashi Y, Takeda-Kamiya N, Kakimoto T, Kawaide H, Natsume M, Estelle M, Zhao Y, Hayashi Ki, Kamiya Y, Kasahara H (2015) Distinct characteristics of indole-3-acetic acid and phenylacetic acid, two common auxins in plants. *Plant Cell Physiol* 56: 1641-1654.
- Sugawara, S., Hishiyama, S., Jikumaru, Y., Hanada, A., Nishimura, T., Koshiba, T., Zhao, Y., Kamiya, Y., Kasahara, H. (2009) Biochemical analyses of indole-3-acetaldoxime-dependent auxin biosynthesis in *Arabidopsis*. *Proc. Natl. Acad. Sci. (USA)*. 106, 5430-5435, <https://doi.org/10.1073/pnas.0811226106>.
- Swarup R, Kramer EM, Perry P, Knox K, Leyser HMO, Haseloff J, Beemster GTS, Bhalerao R, Bennett MJ (2005) Root gravitropism requires lateral root cap and epidermal cells for transport and response to a mobile auxin signal. *Nat Cell Biol* 7: 1057-1065.
- Tahara M, Nakanishi T, Yasuda T, Yamaguchi T (1995) Histological and biological aspects in somatic embryogenesis of *Coffea arabica*. In 16^e Colloque Scientifique Internationale sur le Café, Association Scientifique Internationale du Café: Paris, France; 860–867.

-
- Tao Y, Ferrer JL, Ljung K, Pojer F, Hong F, Long JA, Li L, Moreno JE, Bowman ME, Ivans LJ, Cheng Y, Lim J, Zhao Y, Ballaré CL, Sandberg G, Noel JP, Chory J (2008) Rapid synthesis of auxin via a new tryptophan-dependent pathway is required for shade avoidance in plants. *Cell* 133: 164-176.
- Tang Q, Yu P, Tillmann M, Cohen JD, Slovin JP (2018) Indole-3-acetylaspartate and indole-3-acetylglutamate, the IAA-amide conjugates in the diploid strawberry achene, are hydrolyzed in growing seedlings. *Planta*, 249, 1073–1085, doi:10.1007/s00425-018-3061-0.
- Tanaka H, Kitakura S, Rakusová H, et al. Cell polarity and patterning by PIN trafficking through early endosomal compartments in *Arabidopsis thaliana*. *PLoS Genet.* 2013;9(5):e1003540. doi:10.1371/journal.pgen.1003540.
- Tsugafune S, Mashiguchi K, Fukui K, Takebayashi Y, Nishimura T, Sakai T, Shimada Y, Kasahara H, Koshiba T, Hayashi KI (2017) Yucasin DF, a potent and persistent inhibitor of auxin biosynthesis in plants. *Sci. Rep.* 7, 13992, doi:10.1038/s41598-017-14332-w.
- Tusnady GE, Sarkadi B, Simon I, Varadi A (2006) Membrane topology of human ABC proteins. *FEBS Lett* 580(4):1017-22, doi: 10.1016/j.febslet.2005.11.040.
- Tvorogova E, Fedorova V, Potsenkovskaya YA, Kudriashov EA, Efremova AA, Kvitkovskaya EP, Wolabu VA, Zhang TW, Tadege F, Lutova MLA (2019) The WUSCHEL-related homeobox transcription factor MtWOX9-1 stimulates somatic embryogenesis in *Medicago truncatula*. *Plant Cell, Tissue Organ Cult. (PCTOC)*, 138, 517–527, doi:10.1007/s11240-019-01648-w.
- Uc-Chuc Miguel A, Pérez-Hernández Cleyre, Galaz-Ávalos Rosa M, Brito-Argaez Ligia, Aguilar-Hernández Víctor and Loyola-Vargas VM (2020) YUCCA-Mediated Biosynthesis of the Auxin IAA is Required during the Somatic

-
- Embryogenic Induction Process in *Coffea canephora*. *Int. J. Mol. Sci.* 2020, 21, 4751; doi:10.3390/ijms21134751.
- van der Graaff E, Laux T, Rensing SA (2009) The WUS homeobox-containing (WOX) protein family. *Genome Biol* 10(12):248, doi: 10.1186/gb-2009-10-12-248.
- Vogel G (2005) How does a single somatic cell become a whole plant? *Science* 309 (5731) 86, doi: 10.1126/science.309.5731.86.
- Wang B, Chu J, Yu T, Xu Q, Sun X, Yuan J, Xiong G, Wang G, Wang Y, Li J (2015) Tryptophan-independent auxin biosynthesis contributes to early embryogenesis in *Arabidopsis*. *Proc. Natl. Acad. Sci. USA.* 112, 4821–6, doi:10.1073/pnas.1503998112.
- Wang Y, Liu H, Wang S, Li H (2017) Genome-wide identification and expression analysis of the YUCCA gene family in soybean (*Glycine max* L.). *Plant Growth Regul.* 81, 265–275.
- Wang Y, Yang W, Zuo Y, Zhu L, Hastwell AH, Chen L, Tian Y, Su C, Ferguson BJ, Li X (2019) GmYUC2a mediates auxin biosynthesis during root development and nodulation in soybean. *J. Exp. Bot.* 70, 3165–3176.
- Weijers D, Sauer M, Meurette O, Friml J, Ljung K, Sandberg G, Hooykaas P, Offringa R (2005) Maintenance of embryonic auxin distribution for apical-basal patterning by PIN-FORMED-dependent auxin transport in *Arabidopsis*. *Plant Cell* 17: 2517-2526.
- Weijers D, Wagner D (2016) Transcriptional responses to the auxin hormone. *Annu Rev Plant Biol* 67:539–574, doi:10.1146/annurev-arplant-043015-112122.
- Weller B, Zourelidou M, Frank L, Barbosa ICR, Fastner A, Richter S, Jürgens G, Hammes UZ, Schwechheimer C (2004) Dynamic PIN-FORMED auxin efflux

carrier phosphorylation at the plasma membrane controls auxin efflux-dependent growth. *Proc Natl Acad Sci U S A.* 31:114(5), doi:10.1073/pnas.1614380114.

Westfall CS, Herrmann J, Chen Q, Wang S, and Jez JM (2010) Modulating plant hormones by enzyme action: the GH3 family of acyl acid amido synthetases. *Plant Signal. Behav.* 5, 1607–1612, doi:10.4161/psb.5.12.13941.

West MAL, Yee KM, Danao J, Zimmerman JL, Fischer RL, Goldberg RB (1994) LEAFY COTYLEDON 1 is an essential regulator of late embryogenesis and cotyledon identity in Arabidopsis. *Plant Cell* 6: 1731-1745.

Wightman F, Lighty DL (1982) Identification of phenylacetic acid as a natural auxin in the shoots of higher plants. *Physiol Plant* 55: 17-24.

Wójcik AM, Nodine MD, Gaj MD (2017) miR160 and miR166/165 Contribute to the LEC2-Mediated Auxin Response Involved in the Somatic Embryogenesis Induction in Arabidopsis. *Front. Plant Sci.* 8:2024, doi.org/10.3389/fpls.2017.02024.

Wójcikowska B and Gaj MD (2016) Somatic Embryogenesis in Arabidopsis. In *Somatic Embryogenesis: Fundamental Aspects and Applications*; Springer: Berlin/Heidelberg, Germany; pp. 185–199.

Woo YM, Park HJ, Su'udi M, Yang JI, Park JJ, Back K, Park YM, An G (2007) Constitutively wilted 1, a member of the rice YUCCA gene family, is required for maintaining water homeostasis and an appropriate root to shoot ratio. *Plant Mol. Biol.* 65, 125–136.

Woodward, A. W., and Bartel, B. (2005) Auxin: regulation, action, and interaction. *Ann. Bot.* 95, 707–735.

-
- Xinhua Dai, Kiyoshi Mashiguchi, Qingguo Chen, Hiroyuki Kasahara, Yuji Kamiya, Sunil Ojha, Jennifer DuBois, David Ballou, and Yunde Zhao (2013) The Biochemical Mechanism of Auxin Biosynthesis by an Arabidopsis YUCCA Flavin-containing Monooxygenase. JOURNAL OF BIOLOGICAL CHEMISTRY 288(3):1448 –145.
- Xu D, Miao J, Yumoto E, Yokota T, Asahina M, Watahiki M (2017) YUCCA9-mediated auxin biosynthesis and polar auxin transport synergistically regulate regeneration of root systems following root cutting. Plant Cell Physiol 58: 1710-1723.
- Yamamoto Y, Kamiya N, Morinaka Y, Matsuoka M, and Sazuka T (2007) Auxin biosynthesis by the YUCCA genes in rice. Plant Physiol. 143:1362–1371.
- Yan Y, Tao H, He J, Huang S-Y. (2020) The HDOCK server for integrated protein-protein docking. Nature Protocols 15(5):1829-1852, doi: 10.1038/s41596-020-0312-x.
- Yan Y, Zhang D, Zhou P, Li B, Huang S-Y. (2017) HDOCK: a web server for protein-protein and protein-DNA/RNA docking based on a hybrid strategy. Nucleic Acids Res; 45 (W1):W365-W373.
- Yu J, Zhang Y, Liu W, Wang H, Wen S, Zhang Y, Xu L. Temporarily withdrawn: Molecular evolution of auxin mediated root initiation in plants. Molecular Biology and Evolution. 2019. Ref Type: In Press.
- Yasuda T, Fujii Y, Yamaguchi T (1985) Embryogenic Callus Induction from Coffea arabica Leaf Explants by Benzyladenine. Plant Cell Physiol. 26, 595–597, doi:10.1093/oxfordjournals.pcp.a076946.
- Zazimalová E, Krecek P, Skúpa P, Hoyerová K, Petrášek J (2007) Polar transport of the plant hormone auxin the role of PIN-FORMED (PIN) proteins. Cell Mol Life Sci 64: 1621-1637.

-
- Zazimalová E, Murphy AS, Yang H, Hoyerová K, Hosek P (2010) Auxin transporters - Why so many? *Cold Spring Harbor Perspect Biol* 2(3): a001552, doi: 10.1101/cshperspect.a001552.
- Zhao Y (2012) Auxin biosynthesis: a simple two-step pathway converts tryptophan to indole-3-acetic acid in plants. *Mol Plant* 5: 334-338.
- Zhao Y (2014) Auxin Biosynthesis. *Arab. Book*, 12, e0173, doi:10.1199/tab.0173.
- Zhao Y (2011) Auxin biosynthesis: a simple two-step pathway converts tryptophan to indole-3-acetic acid in plants. *Mol. Plant.* 5, 334–8, doi:10.1093/mp/ssr104.
- Zhao Y (2010) Auxin Biosynthesis and Its Role in Plant Development. *Annu. Rev. Plant Boil.* 61, 49–64, doi:10.1146/annurev-arplant-042809-112308.
- Zhao Y (2018) Essential roles of local auxin biosynthesis in plant development and in adaptation to environmental changes. *Annu. Rev. Plant Biol.* 69, 417–435.
- Zhao Y, Christensen SK, Fankhauser C, Cashman JR, Cohen JD, Weigel D, Chory J (2001) A role for flavin monooxygenase-like enzymes in auxin biosynthesis. *Science*, 291, 306–309.
- Zhao Y, Hull AK, Gupta NR, Goss KA, Alonso JM, Ecker JR, Normanly J, Chory J, Celenza JL (2002) Trp-dependent auxin biosynthesis in *Arabidopsis*: involvement of cytochrome P450s CYP79B2 and CYP79B3. *Genome Res.* 16, 3100–3112, doi:10.1101/gad.1035402.
- Zhang J, Peer WA (2017) Auxin homeostasis: the DAO of catabolism. *J. Exp. Bot.* 68, 3145–3154, doi:10.1093/jxb/erx221.
- Ziegler D. M. (1993) Recent studies on the structure and function of multisubstrate flavin-containing monooxygenases. *Annu Rev Pharmacol Toxicol* 33: 179–199.

Zimmerman JL (1993) Somatic embryogenesis: A model for early development in higher plants. *Plant Cell* 5: 1411-1423.

Zourelidou M, Muller I, Willige BC, Nill C, Jikumaru Y, Li H, Schwechheimer C (2009) The polarly localised D6 PROTEIN KINASE is required for efficient auxin transport in *Arabidopsis thaliana*. *Development* 136: 627-636.

Zourelidou M, Absmanner B, Weller B, et al., (2014) Auxin efflux by PIN-FORMED proteins is activated by two different protein kinases, D6 PROTEIN KINASE and PINOID. *Elife*. 2014;3:e02860, doi:10.7554/eLife.02860.

Zuo J, Niu QW, Frugis G, Chua NH (2002) The WUSCHEL gene promotes vegetative-to-embryonic transition in *Arabidopsis*. *Plant J* 30: 349-359.